Distribution Agreement

In presenting this thesis of dissertation as a partial fulfillment of the requirements for an advanced degree from Emory University, I hereby grant to Emory University and its agents the non-exclusive license to archive, make accessible, and display my thesis or dissertation in whole or in part in all forms of media, now or hereafter known, including display on the world wide web. I understand that I may select some access restrictions as part of the online submission of this thesis or dissertation. I retain all ownership rights to the copyright of the thesis or dissertation. I also retain the right to use in future works (such as articles or books) all or part of this thesis or dissertation.

Signature:

_____ _____

Moe Hein Aung Date

Mechanisms Underlying Early Visual Dysfunctions in Rodent Models of Type 1 Diabetes

By

Moe Hein Aung
Doctor of Philosophy

Graduate Division of Biological and Biomedical Science
Neuroscience

_____
Machelle T. Pardue, Ph.D.
Advisor

_____
P. Michael Iuvone Ph.D.
Committee Member

_____
Peter M. Thule, M.D.
Committee Member

_____
Roy Sutliff, Ph.D.
Committee Member

_____
Kerry Ressler, M.D., Ph.D.
Committee Member

_____
Criss Hartzell, Ph.D.
Committee Member

Accepted:

_____
Lisa A. Tedesco, Ph.D.
Dean of the Graduate School

_____
Date

Mechanisms Underlying Early Visual Dysfunctions in Rodent Models of Type 1 Diabetes

By

Moe Hein Aung
B.A., Grinnell College, 2005

Advisor: Machelle T. Pardue, Ph.D.

An abstract of
A dissertation submitted to the Faculty of the
James T. Laney School of Graduate Studies of Emory University
in partial fulfillment of the requirements for the degree of
Doctor of Philosophy
in
Graduate Division of Biological and Biomedical Science
Neuroscience

2014

ABSTRACT

Mechanisms Underlying Early Visual Dysfunctions in Rodent Models of Type 1 Diabetes

By Moe Hein Aung

Diabetic retinopathy is a devastating ocular complication of diabetes mellitus. Due to the wide prevalence of diabetes, diabetic retinopathy is the leading global cause of blindness in working-age adults. As severe vision loss is associated with microvasculopathy in the retinal vasculature, such as aneurysm, hemorrhage, and neovascularization, clinical diagnosis and treatment of diabetic retinopathy is based on the onset and severity of these irreversible structural lesions. However, diabetic patients with angiographically normal retinas have been found to suffer subtle defects in vision (e.g. scotopic vision, color vision, contrast sensitivity). The appearance of these visual deficits can potentially provide an earlier detection and therapeutic window for diabetic retinopathy. Therefore, the purpose of this thesis project is to elucidate plausible mechanisms underlying early diabetes-induced visual dysfunction. Using rodent models of Type 1 diabetes, I first delineated the temporal relationship of visual deficits with other early diabetes-evoked changes in the retina, namely retinal alterations, vascular dysfunction, and cataract formation. Specifically, I found that visual defects found in early-stage diabetic retinopathy may initially involve dysfunctions of the neural retina and retinal vasculature, and worsen with later development of cataracts. Subsequently, with pharmacologic means and genetic models, I investigated the contributions of two specific abnormalities to the visual deficits - disrupted dopamine neurotransmission and defective functional hyperemia. The results show that both retinal dopamine deficiency and reduced functional hyperemic response due to diabetes result in profound visual deficits in rodent models of diabetes, and restoration of these functions ameliorates the severity of visual defects. Collectively, these findings uncover new therapeutic targets that may yield not only visual improvement but also slowing of disease progression. Moreover, the mechanisms revealed in this thesis work can potentially provide novel biomarkers to characterize preclinical diabetic retinopathy and strengthen the importance of viewing and treating diabetic retinopathy as a neurovascular disorder.

Mechanisms Underlying Early Visual Dysfunctions in Rodent Models of Type 1 Diabetes

By

Moe Hein Aung
B.A., Grinnell College, 2005

Advisor: Machelle T. Pardue, Ph.D.

A dissertation submitted to the Faculty of the Graduate School of Emory University in partial fulfillment of the requirements for the degree of
Doctor of Philosophy
in
Graduate Division of Biological and Biomedical Science
Neuroscience

2014

ACKNOWLEDGEMENT

The work presented in this dissertation would not been successful without the constant support of the following people. First and foremost, I would like to thank my advisor, Dr. Machelle Pardue for teaching me how to be a good scientist and how to see the excitement and joy in doing science. Machelle has been a phenomenal mentor, always making time to discuss science with me and motivating me consistently throughout my thesis work. I am also extremely grateful for her guidance in developing my professional career as a clinical scientist and my enthusiasm to become an ophthalmologist. I can't thank her enough for taking me under her wing during the early stage of my PhD study. I would also like to thank members of my thesis committee: Drs. Michael Iuvone, Kerry Ressler, Peter Thule, Roy Sutliff, and Criss Hartzell, for their outstanding mentorship throughout my PhD study. In particular, I would like thank Dr. Iuvone for his guidance in developing and conducting the study on the role of dopamine in diabetic retinopathy and Dr. Thule for teaching me how to induce diabetes in animals and how to take proper care of them. I truly appreciate the various expertise and insight of my committee members, which have greatly improved the quality of my thesis work and enhanced my development as a scientist. Moreover, I am grateful for the technical helps from the following people: Dr. William Delaune for statistical analyses, Dr. John Falck for providing internal standards for HPLC assay, and Dr. Alexa Mattheyses for guidance in using ImageJ program. I would also like to thank Emory's Neuroscience Program (especially Dr. Yoland Smith and Sonia Hayden) and Emory MD/PhD program (especially Mary Horton, Dr. Chuck Parkos, Dr. Marie Csete, and Dr. Kerry Ressler) for their support throughout this PhD journey.

I thank the current and former members of my lab for helping me succeed my graduate work. I am grateful for Moon Han, Han na Park, and Megan Prunty for their help in taking care of the fragile diabetic animals and carrying out several experiments. I am grateful for Vincent Ciavatta, Cao Yang, and Tracy Obertone for their help and insight in molecular works. I would also like to thank Gregor Schmid for his help in setting up the apparatus for functional hyperemia. Lastly, I would like to thank Christopher Tan, Amanda Mui, Rachel Stewart, Krista You, Eric Lawson, Seema Jabbar, Kip Lacy, Ade Adekunle, Brian Prall, Jake Light, Adam Hanif, Marissa Gogniat, and Ranjay Charkraborty for making lab a fun and friendly environment!

I have been fortunate to have numerous great friends to accompany me throughout this long journey. First, I would like to thank my medical school pals: Michael Lava, Seema Kini, Michael Bryant, Hart Squires, Amalia Aleck, Radhika Datar, and Sachin Garg. Also I would like to acknowledge my MD/PhD comrades: Devon Livingston-Rosanoff, Hiro Nakamura, Christopher Wang, Sammy Lee, Seyed Safavynia, Katie Anderson, and Keli Kolegraff. Also, I would like to thank my good friends: Esteban and Andrea Tan, Young Jae Chung, Myo Kyaw Min, Melonie Wang, Gary Lun, Jason Li, Xu Peng, David and Winnie Wang, Chen Xue, Kenny Wijono, Brian and Xiao Ping Lee, Wu Chan, Xiang Jianxing and Su Wenji. Last but not least, I want to shout out to my neuroscience buddies: Christina Nemeth and Katy Shepard. All of you are the best and thank you for providing fun, support, and sanity to my life.

Of course, I wouldn't be here without my family. I am so fortunate to have such a great caring family – loving parents and supportive sister. Lastly, I would like to thank my dear wife: Win. Her presence has transformed my life nothing less than wonderful and exciting! She has consistently treated me with love and support that I needed to finish my PhD work. I can't ask for more than having her and all of the aforementioned people in my life. Love y'all!

Finally, special appreciations to all the funding sources for making this thesis work a possibility: National Institute of Health, Research to Prevent Blindness, and the Department of Veterans Affairs.

TABLE OF CONTENTS

LIST OF FIGURES

CHAPTER 1:

CHAPTER 2:

CHAPTER 3:

CHAPTER 4:

CHAPTER 5:

LIST OF TABLES

CHAPTER 2:

CHAPTER 3:

CHAPTER 4:

ABBREVIATIONS USED IN THE DISSERTATION

(In alphabetical order, from A to Z based on the abbreviations)

- 2-(3-Adamantan-1-yl-ureido)-dodecanoic acid – AUDA
- Blood glucose – BG
- Control – CTRL
- Cycle threshold – Ct
- Cytochrome P450 – CYP
- Dopamine – DA
- Diabetic – DM
- Dopamine$_1$ receptor – D1R or *Drd1*
- Dopamine$_4$ receptor – D4R or *Drd4*
- Diabetic retinopathy – DR
- 3,4-dihydroxyphenyl-acetic acid – DOPAC
- Epoxyeicosatrienoic acid – EET
- Electroretinogram – ERG
- Full-field electroretinogram – ffERG
- Gamma-aminobutyric acid – GABA
- Ganglion cell layer – GCL
- Glial fibrillary acidic protein – GFAP
- L-glutamate/L-aspartate transporter – GLAST
- N-hydroxyl-N'-(4-n-butyl-2methylphenyl)-formamide – HET0016
- 20-Hydroxyeicosatetraenoic acid – 20-HETE
- Hypoxia-inducible factor-1α – HIF-1α
- High-performance liquid chromatography – HPLC
- Indocyanine green – ICG
- Inner nuclear layer – INL
- Inducible nitric oxide synthase – iNOS
- Inner plexiform layer – IPL
- Intraperitoneal – i.p.
- Inner segment – IS
- Intravenous – i.v.
- L-3,4-dihydroxyphenylalanine – L-DOPA
- Multifocal electroretinogram – mfERG
- Nitric oxide – NO
- Non-proliferative diabetic retinopathy – NPDR
- Neurovascular – NV
- Optical coherence tomography – OCT
- Optokinetic tracking – OKT
- Outer nuclear layer – ONL
- Oscillatory potential – OP
- Outer plexiform layer – OPL
- Outer segment – OS

- Proliferative diabetic retinopathy – PDR
- Retinal pigment epithelium – RPE
- Retinal-specific tyrosine hydroxylase knockout – rTHKO
- Standard error of the mean – SEM
- Scanning laser ophthalmoscope – SLO
- Scotopic threshold response – STR
- Streptozotocin – STZ
- Tyrosine hydroxylase – TH or *Th*
- DNA terminal dUTP nick end labeling – TUNEL
- Vascular endothelial growth factor – VEGF
- Vehicle – Veh
- Wild-type – WT

CHAPTER 1: INTRODUCTION

1.1 Visual Processing by the Retina

"To suppose that the eye, with all its inimitable contrivances for adjusting the focus to different distances, for admitting different amounts of light, and for the correction of spherical and chromatic aberration, could have been formed by natural selection seems, I freely confess, absurd in the highest degree."

Charles Darwin, The Origin of Species (Darwin, 1959)

Although we are accustomed to using our eyesight day to day to perceive our surrounding space and the world, the mechanisms that underlie vision are nothing short of a miracle. As the light enters the pupil, it is focused by the cornea and the lens, and projected onto the back of the eye, i.e. the retina (Figure 1-1A). Retina is a specialized sensory organ comprised of alternating layers of neuronal cells and synaptic connections that convert light into electrical neural signals (Figure 1-1B and 1-1C). Specifically, the light energy is first detected by retinal cells that contain photosensitive visual pigments, the photoreceptors. The light-evoked signals in the photoreceptors are then processed and modified through various interneurons (bipolar, horizontal, and amacrine cells) before conveying to the retinal ganglion cells. The axons of the ganglion cells form the optic nerve and carry the outputs of the retina to higher visual centers in the brain for further processing needed for visual perception (For more info, please refer to Figure 1-1) (Kandel et al., 2000). The region where the optic nerve fibers leave the retina is called the optic disc (Figure 1-2). Since the optic disc is devoid of photoreceptors, it forms a blind spot in the visual field of the eye. However, the blind spot is not often perceived as the

brain interpolates the spot based on surrounding details and constant eye movements along with the visual field of the other eye compensates for the lack of visual input for that spot. This allows us and other vertebrate animals to have a full and unbroken impression of the world (Kandel et al., 2000).

As the eye is designed to focus the visual image on the retina with minimal optical distortion, the retinal layout poses an interesting dilemma. The retina is actually inverted with respect to its optical function and light path such that the light must traverse through layers of other retinal neurons before striking the photoreceptors. So how does the light reach the photoreceptors without being distorted? First, the axons of retinal neurons in the proximal layers are unmyelinated[1], so that these layers of cells are relatively transparent, reducing the potential of light scattering and absorption (Kandel et al., 2000). Second, a recent report suggests that Müller cells, which are radial glial cells spanning the entire retinal thickness, act as optical fibers transferring light through the inner retina directly to the photoreceptors, and thereby minimize image distortion and signal loss (Franze et al., 2007). Third, retinas in certain mammals (including humans) contain a region called the macula that is composed of high density of cone photoreceptors and ganglion cells specialized in visual acuity and color vision. Moreover, there is a central depression within the macula, the fovea, in which the cell bodies of the proximal retinal neurons are shifted to the side, enabling the light to travel unimpeded to the photoreceptors (Figure 1-1A) (Kandel et al., 2000). Lastly, the cells in the retinal pigment epithelium contain melanin, a black pigment that absorbs any light not captured

[1] The axons of ganglion cells that are located in the retina are not myelinated, while axons that are located outside the retina are myelinated.

by the retina. This prevents light from being reflected back to the retina, which could potentially degrade the quality of the visual image (Figure 1-1) (Kandel et al., 2000).

Because of the unique setup of the eye for light transmission and detection, the posterior part of the eye, also referred to as the fundus, can be easily visualized (Figure 1-2). Fundus exam with ophthalmoscope or fundus camera is a test commonly used by trained medical professionals to assess the general health of the retina, either for screening, diagnosis, or monitoring of ocular disease, such as diabetic retinopathy.

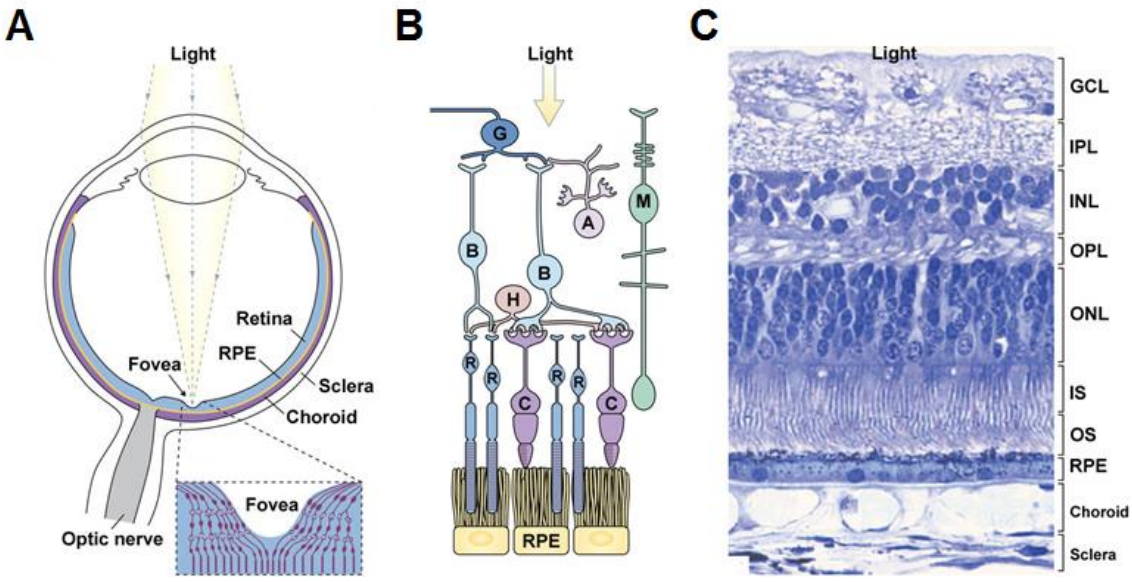

Figure 1-1. Basic overview of the eye and the retina. (A) Diagram illustrating how the incoming light is projected onto the sensory organ located at the back of the eye, the retina. As the light enters through the pupil, it is refracted by the cornea and the lens, and then travels through the vitreous humor that fills the eye cavity before reaching the retina (the blue lining). The fovea is a depression in the retina with a high density of retinal cells responsible for the sharp central vision. **(B)** Diagram depicting the cellular components and structure of the retina. When light reaches the retina, it actually enters from the side of retinal ganglion cells (G) and has to travel through the whole retinal thickness to reach the photoreceptors. Photoreceptors are retinal neurons that detect light and convert it into electrical signals. There are two main types of photoreceptors, rods (R) and cones (C), which mediate night and day vision, respectively. They convey the visual signals onto secondary neurons called bipolar cells (B). The bipolar cells then relay the messages to the ganglion cells, which ultimately transmit the messages onto higher order visual centers in the brain. Amacrine (A) and horizontal (H) cells are interneurons that provide lateral inputs to bipolar cells and ganglion cells. Müller cells (M) are glial cells that span the entire retinal thickness. Some of their supportive roles include recycling of neurotransmitters (e.g. glutamate and GABA), shuttling of energy metabolites to neurons, keeping the ion balance of the retina, and maintaining the blood-retinal barrier. Retinal pigment epithelium (RPE), sandwiched between the retina and the choroid, is composed of a single layer of hexagonal cells that are densely packed with granules of melanin. In brief, its main functions are to shield the retina from excessive incoming light, support the integrity of blood-retinal barrier, maintain the health of the photoreceptors, and supply molecules essential for light detection. [For additional review of the retina and visual perception, please refer to (Kandel et al., 2000)]. **(C)** Histological image of a transverse section of human retina laminated layers. The outer nuclear layer (ONL) contains the nuclei of the photoreceptors, while the processes and synaptic connections between the photoreceptors, horizontal cells, and bipolar cells are located in the outer plexiform layer (OPL). The nuclei of the bipolar cells, amacrine cells, horizontal cells, and Muller glial cells are found in the inner nuclear layer (INL). Next, the processes and terminals of bipolar cells, amacrine cells, and ganglion cells constitute the inner plexiform layer (IPL). The layer closest to the vitreous is the ganglion cell layer (GCL), where the somas and axons of ganglion cells are located. The choroid is a vascularized connective tissue that provides oxygen and nourishment to the photoreceptors and RPE. On the other hand, the metabolic need of the inner retina is supplied by a separate vascular network, the retinal vasculature (not shown here). Image obtained from http://embryology.med.unsw.edu.au/embryology/index.php?title=File:Eye_and_retina_cartoon.jpg with permission (Hill, 2014). Abbreviations used in the figure: A = amacrine cell; B = bipolar cell; C = cone photoreceptor; G = ganglion cell; GCL = ganglion cell layer; H = horizontal cell; INL = inner nuclear layer; IPL = inner plexiform layer; IS = inner segment of the photoreceptor; M = Müller cell; ONL = outer nuclear layer; OPL = outer plexiform layer; OS = outer segment of the photoreceptor; R = rod photoreceptor; RPE = retinal pigment epithelium.

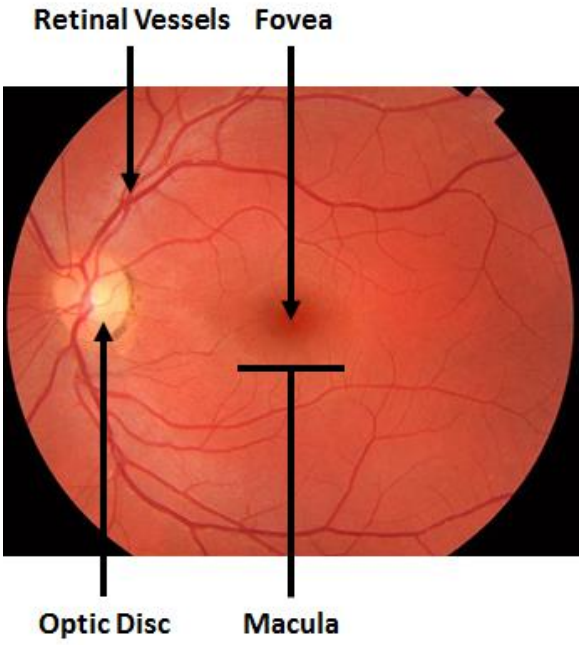

Figure 1-2. A fundus image of a human eye. Using an ophthalmoscope or fundus camera, the posterior part of the eye or the fundus can be observed directly. Key structures that can be visualized (as indicated by black arrows) include optic disc, macula, fovea, and retinal vasculature. Image modified from http://en.wikipedia.org/wiki/Fundus_(eye) with permission (Häggström, 2012). The image is made available under the Creative Commons CC0 1.0 Universal Public Domain Dedication.

1.2 Overview of Diabetic Retinopathy

Diabetes mellitus (from here on referred to as diabetes) is a disorder characterized by uncontrolled and fluctuating glucose levels in the blood due to insulin-related abnormalities. There are two main types of diabetes. Type 1 diabetes (often referred to as juvenile-onset or insulin dependent diabetes) is associated with loss of insulin-producing beta cells of the Islets of Langerhans in the pancreas, leading to inadequate insulin production. Type 2 diabetes (also known as adult-onset or non-insulin-dependent diabetes) is primarily caused by insulin resistance, which can be coupled with insulin deficiency at advanced stages (http://diabetes.niddk.nih.gov/). With the worldwide prevalence of diabetes in adults set to rise by 35% in 2025, the complications arising from diabetes impose an ever-increasing burden on the healthcare systems in both developed and developing countries (King et al., 1998). As one of the most common microvascular complications of this disease, diabetic retinopathy (DR) continues to be the leading cause of vision impairment and blindness among working-age adults globally (Congdon et al., 2003). Epidemiological studies indicate that practically all patients with Type 1 diabetes and nearly 80 percent of those with Type 2 diabetes will have at least some form of retinopathy after 20 years of diabetes (Klein et al., 1989; Roy et al., 2004; Klein, 2007).

Clinically, DR is considered a vascular disorder, characterized by structural defects in the retinal vasculature [Figure 1-3; for more complete review, please see (Frank, 1995, 2004)]. The earliest clinical signs of DR are microaneurysms, small swellings of retinal vessels, as well as dot intraretinal hemorrhages on ophthalmoscopy (Figure 1-3A). When these lesions are observed, the patient is diagnosed with non-

proliferative retinopathy (Figure 1-3B). As the disease progresses, mild to moderate to severe, there is an increase in the size and number of hemorrhages. This may be accompanied by cotton-wool spots, which are indicative of focal retinal infarctions due to occlusion of small arterioles. Retinal arterioles may also appear white and be occluded while the retinal veins become dilated, tortuous, and irregular in caliber. With increasing vascular insufficiency, the retina experiences progressively worse ischemia that ultimately drives an aggressive neovascularization response – development of new blood vessels. This stage of disease is classified as proliferative diabetic retinopathy (Figure 1-3). If left untreated, the neovascularization response can cause severe vision loss. Often, the newly developed vessels are immature and can hemorrhage into the vitreous. Moreover, the vessels can cause retinal detachment due to traction from the accompanying contractile fibrous tissue. Despite proper insulin treatment and glycemic control, neovascularization still occurs in roughly 20% of diabetic patients after 30 years of diabetes (Antonetti et al., 2012). Another important and common reason for visual impairment in diabetic patients, especially of central vision, is macular edema. Macular edema is defined as swelling of the neural retina within the macular region. This is caused by leakage of plasma from the capillaries into the retina from diabetes-induced breakdown of the blood-retinal barrier (Figure 1-4). The edema can also cause lasting alterations to the macular region even when the fluid components are reabsorbed; depositing lipid and lipoprotein elements and forming hard exudates (Figure 1-3A). According to the population-based Wisconsin Epidemiological Study of Diabetic Retinopathy, the incidence of macular edema over 10-year period is roughly 20 percent for Type 1 patients and 14 to 25 percent for Type 2 patients, depending on whether the

individual needs insulin treatment or not (Klein et al., 1989; Frank, 2004; Roy et al., 2004; Klein, 2007). Because the appearance of these late-stage vascular lesions signifies irreversible damage to the retina, there is an urgent need to study early-stage DR so that earlier detection and intervention methods can be developed.

Currently, there are few options for the prevention and treatment of DR. First and foremost, clinical trials have shown that rigorous glycemic control can significantly delay the development and slow the progression of retinopathy in patients with either Type 1 or Type 2 diabetes (The Diabetes Control and Complications Trial (DCCT) Research Group, 1993; UK Prospective Diabetes Study (UKPDS) Group, 1998). Moreover, intensive metabolic control, especially to regulate hypertension and dyslipidemia, can reduce the incidence and progression of DR (Antonetti et al., 2012). However, ideal glycemic and metabolic controls are difficult to achieve and maintain, and are associated with increased risk of hypoglycemia. For patients with symptoms of more advanced DR such as persistent vitreous hemorrhages and fibrovascular complications, vitrectomy is often conducted. However, the standard of care treatment for late-stage DR remains focal and pan-retinal laser photocoagulation, which involves inducing laser burns in the retina. It has served as the primary treatment for severe proliferative DR since the 1970's when the Diabetic Retinopathy Study demonstrated the efficacy of laser therapy in reducing visual impairment due to neovascularization. Although the mechanism(s) of action for laser coagulation therapy still need to be elucidated, it is hypothesized that the laser therapy causes regression of new vessels by destroying presumably hypoxic regions of the peripheral retina that is releasing neovascularization promoting factors, predominantly vascular endothelial growth factor (VEGF) (Frank, 2004). Although the

progression of late-stage retinopathy can be retarded somewhat by vitreoretinal surgery or laser photocoagulation, these treatments are performed at the expense of functional retina and visual performance. It is important to note that direct inhibition of VEGF with biologic antibodies is an emerging and promising treatment for late-stage DR, especially for macular edema (Frank, 2009; Waisbourd et al., 2011). Still, it is of great clinical importance to find novel therapeutic targets at early stages of DR when the retina has not incurred permanent damage.

Figure 1-3. Illustrations of clinically relevant vascular lesions and the stages of Diabetic Retinopathy. **(A)** A schematic of the classic vascular lesions found in non-proliferative DR (NPDR) and proliferative DR (PDR). Images obtained from http://www.eyerisvision.com/diabetic-retinopathy.html. **(B)** Representative fundus photographs of normal, NPDR, and PDR to show how different stages of DR will appear on inspection with an ophthalmoscope. Images modified from http://www.checkdiabetes.org/2011/02/diabetic-retinopathy.html. Abbreviations used in the figure: DR = diabetic retinopathy; NPDR = non-proliferative DR; PDR = proliferative DR.

Figure 1-4. Optical Coherence Tomography images comparing an eye with normal macula and one with diabetic macular edema. In brief, optical coherence tomography (OCT) is a type of optical tomographic technique used to visualize retinal layers *in vivo*. It is based on the use of interferometry of near-infrared light to penetrate into the eye and the retina. In an OCT image from a healthy subject (top), the fovea is clearly delineated as a slight depression in the macular region and the retina appears compact with distinct layers. However, in a diabetic patient with macular edema, the fluid from the leaky blood-retina barrier accumulates in the macular region (indicated by white arrow), disrupting the fovea and retinal structure. OCT Images modified from http://www.medscape.com/viewarticle/704734_3. Abbreviation used in the figure: OCT = optical coherence tomography.

1.3 Signs of Neuronal Dysfunctions in Preclinical Stages of Diabetic Retinopathy

While there has been an emphasis on studying retinal vascular changes in diabetes, alterations to the neural retina, including changes to both retinal neurons and glia, have been identified before the onset of clinically detectable vascular lesions (Barber, 2003; Antonetti et al., 2006). Mounting evidence of early neuronal and glial changes may be crucial for developing methods to predict which diabetic patients may be at risk of developing DR, to monitor disease progression, or to assess the efficacy of new treatment options. The following sections will discuss the changes that have been found in a variety of electrophysiological and psychophysical assessments, which are reflective of neuroglial abnormalities in the retina due to diabetes.

1.3.1 Alterations in Retinal Function

The first hint of neuronal deficits in DR was reported in the 1960s, in which oscillatory potentials (OPs) seen in full-field electroretinogram (ffERG) were diminished and delayed in diabetic patients (For more info on ffERG, please see Figure 1-5). OPs are high-frequency oscillations on the leading edge of the b-wave and they are indicative of amacrine cell activity and/or amacrine to ganglion cell communications (Speros and Price, 1981; Wachtmeister, 1998; Dong et al., 2004). Since then, abnormalities in OPs have been consistently reported in diabetic patients (Bresnick and Palta, 1987; Holopigian et al., 1992; Shirao and Kawasaki, 1998; Kizawa et al., 2006; Holfort et al., 2010; Lecleire-Collet et al., 2011) and in animal models (Hotta et al., 1997; Li et al., 2002; Matsubara et al., 2006; Ramsey et al., 2006; Kohzaki et al., 2008; Kern et al., 2010a; Ly et al., 2011; Aung et al., 2013), even before the appearance of vascular lesions. Furthermore, changes in OPs have been shown to correlate significantly with the

progression of retinopathy and the severity of vision loss (Bresnick and Palta, 1987). The value of OPs in detecting retinal changes due to diabetes most likely stems from its sensitivity in reflecting disturbances in the retinal circulation (i.e. ischemia), which is well-documented in the pathogenesis of DR (Speros and Price, 1981).

Aside from abnormalities in OPs, alterations to another inner retinal component have been consistently reported – ganglion cell function. Ganglion cell function can be elicited with ffERG at extremely dim light intensities and is referred to as scotopic threshold response (STR) (Sieving et al., 1986; Saszik et al., 2002). In Type 1 diabetic patients, STR amplitudes are found to be reduced and implicit time delays correlate with fluorescein leakage and severity of DR (Aylward, 1989). Similarly, STRs are reduced in streptozotocin[2] (STZ)-induced diabetic rats as early as 4 weeks of diabetes, a time-point which is comparable to preclinical stage of DR (Kohzaki et al., 2008; Ly et al., 2011).

Although less robust, some studies have observed changes to other components of ffERG: a- and b-waves, in terms of both reduced amplitudes and delayed implicit times (Phipps et al., 2006; Fletcher et al., 2007). This suggests that dysfunctions due to diabetes are not restricted only to the inner retina, but the retina as a whole. More importantly, these studies show the capability of using ffERG as an objective tool to detect early alterations in retinal function, to predict progression of DR, and to assess efficacies of treatments.

There is, however, a caveat. Because ffERG is a global assessment of retinal function, it is possible that subtle local abnormalities may be missed because responses from remaining healthy retina can potentially predominate the functional measures.

[2] STZ is an alkylating agent used to destroy insulin-producing β cells in the pancreas, and thus creating a model for Type 1 diabetes in rodents.

Therefore, researchers have examined if multifocal ERG (mfERG) would provide better sensitivity in detecting early functional alterations and higher predictive value in assessing local disease progression over time (For more info on mfERG, please see Figure 1-6). They have found (1) presence of mfERG changes in the absence of visible signs of retinopathy, (2) significant spatial association between mfERG abnormalities and early-stage retinopathic lesions, (3) changes in implicit time of mfERG response having good predictive value of DR onset (Han et al., 2004; Bearse et al., 2006; Wolff et al., 2010; Harrison et al., 2011). These benefits of mfERG provide clinicians a powerful tool to identify diabetic patients who may be at risk for DR, to initiate early prophylactic treatments, or to monitor the disease progression of these patients. Although both ffERG and mfERG unequivocally detect early retinal dysfunction due to diabetes and predict potential development of retinopathy, usage of ERG as a screening tool for DR remains limited as certain level of expertise is needed to properly conduct the exam and interpret the ERG responses. Moreover, studies are still needed to systematically compare the reliability and sensitivity of these different ERG modalities and to improve the ease and speed of conducting ERG testing. However, the question as to whether ERG abnormalities reflect worsening visual function in diabetics remains unanswered.

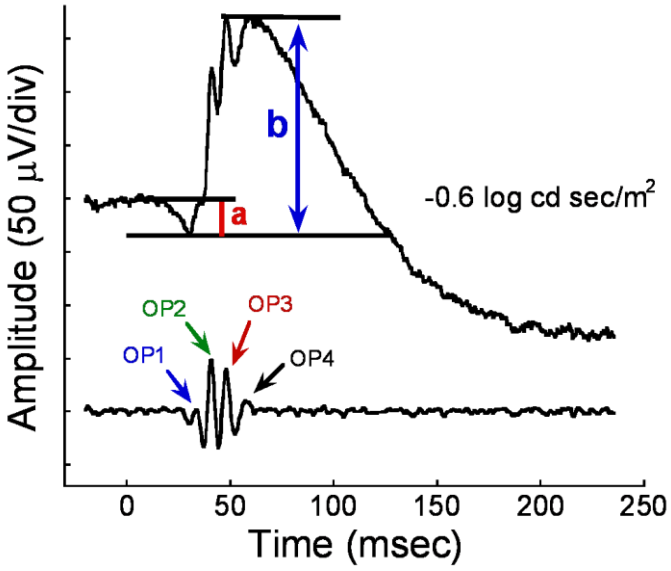

Figure 1-5. Sample full-field ERG waveform (top) and filtered oscillatory potentials (bottom) from an adult rat in response to a -0.6 log cd sec/m^2 flash. In brief, full field ERG (ffERG) is a non-invasive measurement of retinal function that displays the summed response of electrical signals originating from multiple retinal cell populations to a flash of light. Due to differences in timing, amplitude and polarization of synapses, the ERG has a distinct waveform in which the sequential responses from different cell types can be discerned. Specifically, a-wave is generated by photoreceptor activation (Penn and Hagins, 1969; Hood and Birch, 1990), while the b-wave represents the activity of the rod ON bipolar cells (Robson and Frishman, 1999). The oscillatory potentials (OPs), wavelets on the rising phase of the b-wave, are potentially generated by the amacrine cells and retinal ganglion cells (Wachtmeister, 1998). Furthermore, the rod and cone retinal systems can be isolated by manipulating the intensity of the stimulus and the adaptation state of the eye. The figure is created by Dr. Machelle Pardue and reproduced with her permission. Abbreviation used in the figure: OP = oscillatory potential.

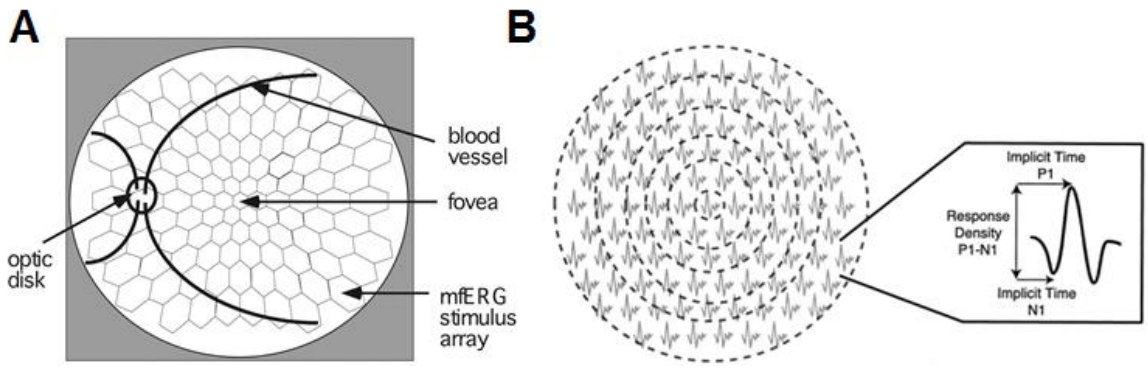

Figure 1-6. Demonstration of how stimuli are delivered in multifocal ERG and the retinal response that it elicits. (A) An example of how multifocal ERG (mfERG) stimulus array overlays to approximate spatial correspondence on a fundus image. In mfERG, a series of stimuli are presented across numerous retinal patches, thereby allowing simultaneous recordings of local retinal response elicited at each individual patch (Hood, 2000). Image modified from http://www.iovs.org/content/45/3/948/F1.expansion.html with permission (Han et al., 2004). **(B)** A sample of typical mfERG responses. Each response corresponds to a region of the retina. The responses extracted are further analyzed in terms of the parameters shown in the right panel. Abbreviations used: P1 – first positive peak; N1 – first negative trough; P1-N1 – difference between P1 and N1. Image modified from http://www.39kf.com/cooperate/qk/American-Society-for-Nutrition/047906/2008-12-28-551328.shtml with permission (Schupp et al., 2004). Abbreviations used in the figure: ERG = electroretinogram; mfERG = multifocal ERG; N = negative; P = positive.

1.3.2 Early Diabetes-associated Visual Dysfunction

Although signs of abnormal neural retina are evident in early-stage DR, typical visual acuity assessment with eye charts is an insensitive diagnostic and clinical trial end-point measurement for early-stage DR. More often, impairments in subtle aspects of vision are detected preceding overt signs of vascular disease (Jackson and Barber, 2010). For example, contrast sensitivity, determined by measuring the contrast level required to detect or recognize a visual target (such as differentiating alternating dark and light bars or checkerboards), has been found to be consistently dysfunctional at preclinical stages of DR (Ghafour et al., 1982; Sokol et al., 1985; Ghirlanda et al., 1997; Lopes de Faria et al., 2001). Similarly, defective color discrimination has been detected in diabetic patients with angiographically normal retinas and normal visual acuity levels (Roy et al., 1986; Greenstein et al., 1990; Hardy et al., 1992; Ghirlanda et al., 1997). Moreover, visual field testing with perimetry has demonstrated superior correlation with the severity of retinopathy than visual acuity tests, and abnormalities found in specific visual fields correspond to actual retinal morphological changes (Ghirlanda et al., 1997; Bengtsson et al., 2005).

However, it is unknown whether these visual deficits originate mostly at the retinal level or involve post-retinal connections. To isolate the retinal contributions to the visual defects, one needs to delineate the temporal relationship of retinal and visual changes in early-stage DR. Once the relationship is determined, further studies can delve into the underlying mechanisms to reveal novel therapeutic targets. As conducting longitudinal studies on diabetic patients and minimizing different confounding variables between human subjects are costly and extremely difficult, animal models that can

sufficiently recapitulate early changes in DR and techniques that can reliably measure retinal and visual function are needed to answer such questions.

1.4 Potential Underlying Pathogenic Mediator(s) for Retinal and Visual Deficits

Though the role of neuronal pathology is increasingly recognized as a major component in the pathogenesis of early retinopathy, the exact mechanisms that lead to the functional deficits (as discussed in the previous section) remain unclear. There is no doubt that the deleterious metabolic effects of hyperglycemia and insulin deficiency as well as the metabolic pathways triggered by diabetes (e.g. up-regulation of polyol and hexosamine pathways, production of advanced glycation end-products, activation of protein kinase C, dysregulation of renin-angiotensin system, inflammatory responses, and presence of oxidative stress) initiate the development of early dysfunctions in DR (Brownlee, 2001, 2005; Cai and Boulton, 2002; Frank, 2004; Giacco and Brownlee, 2010; Tang and Kern, 2011). However, the answers to which cell types are affected and how they are affected in early-stage DR are still under intense investigation. The following sections are dedicated to discuss the subsequent diabetes-induced changes that may potentially contribute to the functional defects in the retina observed in both diabetic patients and animal models.

1.4.1 Neurodegeneration

The observed retinal and visual dysfunctions could be explained by the accelerated loss of neurons due to diabetes (Simó and Hernández, 2013). As neurons are terminally differentiated and unable to proliferate, loss of these cells would be cumulative, leading to chronic neurodegeneration and potentially manifesting as functional deficits. Such sign of neurodegeneration were first detected in the 1960s from

histological studies of postmortem diabetic human eyes (Wolter, 1961; Bloodworth, 1962). This finding has been replicated in recent studies that show an up-regulation of apoptotic markers in diabetic retinas prior to clinical diagnosis of DR (Barber et al., 1998; Abu-El-Asrar et al., 2004; Abu El-Asrar et al., 2007; Carrasco et al., 2008). More importantly, most of the apoptotic cells are not associated with blood vessels and do not co-localize with endothelial cell marker. Furthermore, *in vivo* assessments of retinal thickness with optical coherence tomography (OCT) have found thinning of the inner retina and retinal nerve fiber layer in human patients devoid of vascular compromise, consistent with the loss of retinal neurons found in early-stage DR using histological methods (Kern and Barber, 2008; Oshitari et al., 2009; Cabrera DeBuc and Somfai, 2010; Barber et al., 2011). Moreover, Müller glial cells are found to be activated in diabetic human retinas with upregulation of glial fibrillary acidic protein (GFAP), indicative of retinal injury (Mizutani et al., 1998; Abu-El-Asrar et al., 2004)

Similarly, studies have identified increased apoptosis of neuronal cells in diabetic animals prior to appearances of vascular changes (<6 months of diabetes), using a variety of techniques such as *in situ* end labeling of DNA terminal dUTP nick end labeling (TUNEL) and counting cells immuno-positive for apoptotic markers (Barber et al., 1998, 2011; Lorenzi and Gerhardinger, 2001; Kowluru and Koppolu, 2002; Martin et al., 2004; Feit-Leichman et al., 2005; Kern and Barber, 2008; Ozawa et al., 2011). Likewise, early signs of gliosis are evident in animal models of diabetes, as the glial cells react to the dysfunctional and dying neurons or the cells themselves are directly damaged by diabetes (Rungger-Brändle et al., 2000; Fletcher et al., 2005, 2007, 2010; Pannicke et al., 2006; Curtis et al., 2010; Ly et al., 2011). Although STZ itself is a neurotoxin, the observed

increase in cell death is most likely attributable to diabetes. First, correction of diabetes with intensive insulin treatment attenuates the cell loss (Barber et al., 1998), suggesting that the neuronal death is most likely due to diabetes as insulin will not ameliorate the toxic effects of STZ. Second, neurotoxicity due to STZ should permeate throughout the retina, inducing cell death of all cell types. However, the majority of the cell death is found in the inner retina, most notably affecting ganglion cells and amacrine cells, while sparing the outer retina (Zeng et al., 2000; Gastinger et al., 2006; Kern and Barber, 2008; Barber et al., 2011). Third, degeneration due to STZ should be rapid, but the cell loss observed in STZ-induced animals is gradual and cumulative. Fourth, *in vitro* studies on retinal neural cells show that exposure to high glucose alone is sufficient to induce apoptotic cell death (Santiago et al., 2007). Lastly, signs of neurodegeneration have also been observed in animal models of Type 2 diabetes and diabetic human retinas, in which STZ was clearly not used (Lorenzi and Gerhardinger, 2001).

Collectively, these studies demonstrate that a diabetic retina undergoes an active though slow neurodegenerative process in early phases of DR. The loss of these neurons would be expected to impair the proper function of retinal circuitry, and ultimately affect vision in both diabetic patients and animals. However, since the observed degeneration is gradual and the reduction in neuronal cells is relatively small (approximately 10-20%) after months of diabetes, other detrimental changes may occur and contribute to the functional deficits in early-stage DR.

1.4.2 Abnormalities in Visual Processing

As the retina is composed of complex and elaborate parallel pathways to extract different attributes from the visual scene, slight alterations in the transmission and

processing of the visual signals can lead to profound defects in vision (Schiller, 2010). Increasing evidence has shown that diabetes induces changes in different levels of signal transduction cascades in the retina, from phototransduction to neurotransmission.

Phototransduction. Diabetes has been shown to impede photoactivation by impairing activity levels of transducin and down-regulating levels of transducin protein in STZ-induced diabetic rats (For more info on photoactivation and deactivation, please see Figure 1-7) (Kowluru et al., 1992; Kim et al., 2005). In addition, diabetes alters the expression levels of rhodopsin kinase and recoverin proteins in diabetic retinas, suggesting that deactivation of phototransduction is also affected (Kim et al., 2005). Furthermore, signs of defective visual cycle (a pathway of enzymatic reactions that recycle the retinoids that are used during light detection in photoreceptors) have been detected in both human and animal samples. Specifically, studies have found impaired rhodopsin regeneration and lower 11-*cis*-retinal concentration in diabetic retinas (Ostroy et al., 1994; Tuitoek et al., 1996a, 1996b), which could be due to diabetes-induced reduction in the enzymes responsible for the recycling of retinoids (Garcia-Ramírez et al., 2009; Kirwin et al., 2011).

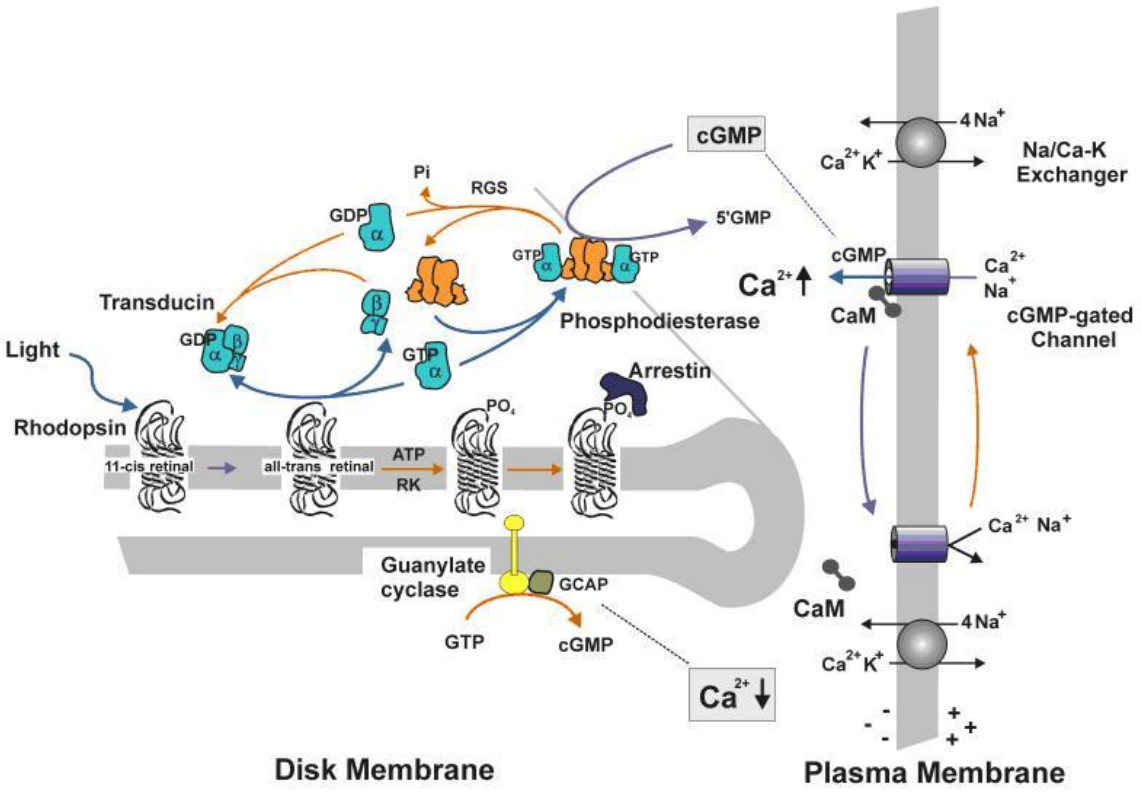

Figure 1-7. Representation of the molecular steps in photoactivation and deactivation of the phototransduction cascade. Photoactivation begins when a photon of light is absorbed by rhodopsin. The rhodopsin then undergoes conformational change and activates the regulatory protein transducin. Once activated, the transducin releases its bound GDP in exchange for cytoplasmic GTP, which then leads to the dissociation of its β and γ subunits. The remaining α subunit-GTP complex then activates phosphodiesterase, which is responsible for breaking down cGMP to 5'-GMP and thereby lowering the concentration of cGMP. The decreased levels of cGMP lead to the closure of cGMP-gated sodium/calcium channels. The resulting hyperpolarization of the cell causes reduction in the amount of neurotransmitter glutamate released. A decrease in the amount of glutamate released by the photoreceptors causes depolarization of ON-center bipolar cells (of both rods and cones) and hyperpolarization of cone OFF-center bipolar cells. The deactivation of the phototransduction occurs as the closure of cGMP-gated sodium/calcium channels lead to a drop in intracellular calcium level, causing the following the events. (1) Recoverin, a calcium binding protein, relieves its inhibition on rhodopsin kinase (RK) once the calcium levels fall during phototransduction. RK then phosphorylates activated rhodopsin, which decreases its affinity for transducin. The phosphorylation also allows arrestin to bind to the activated rhodopsin, and thereby completely deactivates it. (2) GTPase activating protein (GAP), part of the family of regulatory of G-protein signaling proteins (RGS), interacts with the α subunit of transducin, leading to hydrolysis of GTP to GDP, and thus preventing further activation of phosphodiesterase. (3) Guanylate cyclase activating protein (GCAP), another calcium binding protein, activates guanylate cyclase once it is dissociated from calcium. The activation of guanylate cyclase then proceeds to transform GTP to cGMP, and thus replenish the cell's cGMP levels and reopen the sodium/calcium channels. [For more thorough review of phototransduction, please refer to (Lamb and Pugh, 2006)]. Image taken from http://research.biochem.ubc.ca/fac_research/faculty/Molday_2011/Research/Research.html with permission (Molday, 2011). Abbreviations used in the diagram: ATP = adenosine triphosphate; CaM = calmodulin; cGMP = cyclic guanosine monophosphate; GAP = GTPase activating protein; GCAP = guanylate cyclase activating protein; GDP = guanosine diphosphate; GMP = guanosine monophosphate; GTP = guanosine triphosphate; Pi = phosphate; RGS = G-protein signaling proteins; RK = rhodopsin kinase.

Neurotransmission. Aside from phototransduction defects, diabetes has also been suggested to induce dysfunctions in the neurotransmission process and in the ability of Müller cells to regulate the extracellular ionic environment. Impairments have been found in all neurotransmitter systems in the retina, from excitatory to inhibitory as well as essential neuromodulators.

A plausible source of neuronal dysfunction in early-stage DR is a defective glutamatergic system. Glutamate, the main excitatory neurotransmitter in the retina, is required for the proper signal transmission from the photoreceptors to the ganglion cells. Its extracellular level is tightly regulated as high abundance of extracellular glutamate could alter synaptic function and potentially induce excitotoxicity and other unwanted effects (e.g. activation of protein kinase C) (Pulido et al., 2007). Studies have shown that STZ-induced diabetes diminishes the turnover of glutamate in rats, specifically impairing the metabolism of glutamate to α-ketoglutarate by transamination and conversion of glutamate to glutamine by glutamine synthetase (Lieth et al., 1998, 2000). Moreover, these studies have found that inefficient clearance of extracellular glutamate is complicated by diabetes-induced reduction in the re-uptake of glutamate into Müller cells via high-affinity L-glutamate/L-aspartate transporter (GLAST) (Lieth et al., 1998; Li and Puro, 2002; Ward et al., 2005). Interestingly, the capacity for glutamate synthesis is not altered in STZ-induced animals. All these dysfunctions are found to occur within three months of diabetes, well before the appearance of clinically significant injuries to the retinal vasculature in the diabetic animals which typically occur after six months post-STZ (Kern et al., 2010b; Barber et al., 2011). As glutamate turnover is abnormal in diabetes, it is plausible then that retinal glutamate level will be increased. Indeed,

glutamate levels have been reported to be elevated in both diabetic rats and human patients (Ambati et al., 1997; Lieth et al., 1998, 2000; Fletcher et al., 2007; Pulido et al., 2007). As described above, excessive glutamate levels can induce excitotoxicity and potentially contribute to the neurodegeneration observed in early-stage DR. Moreover, glutamate accumulation can result in oxidative stress, further augmenting neuronal damage due to diabetes (Kowluru et al., 2001). Aside from presynaptic abnormalities, studies have identified changes in expression of postsynaptic glutamate receptors, at both transcript and protein levels, in STZ-induced diabetic animals (Santiago et al., 2009; Lau et al., 2013). Altogether, these studies show that diabetes impairs the retinal glutamatergic system, potentially resulting in altered synaptic communications and even neuronal cell death, which may contribute to the functional deficits in early-stage DR.

Aside from excitatory neurotransmission, significant aberrations have been observed in the inhibitory neurotransmitter system of diabetic retinas, mainly systems involving gamma-aminobutyric acid (GABA). GABA is released by horizontal and amacrine cells of the inner retina, to fine-tune the receptive fields of ganglion cells by providing both feedforward and feedback controls on visual signal transmission from the photoreceptors to the ganglion cells via the bipolar cells (Wässle, 2004). Although elevated levels of GABA have been reported in the vitreous of patients with proliferative DR (Ambati et al., 1997), assessment of GABA levels in preclinical DR has been inconsistent. Some studies have found accumulation of GABA, especially in Müller cells after 12 weeks of diabetes in STZ-induced diabetic rats, presumably due to a decrease in the activity of a major GABA degradation enzyme, GABA-transaminase (Ishikawa et al., 1996a, 1996b; Fletcher et al., 2007). Meanwhile, other results have suggested lower

retinal GABA content in STZ-induced rats due to reduction in the activity of GABA synthesizing enzyme, glutamate decarboxylase (Honda et al., 1998). Despite the conflicting results on GABA levels in early-stage DR, abnormal GABA signaling, coupled with signs of modulated GABA responses in diabetic retinas (Ramsey et al., 2007), may have functional significance. This is suggested by Ishikawa et al. in their work showing significant temporal relationship between increased retinal GABA contents and diminished OP responses in STZ diabetic rats (Ishikawa et al., 1996a).

Another intriguing candidate that may underlie the functional deficits in early-stage DR is the neuromodulator, dopamine (DA). As the eye is exposed to an enormous range of light intensity, the retina undergoes rapid dark or light adaptation to optimize its sensitivity and function under different light conditions. Retinal DA, synthesized and released by the dopaminergic amacrine cells, is crucial for modulating retinal circuitry to favor cone-driven pathways during the daylight and sensitizing rod-driven signals to enhance night vision under dim illumination (Witkovsky, 2004; Herrmann et al., 2011). Aberrations in the dopaminergic systems, in terms of both deficiency (e.g. Parkinson's disease and retinitis pigmentosa) and excess (e.g. schizophrenia and Tourette syndrome), have led to serious visual deficits (Brandies and Yehuda, 2008). So, what is happening to the dopaminergic system in early-stage DR? As early as 3 weeks post-STZ, diabetic rats have exhibited reduction in retinal DA levels (Nishimura and Kuriyama, 1985), though such finding has not been confirmed in the vitreous or retinal samples from human patients. Decrease in retinal DA content has been attributed mainly to decreased synthesis of DA, either due to decreased activity and/or level of rate-limiting enzyme, tyrosine hydroxylase (TH) (Fernstrom et al., 1984, 1986; Nishimura and Kuriyama, 1985; Seki et

al., 2004) or simply reduced number of surviving dopaminergic neurons due to diabetes-induced neurodegeneration (Gastinger et al., 2006). Although the evidence of altered DA levels is clear in early-stage DR, several key questions still need to be explored:

1. What is the functional significance of dopamine deficiency in early-stage DR?
2. Is deficiency in retinal DA content an underlying factor for the functional deficits or do the functional deficits originate from changes in the DA levels in the brain?
3. Can therapies targeting the dopaminergic system rescue or restore retinal and visual functions?

Although not discussed in this section, it is imperative to know that the effects of diabetes are not limited to only glutamatergic, GABAergic, and dopaminergic systems. Numerous studies have focused on effects of diabetes on melatonin (do Carmo Buonfiglio et al., 2011; Hikichi et al., 2011), taurine (Hansen, 2001; Yu et al., 2008; Zeng et al., 2010), substance P (Troger et al., 2001), and other neurotransmitters in the retina. Furthermore, diabetes can induce global changes in synaptic transmission [e.g. reducing synaptic proteins (VanGuilder et al., 2008)], impair post-retinal pathways [e.g. thinning of ganglion cell fiber layers (Oshitari et al., 2009; Cabrera DeBuc and Somfai, 2010)], and/or affect higher visual processing centers in the brain [e.g. abnormalities in visual cortex]. Taken together, these results show that the functional deficits in preclinical DR are likely due to direct effects of diabetes on the neural retina. If we can better understand the causal factors for the onset of these deficits, such changes may provide opportunities for earlier interventions.

1.4.3 Abnormal Hemodynamic Responses and Resulting Retinal Hypoperfusion

As the neural retina is a metabolically demanding tissue, retinal and visual dysfunctions found in early-stage DR could also result from abnormalities in retinal perfusion that lead to insufficient oxygen and nutrient delivery (Bursell et al., 1996; Ciulla et al., 2002; Clermont and Bursell, 2007; Pemp and Schmetterer, 2008; Curtis et al., 2009). Indeed, experimental studies have found signs of retinal hypoxia in early phases of diabetes. For instance, long-standing diabetic cats (>6 years of diabetes) display significantly lower retinal PO_2 levels than control cats (Linsenmeier et al., 1998). Others have found evidence of hypoxia within months of diabetes duration in rodents using the oxygen-dependent probe pimonidazole (de Gooyer et al., 2006a, 2006b; Ly et al., 2011). The suggestion of increased hypoxic load with pimonidazole staining in diabetic animals is strengthened by findings of up-regulation of hypoxia-inducible factor-1α (HIF-1α, a transcription factor known to be an early marker for hypoxia) in the same animal models (Mowat et al., 2010; Wright et al., 2010; Ly et al., 2011). Occurring even earlier, intravascular oxygen response to light flicker is abnormal in rats after four weeks of diabetes. The diabetic rats lack the flicker-induced increase in arterial PO_2 and PO_2 difference (arterial PO_2 - venous PO_2) observed in normal control rats (Blair et al., 2009). Moreover, diabetic patients with no retinopathy or minimal lesions show improved contrast sensitivity and color vision when breathing pure oxygen, suggesting that tissue hypoxia does occur early in DR (Harris et al., 1996). **E**lucidating the underlying mechanisms of early retinal hypoxia in DR may reveal preventative or therapeutic measures that can ameliorate this secondary insult to the neural retina function.

A highly plausible culprit for the observed hypoxia in early-stage DR is the pronounced reduction in functional hyperemic response, which has been consistently detected in diabetic patients without retinopathy (Garhofer et al., 2004; Storch et al., 2007; Bek et al., 2008; Mandecka et al., 2009; Nguyen et al., 2009; Pemp et al., 2009; Lecleire-Collet et al., 2011). Functional hyperemia is a hemodynamic response evoked by the central nervous system to increase local blood flow to regions of metabolically active neurons (Roy and Sherrington, 1890; Riva et al., 2005; Pournaras et al., 2008; Attwell et al., 2010; Newman, 2013). Classically, functional hyperemia is thought to be mediated by a metabolic feedback mechanism. The mechanism initiates with increased neuronal activity leading to a drop in energy reserves in active neurons and to the generation of metabolic signals that dilate nearby blood vessels. The resulting increased blood flow then provides additional oxygen and nutrients and replenishes the energy reserve of the neurons (Figure 1-8A) (Roy and Sherrington, 1890; Riva et al., 2005; Pournaras et al., 2008). However, persuasive evidence has emerged in recent years indicating a feedforward neurovascular (NV) coupling mechanism mediated by signaling from the neurons to the glial cells then onto the blood vessels (Figure 1-8B) (Metea and Newman, 2007; Koehler et al., 2009; Attwell et al., 2010; Newman, 2013). Therefore, insufficient functional hyperemic responses in DR could potentially arise from defects in the NV coupling cascade.

Although various molecules have been postulated as putative mediators of functional hyperemia, experimental evidence in diabetic animals has indicated imbalance in vasoactive metabolites of arachidonic acid as an underlying factor for the defective hyperemic response in diabetes (Figure 1-9). The involvement of arachidonic acid

metabolites in light-evoked vasodilatory response was first described by Metea and Newman (Metea and Newman, 2006). Using an *in vitro* preparation of isolated, intact rodent retina, they showed that photic stimulation of the retina leads to a cascade of signaling (for more info, see Figure 1-10) that induce the production of two types of arachidonic acid metabolites, epoxyeicosatrienoic acids (EETs) and 20-hydroxyeicosatetraenoic acid (20-HETE), which dilate and constrict vessels, respectively. Under physiologic conditions, the production of the vasodilators exceeds that of 20-HETE, and thus retinal activation results in vasodilation. They also discovered that nitric oxide (NO) modulates the activity of the enzymes responsible for the synthesis of EET and 20-HETE (Fleming, 2001; Roman, 2002). Specifically, EET production by epoxygenase is more sensitive to NO inhibition than 20-HETE production by ω-hydroxylase. Therefore, increased retinal NO levels, in a pathologic setting (i.e. diabetes), could suppress flicker-induced vasodilation (even though basal blood flow could potentially be augmented since NO is a potent vasodilator) (Figure 1-10). Complementing this hypothesis is the finding that increased NO abundance has been detected in early stages of DR, most likely due to the up-regulation of inducible NO synthase (iNOS) as a part of the inflammatory responses induced by diabetes (Goldstein et al., 1996; Carmo et al., 1999, 2000; Goto et al., 2005; Toda et al., 2007; Giove et al., 2009; Tummala et al., 2009; Zheng and Kern, 2009; Silva et al., 2010). Moreover, studies have found that inhibition of iNOS activity, both in *ex vivo* whole-mount diabetic retinal preparation and in chronic *in vivo* treatment of diabetic rats, restores the functional hyperemic response (Mishra and Newman, 2010, 2011). However, the temporal relationship and the causal linkage of the following events in early-stage DR still require

experimental confirmation: imbalance in arachidonic acid metabolites → defective functional hyperemia → retinal hypoxia → retinal and visual dysfunctions.

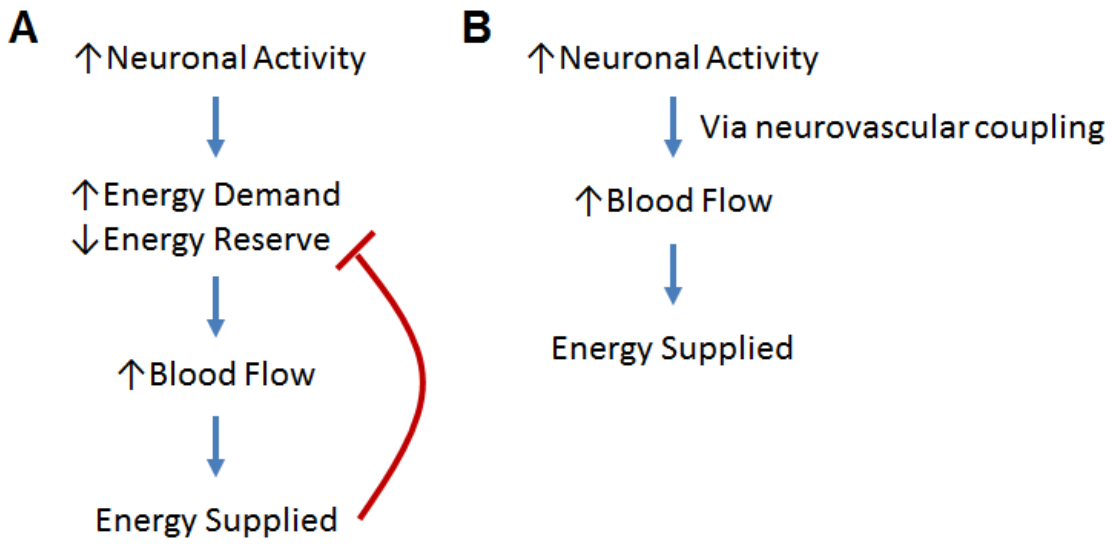

Figure 1-8. Schematics of the potential mechanisms underlying functional hyperemia. (A) The negative-feedback control hypothesis for the hyperemic response. A fall in energy level due to increased activity elicits an increase in blood flow to restore the depleted energy reserve. The fulfillment of the energy demand then causes a negative feedback to regulate the blood flow response. **(B)** The feedforward regulation hypothesis for functional hyperemia, in which the activated neurons, either directly or indirectly (via glial cells), induce increased blood supply to meet their metabolic need.

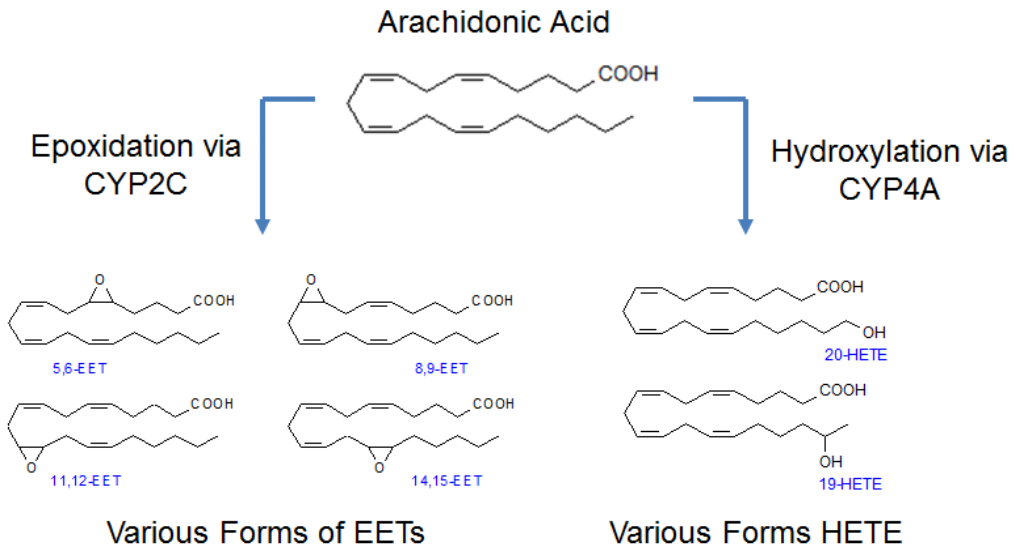

Figure 1-9. Synthesis pathways for the pertinent vasoactive arachidonic acid metabolites that are involved in functional hyperemia. Images of the molecular structure of the EETs and HETEs modified from the http://lipidlibrary.aocs.org/Lipids/eic_hete/index.htm with permission (Christie, 2013). Abbreviations used in the diagram: CYP = cytochrome P450 enzyme; EET = epoxyeicosatrienoic acid; HETE = hydroxyeicosatetraenoic acid.

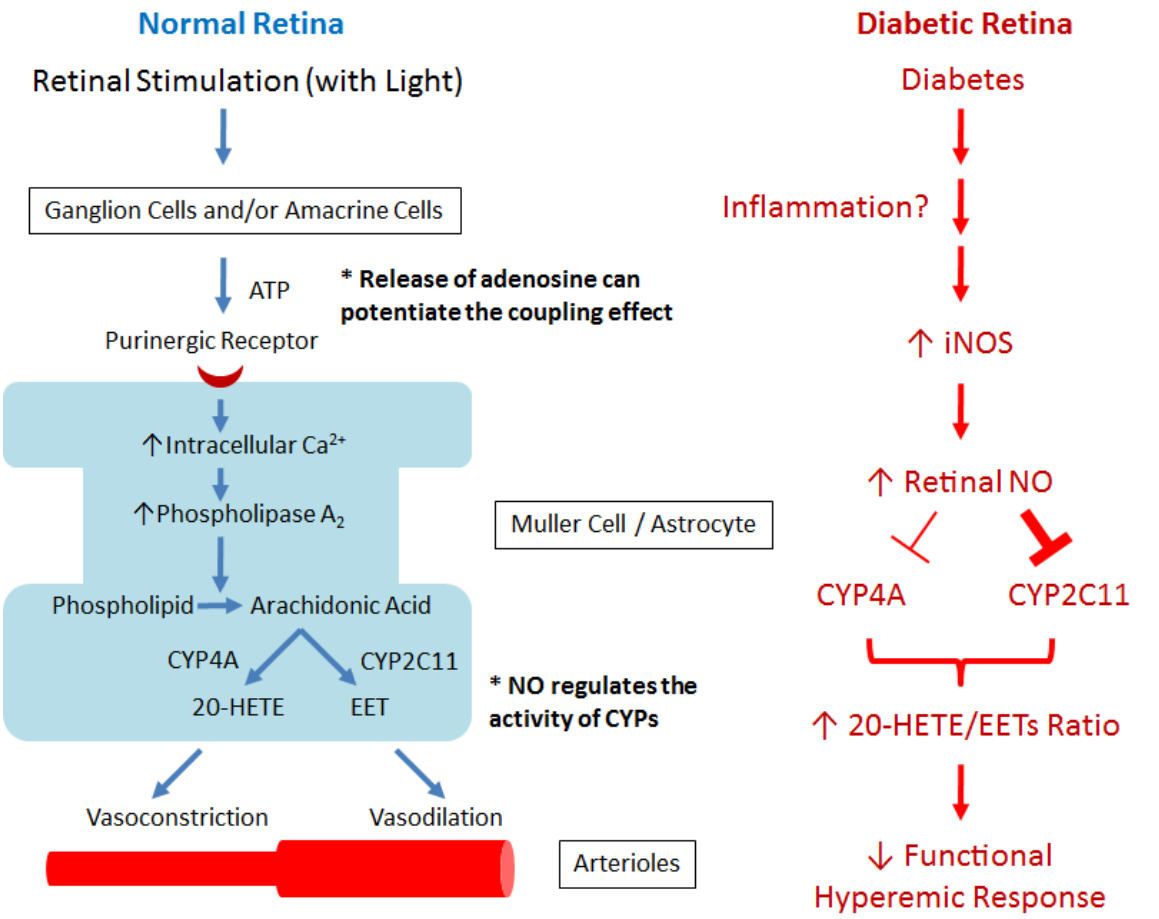

Figure 1-10. Proposed mechanism for arachidonic acid metabolites-mediated neurovascular coupling in the retina and how diabetes may disrupt its functioning. Under physiological conditions, the activated ganglion cells and amacrine cells are postulated to release ATP to nearby glial cells upon light stimulation. Activation of purinergic receptor on the glial cell membrane evokes an increase in the intracellular calcium level, leading to the generation of arachidonic acid. The arachidonic acid is then further metabolized into different vasoactive molecules, 20-hydroxyeicosatetraenoic acids (20-HETEs) and epoxyeicosatrienoic acids (EETs), which constrict and dilate vessels, respectively. [For a more complete review of the signaling cascade, please see (Metea and Newman, 2006, 2007; Newman, 2013)]. In a diabetic retina, there is an up-regulation of iNOS activity and protein levels, presumably due to inflammatory responses associated with diabetes. The resulting increase in retinal NO is hypothesized to cause an imbalance in the productions of 20-HETEs and EETs, such that the effects of 20-HETEs now outweigh those of EETs. Altered levels of 20-HETE and EETs ultimately lead to a diminished functional hyperemia response. Abbreviations used in the diagram: ATP = adenosine triphosphate; CYP = cytochrome P450 enzyme; EET = epoxyeicosatrienoic acid; 20-HETE = 20-hydroxyeicosatetraenoic acid; iNOS = inducible nitric oxide synthase; NO = nitric oxide; NT = neurotransmitter.

1.5 Thesis Overview

The main goals of my thesis are to examine the relationships between retinal dysfunction and visual deficits in early-stage DR and to determine the roles of DA dysregulation and defective functional hyperemia as underlying mechanisms of early diabetes-induced visual deficits. Three main studies, as listed below, were devised to fulfill the goals (Figure 1-11).

In Study 1 (described in Chapter 2), I investigated the hypothesis **that retinal dysfunction contributes to visual defects observed in early-stage DR**. To test this hypothesis, I first determined the temporal relationship between retinal alterations, as assessed with ERGs, and visual deficits, as assessed with optokinetic tracking (OKT) testing (for more info, please see Figure 1-12), by monitoring longitudinal changes in STZ-induced diabetic rats. I also examined the extent of lens opacity over the same disease course in the same animals to evaluate if cataract formation, a common complication of diabetes in humans, is an additional contributing factor to the vision loss. I then correlated ERG changes and cataract scores to the severities of visual deficits to examine the relative contributions of retinal dysfunction and cataract formation to visual defects in early stages of DR. In Study 2 and Study 3, I proceeded to experiments aimed at revealing potential underlying mechanisms for the early functional changes in DR.

For Study 2 (discussed in Chapter 3), I examined the hypothesis **that disruptions in the retinal dopaminergic system may underlie the early retinal and visual dysfunctions in DR.** To test this hypothesis, I first examined changes in retinal DA levels in STZ-induced diabetic animals (both rats and mice) due to diabetes. To establish the causal role of DA deficiency on the neuronal dysfunctions, I then evaluated the

effects of pharmacologically restoring retinal DA levels or directly activating DA pathways on the retinal and visual functions of diabetic animals. Similar pharmacological studies were also performed on a genetic mouse model of retinal DA depletion (by selectively knocking out the gene *tyrosine hydroxylase* only in the retina) to isolate the effects of retinal DA deficiency on retinal and visual functions.

In Study 3 (described in Chapter 4), I tested the hypothesis **that diabetes-induced loss of functional hyperemia is an additional underlying mediator for the early neuronal deficits and the imbalance in the levels of vasoactive arachidonic acid metabolites is the main effector for the diminished flicker-induced vasodilation response.** To test this hypothesis, I first delineated the temporal correlations between insufficiency in functional hyperemia and functional deficits in STZ-induced diabetic rats. To further establish the causal relationship between impairment in NV coupling and the deficits in retinal and visual functions in early-stage DR, I examined the potential benefits of pharmacologically manipulating 20-HETE and EETs levels (with the goal of enhancing hyperemic responses) on the retinal and visual functions of diabetic animals.

In summary, the importance of recognizing and treating neuronal damage early in the course of DR underscore the potential clinical relevance of this study. The discovery of novel mechanisms underlying early diabetes-induced visual deficits in this thesis work could also aid future development of diagnostic tools and therapies targeting these early changes, with the hope of slowing the disease progression and preventing the severe vision loss associated with late-stage vasculopathy in DR.

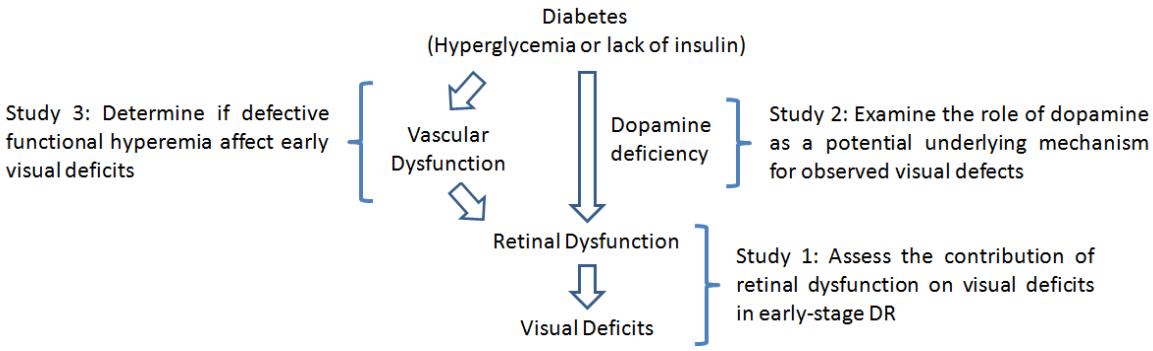

Figure 1-11. Outlines of the proposed studies and the corresponding hypotheses tested for the thesis project.

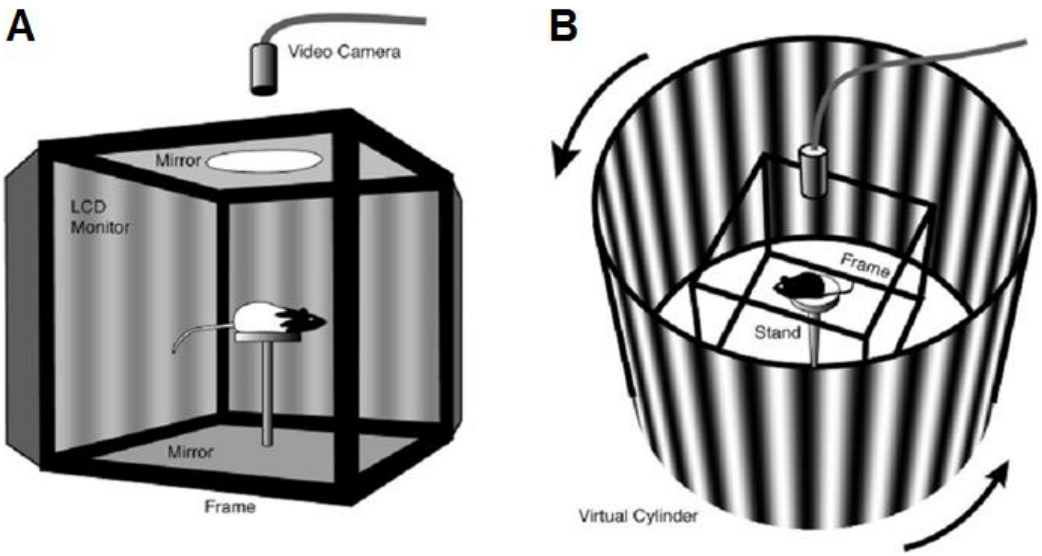

Figure 1-12. Configuration of the virtual optomotor system to assess optokinetic response. (A) Side view of the testing chamber comprised of four computer monitors. Awake, unconstrained animal sits on a pedestal in the middle and its behavior is monitored in real-time by the experimenter with the video camera from above. **(B)** Diagram of how optokinetic stimuli are delivered to the animal. The animal is exposed to sine wave gratings rotating at a speed of 12 deg/sec. Tracking is considered when the animal makes reflexive head movement in response to the rotating gratings in the same direction. Both spatial frequency thresholds and contrast sensitivity function of the animal can be determined using this apparatus. Image taken from http://www.cerebralmechanics.com/how-optomotry-works/ with permission.

CHAPTER 2: ASSOCIATIONS BETWEEN EARLY RETINAL ALTERATIONS AND VISUAL DEFICITS IN STREPTOZOTOCIN-INDUCED DIABETIC LONG EVANS RATS

This chapter was originally published as an article in *Investigative Ophthalmology & Visual Science:*

Aung MH, Kim MK, Olson DE, Thule PM, and Pardue MT. Early visual deficits in streptozotocin-induced diabetic long evans rats. *Investigative Ophthalmology & Visual Science* 2013 54:1370–1377.

2.1 Abstract

Purpose: While diabetic retinopathy (DR) is clinically diagnosed based on vascular pathology, diabetic patients with angiographically normal retinas have been found to exhibit subtle defects in vision. This has led to the theory that diabetes-associated metabolic abnormalities directly impair neural retinal function prior to the development of vasculopathy, thereby resulting in visual deficits. In this study, we sought to delineate the temporal relationship between retinal dysfunctions and visual deficits in a rat model of Type I diabetes. Moreover, we investigated the relative contribution of retinal dysfunction versus diabetes-induced lens opacity, to the visual deficits found in early-stage DR.

Methods: Pigmented Long Evans rats were rendered diabetic with streptozotocin (STZ). Control and diabetic rats were assessed across 12 weeks of hyperglycemia for visual

function with optokinetic tracking (weekly visual acuity and monthly contrast sensitivity), retinal function with dark-adapted electroretinograms (monthly ERGs), and cataract formation with slit lamp exam (biweekly).

Results: Diabetic rats exhibited significantly reduced visual functions and delayed ERG responses by 1 month post-STZ. Significant cataracts did not develop until 6 weeks post-STZ. Moreover, increases in lens opacity (r=-0.728) and ERG implicit time (r=-0.615 for rod-dominated response and r=-0.322 for rod/cone mixed response) showed significant correlations with reductions in visual acuity in diabetic rats.

Conclusions: STZ-induced hyperglycemia reduces visual function, affecting both visual acuity and contrast sensitivity. The data suggest that visual defects found in early-stage DR may initially involve abnormalities of the neural retina and worsen with later development of cataracts.

2.2 Introduction

Diabetic retinopathy (DR) is a common complication of diabetes mellitus and a leading cause of blindness in working-age adults (Congdon et al., 2003; Klein, 2007). Progressive vision loss after the diagnosis of DR has been associated with the severity of lesions in the retinal vasculature, such as hemorrhages, macular edema, and neovascularization (Jackson and Barber, 2010). Unfortunately, by the time these vascular lesions are identified, vision loss is often advanced and irreversible. Interestingly, some studies have found that diabetic patients with angiographically normal retinas experienced subtle visual dysfunctions, including abnormal color vision and decreased contrast sensitivity (Kawasaki et al., 1986; Greenstein et al., 1990; Hardy et al., 1992; Ghirlanda et al., 1997; Jackson and Barber, 2010). Since preventing vision loss is an

important therapeutic goal for diabetic patients, detecting visual deficits at preclinical stages of DR may provide an early window for diagnosis and intervention.

To determine the temporal appearance of visual dysfunction in diabetes, it is important to establish to what degree animal models of diabetes replicate visual defects found in diabetic patients. An effective behavioral test of visual performance in animals is the assessment of optokinetic response, the ability of an animal to track moving stimuli by moving its head (Thomas et al., 2004; Douglas et al., 2005). Both visual acuity and contrast sensitivity can be measured by varying spatial frequency or contrast of the projected gratings. Assessment of optokinetic tracking (OKT) response with head movement has been reliably quantified in rodents (Prusky et al., 2000, 2004; Thomas et al., 2004; Douglas et al., 2005) and can readily distinguish mice with normal vision from those with retinal degeneration (Thaung et al., 2002). A recent report using OKT to evaluate visual function of streptozotocin (STZ)-induced diabetic rats found reductions in visual acuity at 4 weeks post-STZ, which the authors attributed to reduced expressions of visual cycle enzymes (Kirwin et al., 2011). However, it remains unclear how the changes in visual function correlate with the more commonly reported changes in electroretinogram (ERG), an indicator of diabetes-induced retinal dysfunction.

Since the observation of diminished and delayed oscillatory potentials (OPs) in diabetic patients in the 1960's, alterations in ERG response have been consistently found in both humans and animals with diabetes, even prior to the appearance of vascular lesions (Bresnick and Palta, 1987; Holopigian et al., 1992; Shirao and Kawasaki, 1998; Fortune et al., 1999; Li et al., 2002; Bearse et al., 2006; Kizawa et al., 2006; Fletcher et al., 2007; Kohzaki et al., 2008; Wolff et al., 2010; Lecleire-Collet et al., 2011; Ly et al.,

2011). Moreover, multiple reports have established that changes in the multifocal ERG are predictive of DR onset and progression of DR (Bearse et al., 2006; Harrison et al., 2011). Factors underlying ERG changes associated with diabetes may include neuronal dysfunctions [such as decreases in synaptic proteins (VanGuilder et al., 2008) or changes in the levels of various neurotransmitters (Nishimura and Kuriyama, 1985; Northington et al., 1985; Gastinger et al., 2006)] and cell deaths in the neural retina (Barber, 2003; Martin et al., 2004; Fletcher et al., 2007, 2010; Villarroel et al., 2010; Barber et al., 2011). Although visual acuity deficits in early DR may be secondary to retinal dysfunction, the possibility exists that induced lens opacity may contribute to visual loss as epidemiological studies have revealed increased prevalence of cataracts in diabetic patients when compared with non- diabetic population (Obrosova et al., 2010). Thus, a better characterization of the roles of diabetes-associated cataract formation and retinal dysfunction on visual impairment is needed. Therefore, the purposes of this study are (1) to examine longitudinally changes in both visual acuity and contrast sensitivity in a Type I diabetic rat model, and (2) to evaluate relative contribution of cataracts and retinal dysfunction to early visual deficits in our model.

2.3 Materials and Methods

2.3.1 Animals and Experimental Design

Male Long Evans rats (200-225 g; Charles River, Wilmington, MA) were housed in shoe-box cages on a 12:12 light:dark cycle with chow and water provided *ad libitum*. All procedures were approved by the Atlanta VA Institutional Animal Care and Use Committee and conformed to the ARVO Statement for the Use of Animals in Ophthalmic and Vision Research.

Hyperglycemia was induced with a single intravenous injection of streptozotocin (STZ: 100 mg/kg; Ferro Pfanstiehl Laboratories, Waukegan, IL) dissolved in citrate buffer/50% glucose solution (8:1 ratio), and control (CTRL) rats were injected with vehicle alone (Thulé et al., 2006). Diabetes was defined as two successive daily blood glucose levels >250 mg/dL (Freestyle hand-held blood glucose meter from tail-prick blood), which routinely occurred 2-3 days after STZ injection. Body weights and blood glucose were monitored 2-3 times per week. Diabetic (DM) rats were treated with small pellets of sustained-release subcutaneous insulin (Linplant; Linshin Canada, Scarborough, ON, Canada) at a dose sufficient to prevent excessive weight loss and catabolic response but insufficient to control hyperglycemia (Thulé et al., 2006). For our first set of animals (n=6 per group), visual acuity threshold was assessed weekly, contrast sensitivity was measured monthly (± one week), and cataract exam was evaluated biweekly for 12 weeks. A second set of CTRL and DM animals (n=8 per group) underwent monthly ERG recordings to assess retinal function. We also examined their visual acuity weekly and lens clarity biweekly to ensure that these animals exhibited similar phenotypes to our first set of animals. As responses were similar for both right and left eyes, only the responses from the right eye for each animal are reported here.

2.3.2 Visual Function Tests

Visual function of each rat, without movement restriction, was tested using the virtual optokinetic system (OptoMotry system; Cerebral-Mechanics, Lethbridge, AB, Canada), as previously described (Douglas et al., 2005). Briefly, the rat was placed on a platform at the center of a virtual-reality chamber composed of four computer monitors that display vertical sine wave gratings rotating at a speed of 12 deg/s. The experimenter

monitored the rat in real-time through a video camera positioned above the animal and noted the presence or absence of reflexive head movements (tracking) in response to the rotating gratings in the same direction. The experimenter also manually tracked the head of the rat to align the center of the virtual cylinder to the viewing position of the rat. For visual acuity assessment, the grating started at a spatial frequency of 0.042 cyc/deg with 100% contrast. The acuity threshold was determined automatically by the OKT software using a staircase paradigm based on observations of head-tracking movements. Similarly, the contrast sensitivity threshold was determined by reducing the contrast of the black and white gradients from 100% in a staircase paradigm until animal head-tracking movements were no longer observed. Contrast sensitivity was measured at the spatial frequency of 0.064 cyc/deg for the study. This was the spatial frequency that elicited the maximum sensitivity obtained from the rats at baseline when a contrast sensitivity curve was assessed across five spatial frequencies (0.031, 0.064, 0.092, 0.103, and 0.119 cyc/deg). The contrast sensitivity was calculated as a reciprocal of the Michelson contrast from the screen's luminance [i.e. (maximum + minimum) / (maximum – minimum)], as previously described(Prusky et al., 2006).

2.3.3 Cataract Examination and Scoring

After dilating the pupils of unanesthetized animals with 1% tropicamide, a researcher (blinded to the treatment condition) examined the animals for the presence of lens opacification by using slit lamp illumination and graded the severity based on a cataract grading scale as described in Muranov et al (Muranov et al., 2004). Briefly, the classifications are as follows: Grade 0 – a clear lens; Grade 1 – swollen fibers and subcapsular opacities; Grade 2 – nuclear cataract in lens and swollen fibers in lens cortex;

Grade 3 – severe nuclear cataract with perinuclear area opacity in lens; Grade 4 – total opacity of lens. To ensure equivalent assessment of the cataract severity for each observation, the slit lamp illumination was standardized to the same slit width and light intensity for all examinations.

2.3.4 Retinal Function Test with ERG

Rats were dark-adapted overnight and then prepared under dim red illumination as previously described (Ciavatta et al., 2009). In brief, rats were anesthetized [ketamine (60 mg/kg) and xylazine (7.5 mg/kg)], pupils dilated (1% tropicamide), and the corneal surface anesthetized (0.5% tetracaine HCl). Using custom-made DTL fiber electrode, responses were recorded to flash stimuli presented in order of increasing luminance using a signal averaging system (UTAS BigShot; LKC Technologies, Gaithersburg, MD). ERG stimuli consisted of a 12-step dark-adapted series (-3.4 to 2.1 $\log \cdot cd \cdot s/m^2$) to isolate rod-dominated and rod/cone mixed responses. After testing, rats received yohimbine (2.1 mg/kg) to reverse the effects of xylazine and prevent corneal ulcers (Turner and Albassam, 2005).

Amplitudes and implicit times were measured for both a- and b-waves. Oscillatory potentials (OPs) were digitally filtered using the ERG system software (75-500 Hz; EM Version 8.1.2, 2008; LKC Technologies, Gaithersburg, MD). The amplitudes and implicit times of individual OP1 through OP4 were determined, but only OP2 and OP4 results are reported here.

2.3.5 Statistical Analysis

Statistical analysis was performed using statistical software (SigmaStat 3.5, Aspire Software International, Ashburn, VA). Two-way repeated-measures ANOVA was

used to compare treatment groups across time-points after STZ injection. Post-hoc multiple comparisons were performed when appropriate using the Holm-Sidak method. All statistics reported are the two-way repeated-measures ANOVA interaction effect, unless otherwise noted. For correlation analysis, relationship between visual acuity and ERG implicit time was determined using Pearson's product-moment correlation coefficient while relationship between visual acuity and cataract score was determined using Spearman's rank correlation coefficient. All analyses were performed with significance set at $p<0.05$.

2.4 Results

Average weights and blood glucose levels for both CTRL and DM groups at baseline and by the end of the 12-week study are summarized in Table 2-1. Although the two treatment groups were indistinguishable at baseline, DM rats were smaller than CTRL rats [post-hoc analysis, $p<0.001$] and had higher blood glucose levels [post-hoc analysis, $p<0.001$] at the 12-week time-point. Moreover, DM rats were hyperglycemic (all values >250mg/dl) throughout the 12-week study (data not shown).

Set	Treatment Group	n	Baseline		12 weeks post-STZ	
			Weight (g)	BG (mg/dl)	Weight (g)	BG (mg/dl)
1	Control (CTRL)	6	340 ± 15	129 ± 6	587 ± 23	120 ± 6
	Diabetic (DM)	6	319 ± 16	128 ± 1	392 ± 15	557 ± 22
2	Control (CTRL)	8	211 ± 5	144 ± 8	578 ± 18	119 ± 2
	Diabetic (DM)	8	226 ± 5	131 ± 3	382 ± 13	538 ± 32

Table 2-1. Average weight and blood glucose levels of the two treatment groups (± SEM) for the two sets of experiments. In both sets, both treatment groups gained significant weight by the end of the study [Main Duration Effect: $p<0.001$], but DM rats were significantly smaller than CTRL rats and had significantly higher BG levels [$p<0.001$]. Abbreviations used in the table: BG = blood glucose; n = sample size.

2.4.1 Diabetes resulted in profound visual deficits

To assess the effects of sustained hyperglycemia on visual function, we measured visual acuity weekly and contrast sensitivity monthly. Although CTRL and DM groups had similar visual acuity thresholds at baseline to those reported previously in Long Evans rats (Douglas et al., 2005), DM rats had significantly reduced visual acuity levels as early as 3 weeks post-STZ compared to CTRL rats [Figure 2-1A, $F(9,119)=6.802$, $p<0.001$]. The deficits in visual acuity threshold worsened with duration of hyperglycemia, starting with 22% reduction (in comparison to CTRL group) at 3 weeks post-STZ and deteriorating to 70% reduction at 12 weeks post-STZ. Additionally, DM rats showed a significant decrease in contrast sensitivity after 9 weeks post-STZ [Figure 2-1B, $F(3,47)=4.426$, $p=0.011$]. Similarly, the decline in contrast sensitivity worsened with hyperglycemic duration, starting with 34% reduction at 5 weeks post-STZ and reaching 72% reduction by the end of the study. Collectively, these data show the presence of visual dysfunction at preclinical stages of DR in a rat model of Type 1 diabetes.

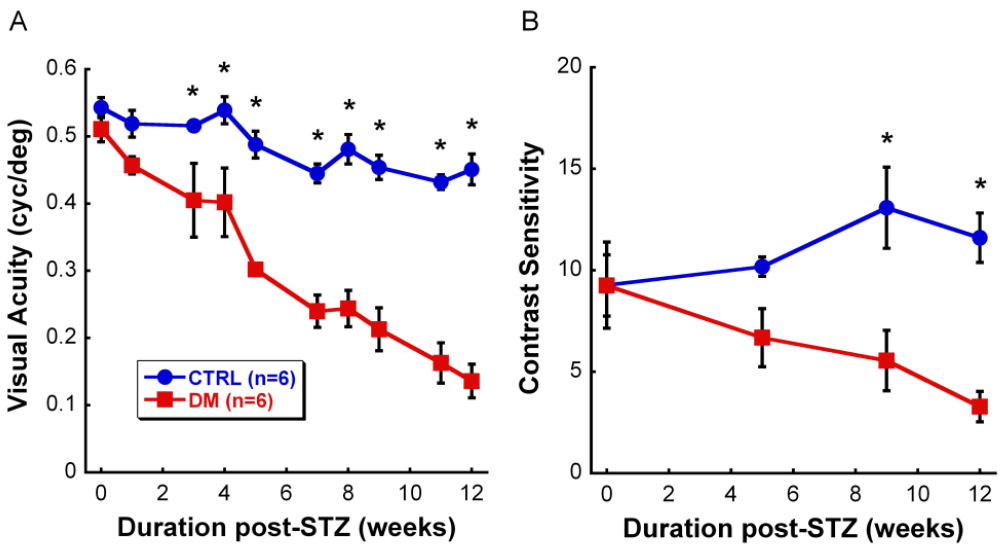

Figure 2-1. Reduced visual function due to hyperglycemia over the 12-week study. (A) Significantly reduced visual acuity (22%) was observed in DM rats starting at 3 weeks post-STZ [$p<0.001$] when compared to CTRL rats, and continued to decrease with disease duration. **(B)** Contrast sensitivity at 0.064 cyc/deg spatial frequency was reduced in DM rats starting at 9 weeks post-STZ [$p=0.011$] when compared to CTRL rats, and worsened with disease progression. Although the deficit seemed to appear at 5 weeks post-STZ, the change was not statistically significant. Data shown are Mean ± SEM. Asterisks represent significant post-hoc comparisons, $p<0.05$.

2.4.2 Cataract formation impaired visual functions in diabetic animals

To evaluate the possibility of early cataract formation contributing to the diminished vision, each rat was examined for lens opacity biweekly. While some DM rats developed mild cataracts starting at 4 weeks, the average cataract score of the DM group was not significantly greater than the CTRL group until 6 weeks post-STZ [Figure 2-2, $F(8,107)=7.136$, $p<0.001$]. The clarity of the lens also worsened with the duration of hyperglycemia, gradually increasing from a score of 0.83 at 6 weeks post-STZ to a score of 1.92 at 12 weeks post-STZ.

To determine the relative contribution of cataracts to visual deficits of the DM rats, we stratified the DM animals based on the presence or absence of cataracts at 4 and 8 weeks post-STZ. No stratification was done at 12 weeks post-STZ as all DM rats developed significant cataracts by that time-point. Figure 2-3A shows that the three groups had significantly different visual acuity thresholds [Main Treatment Effect: $F(2, 23)=49.186$, $p<0.001$]. DM rats with any form of cataracts had the worst acuities [post-hoc analysis, $p<0.001$]. More importantly, DM rats without cataracts also had significantly lower visual acuity values than CTRL animals [post-hoc analysis, $p<0.001$], but higher than those with cataract [post-hoc analysis, $p<0.01$]. Figure 2-3B shows that the three groups also had significantly different contrast sensitivity levels [Main Treatment Effect: $F(2, 23)=6.263$, $p=0.02$]. CTRL rats had the highest sensitivities when compared to the two stratified DM groups [post-hoc analysis, $p<0.05$]. Interestingly, cataract development in DM rats did not seem to further reduce contrast sensitivity as there was no significant difference in the sensitivity between DM rats that did develop cataracts and those that did not [post-hoc analysis, $p=0.788$]. This finding not only

provides additional evidence of other contributing factor(s), aside from cataract, to the early visual dysfunction in DR, but also suggests that visual acuity seems more susceptible than contrast sensitivity to disruption due to cataract formation.

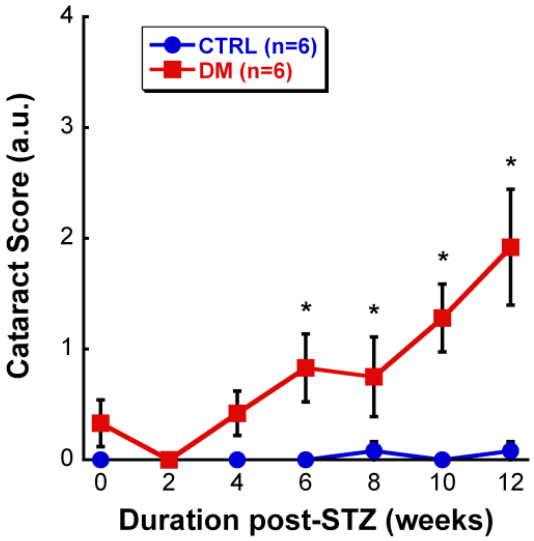

Figure 2-2. Cataract scores for CTRL and DM groups over time. At 6 weeks post-STZ, DM animals had significantly higher cataract scores in comparison to CTRL rats [$p<0.001$]. Moreover, the cataract worsened over the course of the study. Data shown are Mean ± SEM. Asterisks represent significant post-hoc comparisons, $p<0.05$.

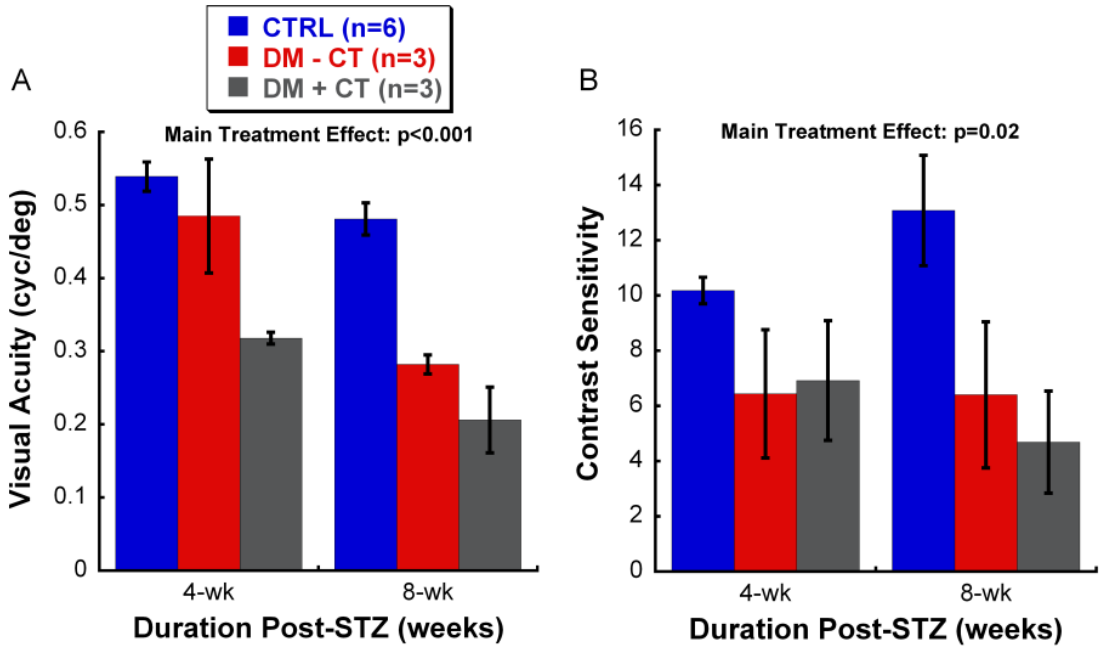

Figure 2-3. Stratification of visual acuity (A) and contrast sensitivity (B) of DM animals based on the presence or absence of cataract. For visual acuity **(A),** a significant difference between the groups was found [Main Treatment Effect: $p<0.001$] such that visual acuity decreased with the presence of hyperglycemia (DM-CT group) and further reduced by the addition of cataract (DM+CT group). These results indicate that other factor(s) besides optical opacity due to diabetes contribute to the reduction of visual function. For contrast sensitivity **(B)**, CTRL rats had the highest thresholds among the three groups examined [Main Treatment Effect: $p=0.02$]. We did not observe a further reduction in contrast sensitivity of DM rats due to cataract formation. Data shown are Mean ± SEM. Abbreviation used in the figure: CT = presence of cataract.

2.4.3 Retinal dysfunction may be a potential contributor to early visual deficits

ERG responses, cataract formation, and visual acuity values were measured in a different set of CTRL and DM animals to further correlate retinal dysfunctions to early visual deficits in DM rats. DM rats in this group also showed a significant reduction in their visual acuity starting at 1 month post-STZ and developed significant cataracts by 6 weeks post-STZ (data not shown). Serial ERGs obtained in this second set of rats revealed that both amplitudes and implicit times of a- and b-waves did not differ consistently between CTRL and DM animals over the experimental period (data not shown). However, consistent with previous ERG studies, DM animals displayed robustly delayed OP responses starting at 4 weeks post-STZ (Figure 2-4) (Li et al., 2002; Kohzaki et al., 2008). Figure 2-4 shows a summary of OP2 and OP4 implicit times from 4 to 12 weeks after hyperglycemia at representative dim (-1.8 log·cd·s/m^2) and bright (0.6 log·cd·s/m^2) flash stimuli. Significant delays in OP2 (Figure 2-4C) and OP4 (Figure 2-4E) implicit times were found under dim stimulus stimulation, as early as 8 weeks post-STZ for OP2 [$F(2, 42)=5.417$, $p=0.012$] and 4 weeks post-STZ for OP4 [$F(2,42)=3.809$, $p=0.037$]. Moreover, the deficit worsened significantly with the duration of hyperglycemia, especially for OP4, increasing from 7% delay (in comparison to CTRL group) at 4 weeks post-STZ to 19% delay at 12 weeks post-STZ. In contrast, we observed no difference between CTRL and DM responses for OP2 in response to bright stimuli (Figure 2-4D) and OP4 revealed a non-progressive delay (on average 8%) due to DM treatment [Figure 2-4F, Main Treatment Effect: $F(1, 43)=9.060$, $p=0.008$].

Figure 5 presents correlation analyses of the visual acuity of each animal against its corresponding cataract score and OP4 responses (elicited with either dim or bright

flash) over the course of the study. Regardless of treatment conditions, cataract severity correlated strongly with visual acuity [Figure 2-5A, Spearman Rank Order: $r=-0.728$, $p<0.0001$]. More interestingly, changes in visual acuity also correlated significantly with OP4 latency (Figure 2-5B and 2-5C), whether collected from rod-dominated responses [Pearson Product: $r=-0.615$, $p<0.0001$] or mixed rod/cone responses [Pearson Product: $r=-0.322$, $p=0.04$]. However, it is important to note that only DM rats, not CTRL rats, maintained the correlation between OP4 implicit times and visual acuities when we separated animals based on their disease state (data not shown). Moreover, it is interesting to note the segregation of the two treatment groups (CTRL vs. DM) on all the scattered plots, demonstrating the effects of hyperglycemia on cataract formation, retinal function, and OKT responses (Figure 2-5).

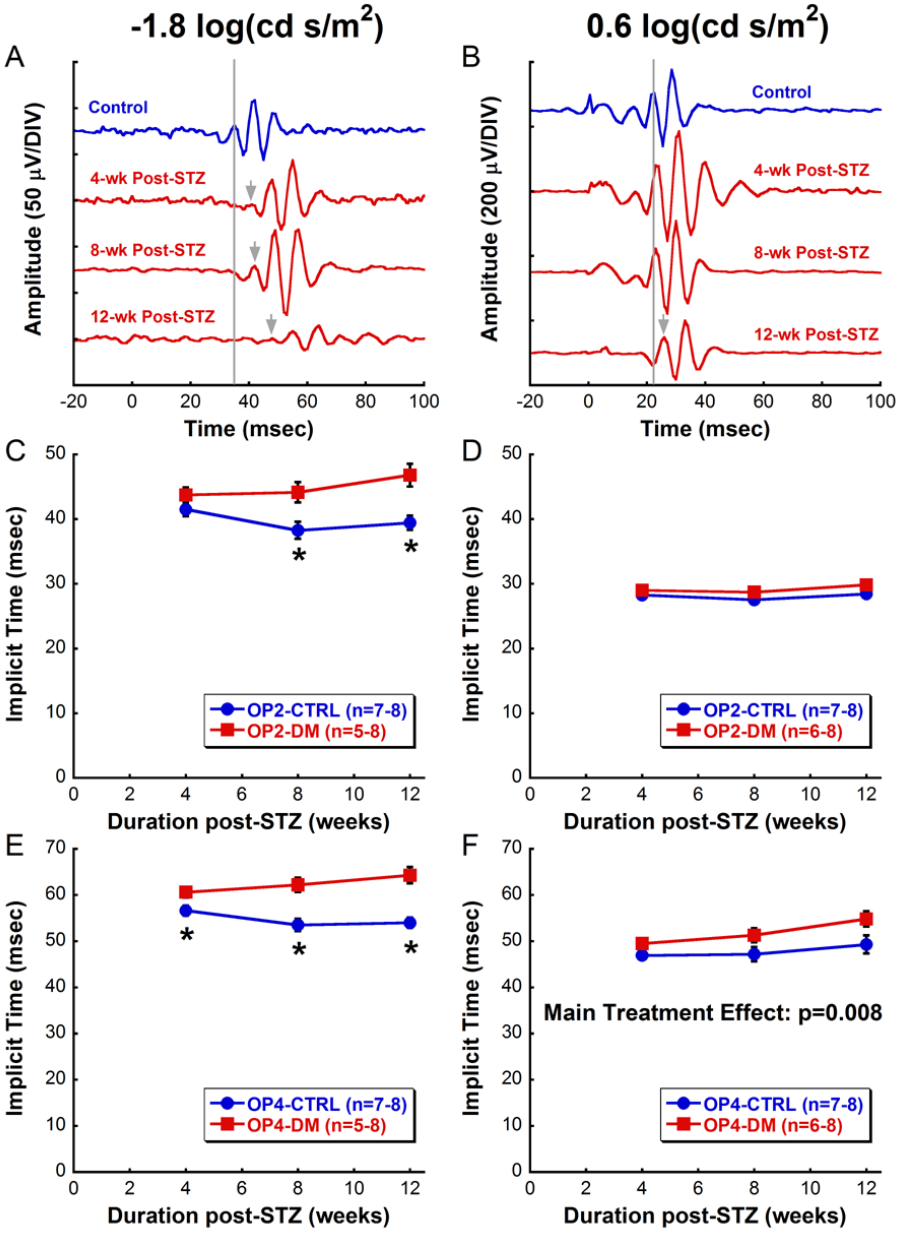

Figure 2-4. Retinal dysfunction due to diabetes. (A, B) Representative OP waveforms to a dim-flash **(A: -1.8 log·cd·s/m^2)** or bright-flash **(B: 0.6 log·cd·s/m^2)** stimulus from a CTRL rat (**blue**) at 4-week time-point and a DM rat (**red**) at 4-week, 8-week, and 12-week time-points. The grey lines indicate the peak of OP1 in the CTRL rat, while the grey arrows indicate the peak of OP1 in the diabetic rat when delayed. **(C, D)** Average OP2 implicit times (± SEM) in response to dim flash **(C)** and bright flash **(D)** over the 12-week study. As early as 8 weeks post-STZ, OP2 of the DM group showed a significant delay in comparison to that of the CTRL group in response to only dim stimulus [p=0.012]. **(E, F)** Average OP4 implicit times (± SEM) in response to dim flash **(E)** and bright flash **(F)** over the 12-week study. OP4 of DM group in response to dim flash displayed a significant delay at 4 weeks post-STZ [p=0.037]. In contrast, OP4 elicited with bright flash showed only a main treatment effect between CTRL and DM groups [Main Treatment Effect: p=0.008]. Data shown are Mean ± SEM. Asterisks represent significant post-hoc comparisons, $p<0.05$.

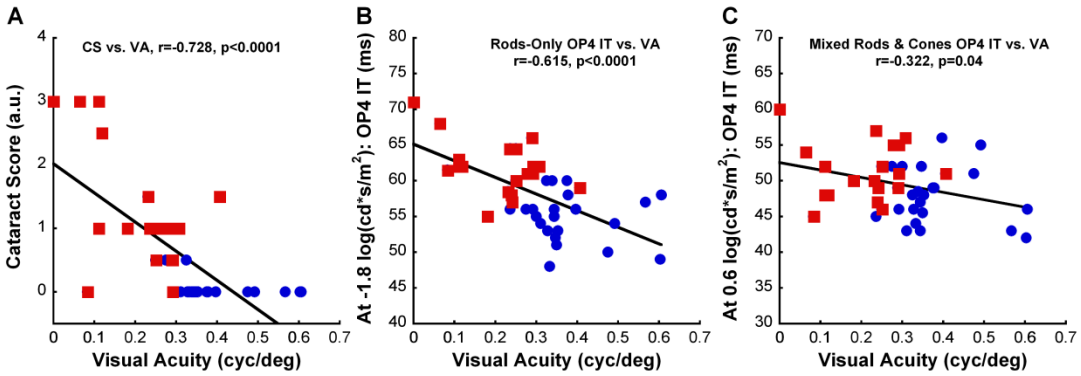

Figure 2-5. Scatter plots of visual acuity threshold against corresponding (A) cataract score, (B) dim-flash OP4 latency, and (C) bright-flash OP4 latency for CTRL (n=7-8) and DM (n=5-8) rats at 4 weeks, 8 weeks, and 12 weeks post-injection. As expected, the visual acuities of our animals significantly correlated to their respective cataract scores [Spearman Rank Order: $p<0.0001$]. More interestingly, changes in visual acuity also significantly correlated with OP4 implicit times elicited from rod-dominated response [Pearson Product: $p<0.0001$] and mixed rod/cone response [Pearson Product: $p=0.04$] conditions. The **blue circle** symbols represent data points for CTRL animals while the **red square** symbols represent data points for DM animals. Abbreviations used in the figure: CS = cataract score; IT = implicit time; r = correlation coefficient; VA = visual acuity.

2.5 Discussion

The present study detected abnormalities in visual acuity and contrast sensitivity in STZ-induced DM rats prior to expected onset of diabetes-associated retinal vascular lesions (Figure 2-6), such as vascular leakage, pericyte dropout, and acellular capillaries (based on published studies: Lorenzi and Gerhardinger, 2001; Curtis et al., 2009; Barber et al., 2011) Some of this early visual loss can be attributed to the development of cataract. However, significant decreases in visual acuity and contrast sensitivity were also found in DM rats with no signs of cataract, suggesting that other factor(s) contributed to decreased visual function. We hypothesize that early visual deficits may result from retinal dysfunction due to STZ-induced hyperglycemia or hypoinsulinemia. Supporting this hypothesis, we found that DM rats exhibited delayed ERG responses, specifically in OP implicit times (indicative of inner retinal dysfunction), at 4 weeks post-STZ, which was the time-point when the DM rats first displayed visual deficits. Similar to our previous findings, the ERG abnormalities were most prominent and consistent under scotopic condition, suggesting rod pathways are more susceptible to diabetic insults (Kim, MH et al. *IOVS* 2008; 49: ARVO E-Abstract 2212). In addition, according to our correlation analyses, visual acuity declines among DM rats were associated with ERG changes elicited by both dim and bright flashes. Interestingly, we also observed that early scotopic ERG changes were associated with diminished scotopic OKT responses, with scotopic visual function declining one week earlier than photopic visual function (data not shown). Collectively, the results of this study suggest that visual deficits in the early-stage DR rat model are initially related to retinal dysfunction then subsequently worsen with the formation of cataracts.

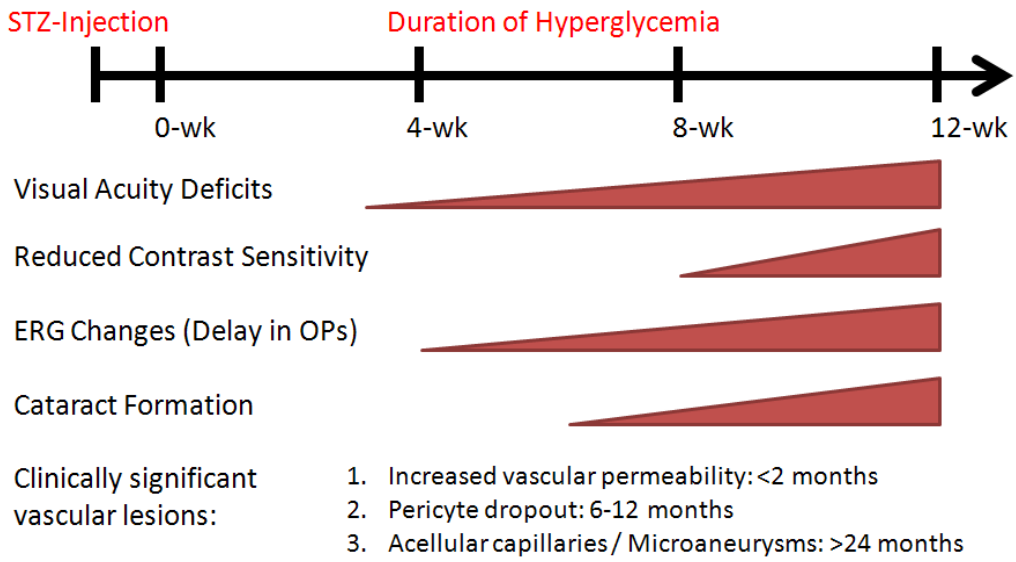

Figure 2-6. Chronological summary of the functional deficits found in our study. The onsets of clinically significant vascular lesions listed were estimates based on published reports on STZ-induced diabetic rat model (Lorenzi and Gerhardinger, 2001; Curtis et al., 2009; Barber et al., 2011).

2.5.1 Cataract and Visual Dysfunction in Early-stage DR

The effects of cataracts on early visual loss in diabetes have been observed in insulin dependent diabetic (IDDM) patients without clinically diagnosed retinopathy (Hardy et al., 1992, 1994). In these studies, the authors noted that color discrimination is abnormal in uncomplicated IDDM patients before the onset of vascular retinopathy. More interestingly, while IDDM patients with increased lens optical density had the worst visual deficit, IDDM patients with clear lenses also had abnormal color discrimination when compared to age-matched control subjects, suggesting underlying retinal dysfunction. Although diabetes-induced cataracts and their effects on visual function are well-documented (Bron and Cheng, 1986), findings from this study reinforce the importance of other underlying factor(s) in contributing to the visual deficits in preclinical stages of DR. Further studies are needed to determine the exact contribution of ocular opacity on visual function, independent of diabetes-induced neuronal defects.

2.5.2 Current OKT Findings on Animal Models of Diabetes

Report by Kirwin et al. has similarly found decreased visual acuity in STZ-induced diabetic rats at 4 weeks post-STZ (Kirwin et al., 2011). Kirwin et al. performed microarray analysis over several time-points post-STZ and revealed that expression levels of several genes encoding visual cycle proteins, such as retinal pigment epithelium-specific protein 65 kDa, were down-regulated. They concluded that OKT deficits in their animals were most likely due to direct hyperglycemic insult on the neural retina. Further supporting the hypothesis of a neuronal pathology in early stages of DR, we found similar onsets of inner retinal dysfunction, as measured with ERG alterations, and decreasing visual function. Interestingly, Kirwin et al. also observed some rats with

cataracts at 6 weeks post-STZ, though contrary to our results, they did not find that cataracts significantly affected visual acuity. It is possible that the impact of cataracts on visual acuity may have reached significance if these diabetic rats had been examined at later time-points.

A more recent study that examined both visual acuity and contrast sensitivity in a different Type 1 diabetic model, $Ins2^{Akita}$ mice, showed reduction in both aspects of vision after developing diabetes for 4-5 months (Akimov and Rentería, 2012). Similar to our study, the authors also found progressive worsening of visual dysfunction with increasing duration of hyperglycemia. Although the authors did not conduct further functional or mechanistic experiments, they also hypothesized retinal pathology as a major contributor for the early visual deficits in $Ins2^{Akita}$ mice. The finding of visual deficits in $Ins2^{Akita}$ mice has been replicated in a separate study that examined the changes in visual function and ocular blood flow in this diabetic mouse model (Muir et al., 2012).

2.5.3 Retinal Origins of Visual Defects in Diabetes

OKT is a reflex response that does not rely on the visual cortex (Douglas et al., 2005), but rather depends on the accessory optic system (AOS) (Schiller, 2010). AOS originates from the retina, with direction-selective and velocity-selective ganglion cells projecting to various nuclei in the midbrain region (Thomas et al., 2004; Giolli et al., 2006; Schiller, 2010). The goal of AOS is to detect slip of the visual world on the retina, which then triggers corrective eye and head movements to stabilize the images (Schiller, 2010). Therefore, it is not surprising that defects in OKT response occur at a similar time-point as OP abnormalities since retinal ganglion cells and amacrine cells are also potential generators of OPs (Shirao and Kawasaki, 1998; Wachtmeister, 1998).

The observed OP changes in our study also agree with other published studies on the effects of diabetes on inner retina. From a molecular biology standpoint, diabetes has been shown to alter the levels and receptors of several inner retinal neurotransmitters [most notably dopamine and gamma-amino-butyric acid (GABA)], as early as 4 weeks post-STZ (Northington et al., 1985; Ramsey et al., 2007; Santiago et al., 2009). Cellularly, increased cell deaths of amacrine and ganglion cells has been observed within weeks of STZ injection (Gastinger et al., 2006; Kern and Barber, 2008; Barber et al., 2011). Functionally, other ERG studies have reported dysfunction in amacrine- and ganglion cell-dominated OPs and scotopic threshold response (STR) at 4 weeks post-STZ (Ghirlanda et al., 1997; Shirao and Kawasaki, 1998; Matsubara et al., 2006; Ramsey et al., 2006; Kohzaki et al., 2008; Wolff et al., 2010; Ly et al., 2011). Amongst these pathological changes, disruption of the retinal dopaminergic system is a highly plausible underlying factor that can lead to both ERG changes and OKT defects as retinal dopamine has been shown to directly modulate OP generation (Wachtmeister, 1998) and visual function (Jackson et al., 2012). It is intriguing that other studies have detected a-wave losses as the major feature of DR neuronal dysfunction, though the difference in the ERG findings may be due to difference in animal strains, extent of glycemic control (i.e. frequency and dosage of insulin treatment), duration of hyperglycemia, or stimulation protocol (Phipps et al., 2006; Fletcher et al., 2007).

Aside from direct hyperglycemic insults on the retinal neurons, it is possible that retinal dysfunction may be secondary to hypoxia due to vascular dysfunction. Numerous studies have found defective vascular function at early stages of DR (Ciulla et al., 2002; Clermont and Bursell, 2007; Curtis et al., 2009; Wang et al., 2011). More importantly, a

recent report has not only demonstrated hypoxia in diabetic rat retina (at the retinal ganglion cell layer) at 4 weeks post-STZ but also detected corresponding functional ganglion cell deficits with ERG (reduced STR amplitude) (Ly et al., 2011). This hypothesis of hypoxia-induced retinal dysfunction leading to visual defects in diabetes was also supported in an earlier study when breathing 100% oxygen improved contrast sensitivity of diabetic patients with minimal retinopathy (Harris et al., 1996).

Taken together with these reports, our findings provide evidence of early inner retinal dysfunction due to diabetes, either directly or indirectly, which can then result in defects in different aspects of vision, including visual acuity and contrast sensitivity. However, it is important to recognize the possibility that defects in OKT response could also be due to disturbances in post-retinal connections, such as downstream components of AOS.

2.5.4 Future Implications

It is intriguing that we were able to detect substantial reduction in OKT responses in our diabetic rats following such a short duration of hyperglycemia, since visual acuity determined with acuity eye charts as a diagnostic and clinical trial end-point in humans has been insensitive to early-stage DR (Ghirlanda et al., 1997; Jackson and Barber, 2010). This suggests that certain aspects of vision are selectively affected in early-stage DR (e.g. contrast sensitivity, scotopic vision, or optokinetic response), and may serve as better diagnostic and screening tools. Furthermore, the present study provides a temporal relationship of the observed visual defects in STZ-induced diabetic rats with corresponding ERG alterations and cataract development. Further research is warranted to establish the causal relationships between these pathologies and determine the best

way to detect the pathologies in diabetic patients in which detection can be confounded by other factors such as aging and other ocular diseases. Nonetheless, STZ-induced diabetic rats can serve as a valuable model to investigate the underlying mechanisms for the visual dysfunction in early-stage DR, in hope of revealing a potential therapeutic target to ameliorate such deficits. Moreover, the reproducibility of the visual deficits in this model can allow us to reliably test the efficacy of future treatment options to prevent or delay vision loss in DR. Lastly, as DR is a multi-faceted disease, it is important to study DR with multi-disciplinary approach. Therefore, future studies to elucidate the underlying causes of vision loss should consider how diabetes differentially affects the neuronal and vascular tissues of the retina, and ultimately vision.

CHAPTER 3: DOPAMINE DEFICIENCY CONTRIBUTES TO EARLY VISUAL DYSFUNCTION IN A RODENT MODEL OF TYPE 1 DIABETES

This chapter was originally published as an article in *Journal of Neuroscience:*

Aung MH, Park HN, Han MK, Obertone TS, Abey Jm Aseem F, Thule PM, Iuvone PM, and Pardue MT. Dopamine deficiency contributes to early visual dysfunction in a rodent model of type 1 diabetes. *Journal of Neuroscience* 2014 34(3):726-736.

3.1 Abstract

Purpose: Dopamine (DA) functions as an essential neuromodulator in the brain and retina such that disruptions in the dopaminergic system are associated with common neurologic disorders such as Parkinson's disease. Although a reduction in DA content has been observed in diabetes, its effects in the development of diabetes-induced neuropathy remains unknown. As the retina is rich in DA and has a well-known diabetes-induced pathology (diabetic retinopathy or DR), this study was designed to examine the role of retinal DA deficiency in early visual defects in DR.

Methods: Using rodent models of Type 1 diabetes, we first determined if diabetes caused reduction in retinal DA content, as assessed with high-performance liquid chromatography, in both rats and mice. We then examined if pharmacologically restoring DA levels (with chronic L-DOPA treatment, a DA precursor) or activating specific DA receptor pathways (with acute delivery of agonists for different DA receptors) could improve the visual functions of diabetic mice, as assessed with optokinetic tracking. We

also probed the retinal functions of L-DOPA treated animals with electroretinography to assess if improvement in visual function could be mediated through improvement in retinal function.

Results: We found that diabetes significantly reduced DA levels by 4 weeks in rats and by 5 weeks in mice, coincident with the initial detection of visual deficits. Treatment with L-DOPA improved overall retinal and visual functions in diabetic mice while acute treatment with DA D1 or D4 receptor agonists improved visual acuity or contrast sensitivity, respectively.

Conclusions: Our results indicate that retinal DA deficiency is an underlying mechanism for early diabetes-induced visual dysfunctions and suggest that therapies targeting the retinal dopaminergic system may be beneficial in early-stage DR.

3.2 Introduction

The catecholamine dopamine (DA) is a crucial neurotransmitter in both the brain and retina. DA is synthesized from tyrosine via L-3,4-dihydroxyphenylalanine (L-DOPA), with the enzyme tyrosine hydroxylase (TH) being the rate-limiting step (Björklund and Dunnett, 2007; Fernstrom and Fernstrom, 2007). In addition to regulating a host of neural processes that include motor, cognition, and retinal function (Witkovsky, 2004), retinal DA directly modulates multiple aspects of light-adapted vision through activation of selective receptors and retinal pathways (Jackson et al., 2012). Although studies have investigated the role of DA malfunction on visual deficits in multiple disorders (e.g. Parkinson's disease, schizophrenia, etc.) (Brandies and Yehuda, 2008), its potential contribution to the pathogenesis of diabetic retinopathy (DR), a leading cause of

vision impairment in working-age adults (King et al., 1998; Congdon et al., 2003; Klein, 2007), remains unclear.

Historically, DR has been primarily considered a vascular disorder due to its association with late-stage structural defects in the retinal vasculature (Cai and Boulton, 2002). Typically, after decades of hyperglycemia, increasing retinal vascular occlusions produce ischemia that drives an aggressive neovascularization response (also known as proliferative DR) and/or macular edema (Frank, 2004). These late-stage vascular lesions are the direct antecedents of severe vision loss associated with DR. While clinical research has emphasized retinal vascular changes in diabetes, retinal neuronal dysfunction that predates clinically detectable vascular lesions is increasingly recognized (Barber, 2003; Antonetti et al., 2006). Electroretinogram (ERG) responses are consistently diminished and delayed in diabetic patients without vascular pathologies (Ghirlanda et al., 1997; Shirao and Kawasaki, 1998). Moreover, several neuronal cell types are less abundant in diabetic retinas when compared to age-matched control retinas (Abu-El-Asrar et al., 2004; Martin et al., 2004; Abu El-Asrar et al., 2007; Fletcher et al., 2007; Kern and Barber, 2008). Additionally, diabetic patients with angiographically normal retinas experience subtle visual dysfunctions, including abnormal color vision and decreased contrast sensitivity (Jackson and Barber, 2010). Similar early visual dysfunctions have been consistently replicated in rodent models of diabetes (Kirwin et al., 2011; Akimov and Rentería, 2012; Muir et al., 2012; Aung et al., 2013). Although most reports emphasized the potential role of retinal defects as a contributing factor for the visual deficits, little is known about the underlying mediator(s).

Interestingly, disruption in the retinal dopaminergic system has also been observed in diabetes. DA levels are reduced in diabetic rat retinas at 1 month after diabetes induction (Nishimura and Kuriyama, 1985). Furthermore, loss of TH-positive retinal neurons has been reported after six months of diabetes (Gastinger et al., 2006). Since retinal DA modulates ERG and visual function (Herrmann et al., 2011; Jackson et al., 2012), we hypothesized that diabetes causes reduced retinal DA content, which then leads to the visual dysfunction observed in early-stage DR. To test this hypothesis, we evaluated the effects of diabetes on retinal DA levels in our diabetic rodent models. We then determined if chronic restoration of DA levels or acute activation of specific DA receptor pathways ameliorated early diabetes-associated visual deficits.

3.3 Materials and Methods

3.3.1 Animals and Experimental Design

All animals were housed in ventilated cages on a 12 hour light-dark cycle (light onset at 6 am) with food and water provided *ad libitum*. All procedures were approved by the Atlanta VA Institutional Animal Care and Use Committee and conformed to the ARVO Statement for the Use of Animals in Ophthalmic and Vision Research.

Comparison of Dopamine levels between Control and Diabetic animals. Diabetes was induced in two month old male Long Evans rats (Charles River, Wilmington, MA) with a single intravenous injection of streptozotocin (STZ: 100 mg/kg; Sigma-Aldrich, St. Louis, MO) dissolved in citrate buffer/50% glucose solution (8:1 ratio), serving as a model for Type 1 diabetes (DM). Age-matched male control (CTRL) rats were injected with citrate buffer/50% glucose solution alone. Diabetes was defined as two successive daily blood glucose levels >250 mg/dL (determined with hand-held blood glucose meter

from tail-prick blood) (Clee and Attie, 2007), which routinely occurred 2-3 days after STZ injection. Weights and blood glucose levels of the animals were monitored twice a week for the entire duration of the experiment. When DM rats were found to be losing weight, they were treated with a pellet of sustained-release subcutaneous insulin (Linplant; Linshin Canada, Scarborough, ON, Canada) at a dose adequate to prevent weight loss, but insufficient to control hyperglycemia (13 ± 3 mg/pellet with a release rate of approximately 2 U/day) (Thulé et al., 2006). Rats were maintained for either 4 or 12 weeks (n=6 per treatment group at each time-point).

To assess the effects of diabetes on retinal DA content in mouse, one and a half month old male CD-1 albino mice (Charles River, Wilmington, MA) were injected intraperitoneally (i.p.) daily for 5 consecutive days with either vehicle (citrate buffer/50% glucose solution in 8:1 ratio) or STZ (50 mg/kg). Diabetes was defined similarly to the rat experiment described above (successive blood glucose levels of >250 mg/dL). Weights and blood glucose levels of the animals were also monitored twice a week. DM mice that lost >10% body weight were given an i.p. injection of 1 U of insulin (NovoLog; Novo Nordisk Inc., Princeton, NJ) diluted 1:10 in Ringer's solution, to prevent catabolic weight loss. Both CTRL and DM mice (n=8 per treatment group) were then followed for 5 weeks.

All animals, both rats and mice, were euthanized between 4-6 hours after light onset to prevent diurnal differences in DA and 3,4-dihydroxyphenyl-acetic acid (DOPAC, a major metabolite of DA that is catalyzed by the enzyme monoamine oxidase) levels (Nir et al., 2000; Witkovsky, 2004). Retinas were collected in amber tubes, stored

at -80^{o}C, and analyzed for DA and DOPAC levels using high-performance liquid chromatography (HPLC) with coulometric detection, as described below.

Chronic Treatment with L-DOPA. In this experiment, we used two month old pigmented mice on C57 background (mixture of males and females) with the gene tyrosine hydroxylase (*Th*) and consequently with DA selectively deleted in the retina. As previously described (Jackson et al., 2012), these mice were created by crossing *Chx10-Cre* recombinase expressing mice with mice expressing floxed *Th* gene. Wild-type mice ($Th^{loxP/loxP}$, herein referred to as WT) and conditional *Th* knockout ($Chx10\text{-}Cre{:}Th^{loxP/loxP}$, herein referred to as rTHKO) mice were rendered diabetic, as described above. DM mice that lost >10% body weight were given an i.p. injection of 1 U of insulin (NovoLog; Novo Nordisk Inc., Princeton, NJ) diluted 1:10 in Ringer's solution, to prevent cachexia. CTRL mice were injected with citrate buffer/50% glucose solution. CTRL and DM mice of both WT and rTHKO genotypes then received daily i.p. injections of either L-DOPA (10 mg/kg; Sigma-Aldrich, St. Louis, MO) dissolved in 0.1% ascorbic acid in saline solution or vehicle alone (Veh) between 4 to 8 hours after light onset. The treatment injections (vehicle and L-DOPA) initiated when majority of the DM animals had elevated blood glucose levels of >250 mg/dL. The sample size for each treatment group is shown in the figure legends. L-DOPA was made fresh daily at a concentration of 1 mg/ml. Mice were maintained for 6 weeks, with their visual function assessed weekly and retinal function assessed with ERG at 5-week time-point. All functional tests were conducted 30 min to 1 hour after L-DOPA or vehicle injection.

Acute Treatment with Selective Dopamine Receptor Agonists. Diabetes was induced in two month old pigmented male WT mice (n=7) with the protocol described

above. Pigmented mice were used in this experiment due to lack of OKT responses from albino mice (Puk et al., 2008). After 8 weeks of diabetes, all mice were successively injected i.p. once with (1) D1 receptor agonist SKF38393 (1 mg/kg; Tocris Biosciences, Ellisvile, MO), (2) vehicle (0.9% NaCl solution), and (3) D4 receptor agonist PD168077 (1 mg/kg; Tocris Biosciences, Ellisvile, MO) (Jackson et al., 2012). There was a 1-2 day interval between each treatment to clear the previous drug effects, which should be adequate as the half-lives of SKF38393 and PD168077 are approximately 1-3 hours (Moreland et al., 2005; Jackson et al., 2006). Visual acuity threshold and contrast sensitivity level of each animal were measured 30 min after each treatment.

3.3.2 Visual Psychophysical Testing

Visual function of each animal was tested using the virtual optokinetic system (OptoMotry system; Cerebral-Mechanics, Lethbridge, AB, Canada), as previously described (Douglas et al., 2005; Aung et al., 2013). Briefly, the animal was placed on a platform surrounded by four computer monitors that displayed vertical sine wave gratings rotating at 12 deg/s. A video camera, positioned above the animal, allowed an observer to determine the presence or absence of visual tracking. Tracking was defined as slow head movements in the same direction and speed as the rotating gratings. For visual acuity assessment, the grating started at a spatial frequency of 0.042 cyc/deg with 100% contrast and increased in a staircase paradigm until the response threshold was crossed three times. Similarly, contrast sensitivity was determined by reducing the contrast between the black and white gradients from 100% in a staircase paradigm until animal head-tracking movements were no longer observed. Contrast sensitivity was measured at the spatial frequency of 0.064 cyc/deg for all the animals (both rats and mice) in the study. This was

the spatial frequency that elicited the maximal sensitivity from both rats and mice at baseline (data not shown). The contrast sensitivity was calculated as a reciprocal of the Michelson contrast from the screen's luminance [i.e. (maximum + minimum) / (maximum – minimum)] as previously described (Prusky et al., 2006). All OKTs were done 30 min to 1 hour after any treatment given (vehicle, L-DOPA, or DA receptor agonists), which usually occurred between 5 to 10 hours after light onset.

3.3.3 Retinal Function Test

To assess retinal function with ERG, we performed dark-adapted ERG luminance series and light-adapted flicker exposure. All ERGs were done 30 min to 1 hour after any treatment given (vehicle or L-DOPA), which usually occurred between 5 to 10 hours after light onset. In brief, mice were dark-adapted overnight and then prepared under dim red illumination. After being anesthetized with ketamine (80 mg/kg) and xylazine (16 mg/kg), we dilated the pupils (1% tropicamide) and numbed the corneal surface (0.5% tetracaine HCl). Using a gold loop electrode, dark-adapted responses were recorded with a signal averaging system (UTAS BigShot; LKC Technologies, Gaithersburg, MD) to flash stimuli presented in order of increasing luminance (Scotopic: -3.0 to 2.1 $\log \cdot cd \cdot s/m^2$), so that rod-dominated and mixed rods and cones responses can be isolated.

To further isolate the cone pathway function, mice were then exposed to a steady background adapting field (30 cd/m^2) for 10 min to saturate the rod photoreceptors. After the light-adaptation period, animals were presented with 2.0 $\log \cdot cd \cdot s/m^2$ flicker stimuli at 6 Hz in the presence of the background light. Responses were recorded using the same signal averaging system (UTAS BigShot; LKC Technologies, Gaithersburg, MD). After

testing, rats received yohimbine (2.1 mg/kg) to reverse the effects of xylazine and prevent corneal ulcers (Turner and Albassam, 2005).

Data were analyzed off-line. For the dark-adapted ERG responses, amplitudes and implicit times were measured for both a- and b-waves. For the light-adapted ERG responses, amplitudes of the flicker responses were measured from the trough of the signal after the flash onset to the peak. Implicit times were determined from flash onset to the peak.

3.3.4 Dopamine and DOPAC Analysis

DA and DOPAC levels were assessed by ion-pair reverse-phase HPLC with coulometric detection, as previously described (Pozdeyev et al., 2008). Frozen retinas were homogenized in 0.2 N $HClO_4$ solution containing 0.01% sodium meta-bisulfate and 25 ng/ml 3,4-dihydroxybenzylamine hydrobromide as an internal standard and centrifuged. Each supernatant fraction was separated on an Ultrasphere ODS 5 µm 250×4.6 mm column (Beckman Coulter, Fullerton, CA) with a mobile phase containing 0.1 M sodium phosphate, 0.1 mM EDTA, 0.35 mM sodium octyl-sulfate, and 6% acetonitrile (pH 2.7). The DA and DOPAC signals from each sample were quantified using a detection curve established by standards ranging from 2 to 20 ng/ml. Levels of DA and DOPAC were then presented as pg of DA or DOPAC per retina.

3.3.5 RT-PCR Analysis

Single retinas were placed in a 1.5 ml tube and homogenized with 50 µl zirconium oxide beads (0.5 mm) and 100 µl Trizol in a Bullet Blender (Next Advance, Inc., Averill Park, NY) for 3-6 minutes. Chloroform (20 µl $CHCl_4$) was added to each sample, shaken, and then centrifuged for 15 minutes at 4°C. The RNA-containing

aqueous phase was then transferred to a fresh tube and cleaned using an RNA purification kit (RNeasy Mini, Qiagen, Germantown, MD) according to manufacturer's instructions, using a final elution volume of 30 µl. For each sample, 1 ug of RNA was reverse-transcribed to cDNA with the QuantiTect kit (Qiagen, Germantown, MD). Resulting cDNA was diluted 1:20 with water and 1.5 µl was used in each real-time quantitative PCR (RT-PCR) reaction. RT-PCR reactions were performed in a 10 µl volume with SYBR green 2X master mix (Bio-Rad, Inc., Hercules, CA) in a RealPlex 4 cycler (Eppendorf North America, Hauppauge, NY). The primer sequences are listed in Table 3-1. Conditions for the RT-PCR reactions were 95°C, 3 minutes; 40 cycles of 94°C, 30 seconds denaturation; 65°C, 30 seconds annealing; 72°C, 30 seconds extension; 72°C, 7 minutes, with fluorescence recorded at the end of each 72°C extension. Melt curve analysis conditions were heating from 55°C to 95°C in 0.5°C increments, 15 seconds per increment, with fluorescence recorded at each increment. The cycle threshold (Ct) value of each reaction was determined as the cycle number in which the log increasing fluorescence intersects the threshold level as determined by the software. Three replicates were performed for each cDNA sample-primer pair combination and the average Ct was calculated. Using 18S as the internal control, the expression of each gene of interest was calculated from the average PCR cycle thresholds using the $2^{-\Delta Ct}$ method (Livak and Schmittgen, 2001; Schmittgen and Livak, 2008). Fold change of the gene expression was further calculated by taking the ratio of the $2^{-\Delta Ct}$ average of the treatment group over the $2^{-\Delta Ct}$ average of the control group.

Gene of Interest	Primer Sequence	
Th	Forward	5'-TGCCCGTGATTTTCTGGCCAGT-3'
	Reverse	5'-TGTCCTGGGAGAACTGGGCAAA-3'
Drd1	Forward	5'-CAGCCTTCATCCTGATTAGCGTAG-3'
	Reverse	5'-CTTATGAGGGAGGATGAAATGGCG-3'
Drd4	Forward	5'- TCTTTGTCTACTCCGAGGTCCAG-3'
	Reverse	5'-TCACGGCCACGAACCTGTCCA-3'
18S	Forward	5'-GTTGGTTTTCGGAACTGAGGC-3'
	Reverse	5'-GTCGGCATCGTTTATGGTCG-3'

Table 3-1. Sequences of the primers used in RT-PCR reactions for genes of interest.

3.3.6 Statistical Analysis

Statistical analysis was performed using commercial statistical software (SigmaStat 3.5, Aspire Software International, Ashburn, VA). Two-way repeated-measures ANOVAs were used to compare DA and DOPAC levels and visual function of treatment groups across time-points after STZ injection. For ERG analysis, one-way ANOVAs were used to compare between treatment groups. Due to failed normality test for the analysis of the efficacy of systemic L-DOPA treatment in increasing retinal DA content, one-way ANOVAs on rank were used instead to compare between treatment groups. Post-hoc multiple comparisons for all ANOVA tests were performed when appropriate with p-value corrected with Rough False Discovery Rate method [RFDR, calculated as (p*(#tests+1))/(2*(#tests))]. For DA and DOPAC analysis in mice, Student's t-test was performed to determine if retinal DA content differed between the experimental groups. For RT-PCR analysis, multiple Student's t-tests were used to determine if the expressions of the treatment groups were different from the control group, with the critical levels corrected with RFDR method. All analyses were performed with *a priori* significance set at $\alpha<0.05$. For the asterisk symbol: * indicates $p<0.05$, ** defines $p<0.01$, and *** means $p<0.001$. All data are presented as Mean ± SEM.

3.4 Results

3.4.1 Diabetes significantly reduced retinal dopamine level

To assess the effects of diabetes on retinal DA level, we induced diabetes in rats for either 4 or 12 weeks and compared their retinal DA levels to age-matched CTRL rats. All rats receiving STZ became hyperglycemic with reduced weights compared to vehicle-treated rats (Table 3-2). Overall, retinal DA levels were significantly decreased in DM

rats compared to CTRL rats [Figure 3-1A, Main Treatment Effect: $F(1,17)=38.233$, $p<0.001$]. DA levels also increased as the animals aged, regardless of diabetes status [Figure 3-1A, Main Duration Effect: $F(1,17)=9.407$, $p=0.007$]. Moreover, DA reduction worsened from approximately 25% (of the CTRL group) at 4-week time-point to 32% at 12-week time-point. Interestingly, only age, not diabetes, altered the levels of DOPAC [Figure 3-1B, Main Duration Effect: $F(1,17)=16.796$, $p<0.001$]. In terms of DA metabolism, the ratios of DA to DOPAC were not significantly altered due to diabetes, but did increase as the animals aged [Figure 3-1C, Main Duration Effect: $F(1,17)=15.492$, $p=0.001$]. Next, we assessed if similar DA reduction occurred in DM mice. All mice injected with repeated low-dose STZ developed diabetes and maintained it throughout the experiment duration (Table 3-2). More importantly, similar to DM rats, DM mice had significantly lower DA levels, approximately 15% reduction, compared to CTRL mice [Figure 3-2A, Student's t value=2.312, $p=0.039$] at 5-week time-point. No significant differences were found in DOPAC levels or DOPAC/DA ratios between the two groups (Figure 3-2B and 3-2C). These results confirmed that diabetes leads to diminished retinal DA levels, as previously reported (Nishimura and Kuriyama, 1985).

Species	Time-pt (weeks)	Treatment Group	Baseline		End of Study	
			Weight (g)	BG (mg/dl)	Weight (g)	BG (mg/dl)
Rat	4	CTRL	209 ± 4.5	147 ± 4	382 ± 11.2	141 ± 8
		DM	212 ± 6.6	149 ± 3	294 ± 7.5	547 ± 15
	12	CTRL	334 ± 15.0	129 ± 6	588 ± 23.5	124 ± 7
		DM	325 ± 12.3	125 ± 2	380 ± 15.6	546 ± 19
Mouse	5	CTRL	26.3 ± 0.5	187 ± 10	37.8 ± 1.1	138 ± 6
		DM	26.6 ± 0.6	186 ± 9	30.9 ± 0.7	508 ± 31
Mouse	6	CTRL WT +Veh	21.7 ± 2.6	165 ± 5	22.6 ± 2.3	168 ± 11
		CTRL WT +L-DOPA	20.0 ± 2.3	147 ± 8	20.8 ± 2.2	139 ± 19
		DM WT +Veh	23.3 ± 0.8	165 ± 10	23.0 ± 0.7	349 ± 29
		DM WT +L-DOPA	21.9 ± 1.0	187 ± 11	19.1 ± 0.9	504 ± 29
		DM rTHKO +Veh	22.2 ± 1.1	185 ± 10	21.2 ± 1.0	426 ± 43
		DM rTHKO +L-DOPA	23.4 ± 1.5	182 ± 14	20.9 ± 1.2	431 ± 35
Mouse	8	DM	32.9 ± 0.8	187 ± 7	26.7 ± 0.6	437 ± 18

Table 3-2. Average weight and blood glucose levels of the experimental groups (± SEM) used for this project. Abbreviation used in the table: BG = blood glucose.

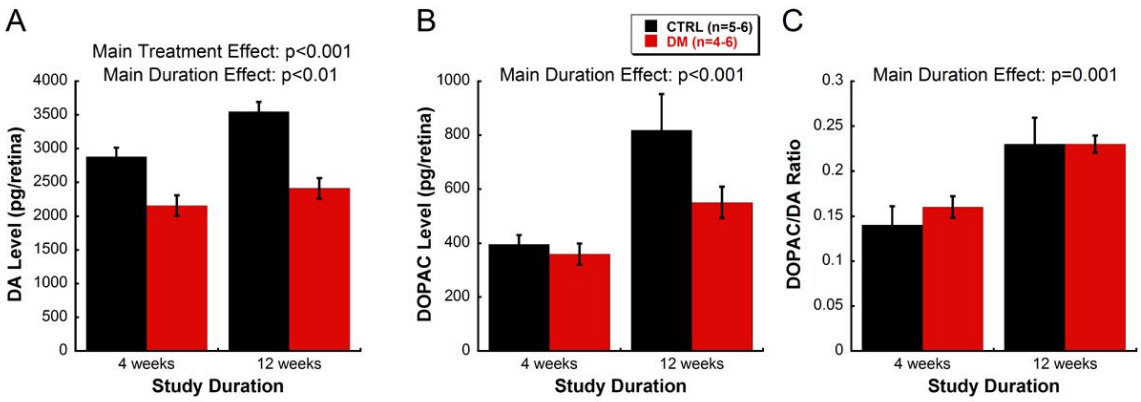

Figure 3-1. Diabetes reduced retinal DA contents in STZ-induced DM rats. (A) Overall, DM rats exhibited significantly reduced DA levels compared to CTRL animals [Main Treatment Effect: $p<0.001$]. There was also a significant age-dependent increase in DA level of all animals [Main Duration Effect: $p<0.01$]. **(B)** Regardless of diabetes status, rats had significantly higher DOPAC levels at 12-week time-point than at 4-week time-point [Main Duration Effect: $p<0.001$]. DM animals showed a trend toward lower DOPAC levels compared to CTRL animals at 12-week time-point. **(C)** Metabolism of DA to DOPAC did not differ between CTRL and DM animals. No significant change in DOPAC/DA ratio was detected due to diabetes in Long-Evans rats. However, there was an increase in dopamine metabolism due to age [Main Duration Effect: $p=0.001$].

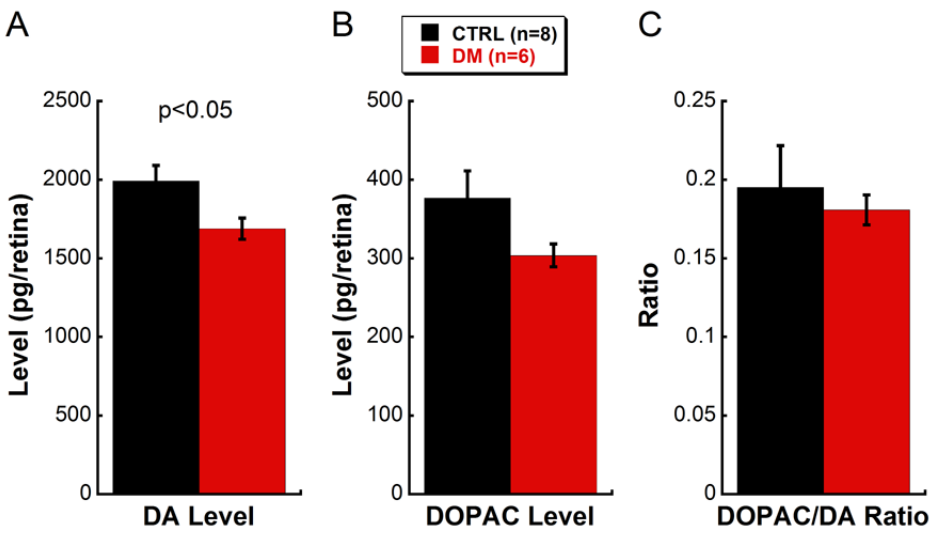

Figure 3-2. Diabetes lowered retinal DA levels in STZ-induced DM mice. (A) At 5-week time-point, DM mice had significantly reduced retinal DA contents than the CTRL mice [p=0.039]. **(B, C)** A slight trend for decreased DOPAC level or DOPAC/DA ratio due to diabetes was observed.

3.4.2 Restoring dopamine content delayed diabetes-induced visual dysfunction

To examine whether DA deficiency causes visual deficits in early DR, we investigated the effects of restoring DA levels with L-DOPA on visual functions of DM mice. All STZ-treated DM mice were significantly hyperglycemic compared to CTRL mice (Table 3-2). Similar to our previous report in STZ-induced diabetic rats (Aung et al., 2013), DM WT+Veh mice exhibited significantly reduced visual acuities [Figure 3-3A, Interaction Effect: $F(12,82)=4.644$, $p<0.001$] and contrast sensitivities [Figure 3-3B, Interaction Effect: $F(12,82)=6.425$, $p<0.001$], as early as 3 to 4 weeks post-STZ. Moreover, the severity of visual deficits progressed over time. The deficit in visual acuity of DM WT+Veh group worsened from 7.0% (in comparison to CTRL WT+Veh group) at 3 weeks post-STZ to 12.3% at 6 weeks post-STZ, while the reduction in contrast sensitivity deteriorated from 12.8% at 3 weeks post-STZ to 43.6% at 6 weeks post-STZ. On the other hand, the onset and progression of visual dysfunction was significantly delayed by chronic L-DOPA treatment (Figure 3-3). The reduction in visual acuity of DM WT+L-DOPA group progressed from 2.4% at 3 weeks post-STZ to 7.2% at 6 weeks post-STZ, while the deficit in contrast sensitivity was only significant at 6 weeks post-STZ with an 18.0% reduction from CTRL WT+Veh group. For comparison, L-DOPA treatment in CTRL mice did not cause significant changes in either visual acuity or contrast sensitivity. Furthermore, we did not observe any behavioral side-effects, i.e. dyskinesia, with our current dosage for L-DOPA (10 mg/kg daily) in either CTRL or DM mice. We were cautious to select a dosage that was lower than the typical dosage used to induce dyskinesia (25 mg/kg) (Cao et al., 2010; Aguiar et al., 2013), yet could still increase retinal DA levels (Mao et al., 2010).

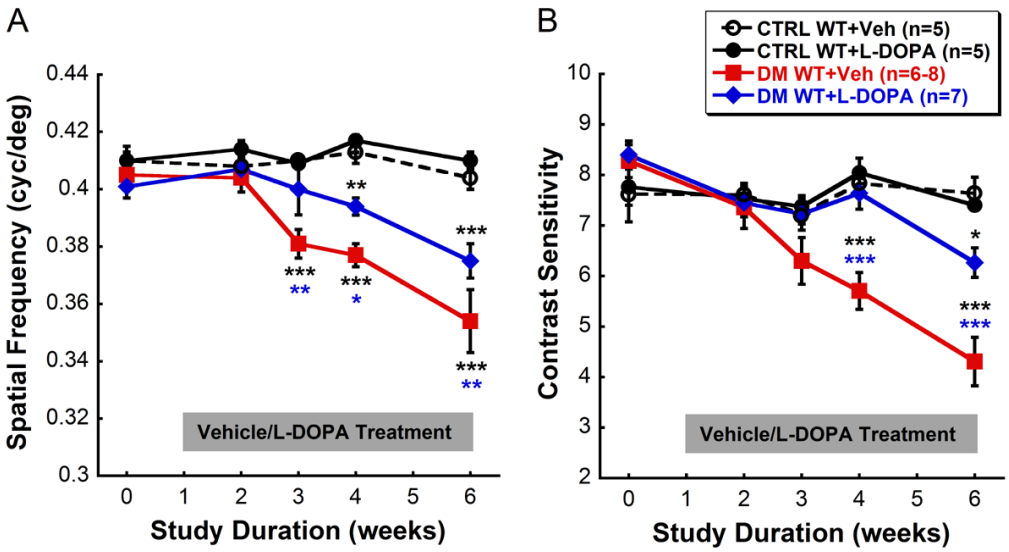

Figure 3-3. Chronic L-DOPA treatment delayed early diabetes-induced visual dysfunction. (A) Visual acuity thresholds of DM WT+Veh mice showed significant reductions from CTRL animals as early as 3 weeks post-STZ (post-hoc comparison, $p<0.001$]. In contrast, the visual deficits appeared in DM WT+L-DOPA mice a week later, starting at 4 weeks post-STZ [post-hoc comparison, $p<0.01$] with a slower and less severe progression. **(B)** Contrast sensitivity levels were also significantly reduced in DM WT+Veh mice [post-hoc comparison, $p<0.001$] at 4 weeks post-STZ, while DM WT+L-DOPA mice only exhibited a slight decrease in sensitivity at 6 weeks post-STZ [post-hoc comparison, $p<0.05$]. The color of the asterisk indicates the treatment group for which significance was reached, with the exception of the black asterisk, which refers to both CTRL WT+Veh and CTRL WT+L-DOPA groups. Note that the Y-axis does not start at zero; this is modified to more clearly show the differences between treatment groups.

3.4.3 Retinal dysfunction underlies the dopamine-mediated visual deficits in diabetes

Since systemic injections of L-DOPA affect both brain and retinal dopaminergic systems, we tested the role of ***retinal*** DA deficiency underlying visual deficits in early-stage DR by assessing the effects of diabetes in mice with loss of retinal DA, rTHKO mice. We hypothesized that reduced retinal DA content is a major contributing factor to the early visual deficits, and thus, diabetes in rTHKO mice should not result in further decline in their visual functions. First, we found that rTHKO mice had reduced visual acuity thresholds (Figure 3-4A and 3-4C: 10.4% lower than CTRL) and contrast sensitivity levels (Figure 3-4B and 3-4D: 39.3% lower than CTRL) at baseline (prior to diabetes induction), which were similar in severity as previously reported (Jackson et al., 2012). More importantly, visual functions of DM rTHKO+Veh mice did not further deteriorate after induction of diabetes and maintained the same levels of visual deficits compared to the CTRL group throughout the study period (Figure 3-4A and 3-4B). While DM rTHKO+Veh mice began the study with significantly lower visual acuities [Figure 3-4A, Interaction Effect: $F(12,95)=8.861$, $p<0.001$] and contrast sensitivities [Figure 3-4B, Interaction Effect: $F(12,95)=13.348$, $p<0.001$] than those of DM WT+Veh mice, the levels of visual functions of both groups began to coincide starting at 3 weeks post-STZ. To show that DA deficiency could account for the visual dysfunction observed in DM rTHKO mice, we treated a separate cohort of DM rTHKO mice with L-DOPA. As shown in Figure 3-4C and 3-4D, L-DOPA treatment significantly improved visual functions of DM rTHKO+L-DOPA mice that lasted for the duration of the study [post-hoc comparison, $p<0.001$].

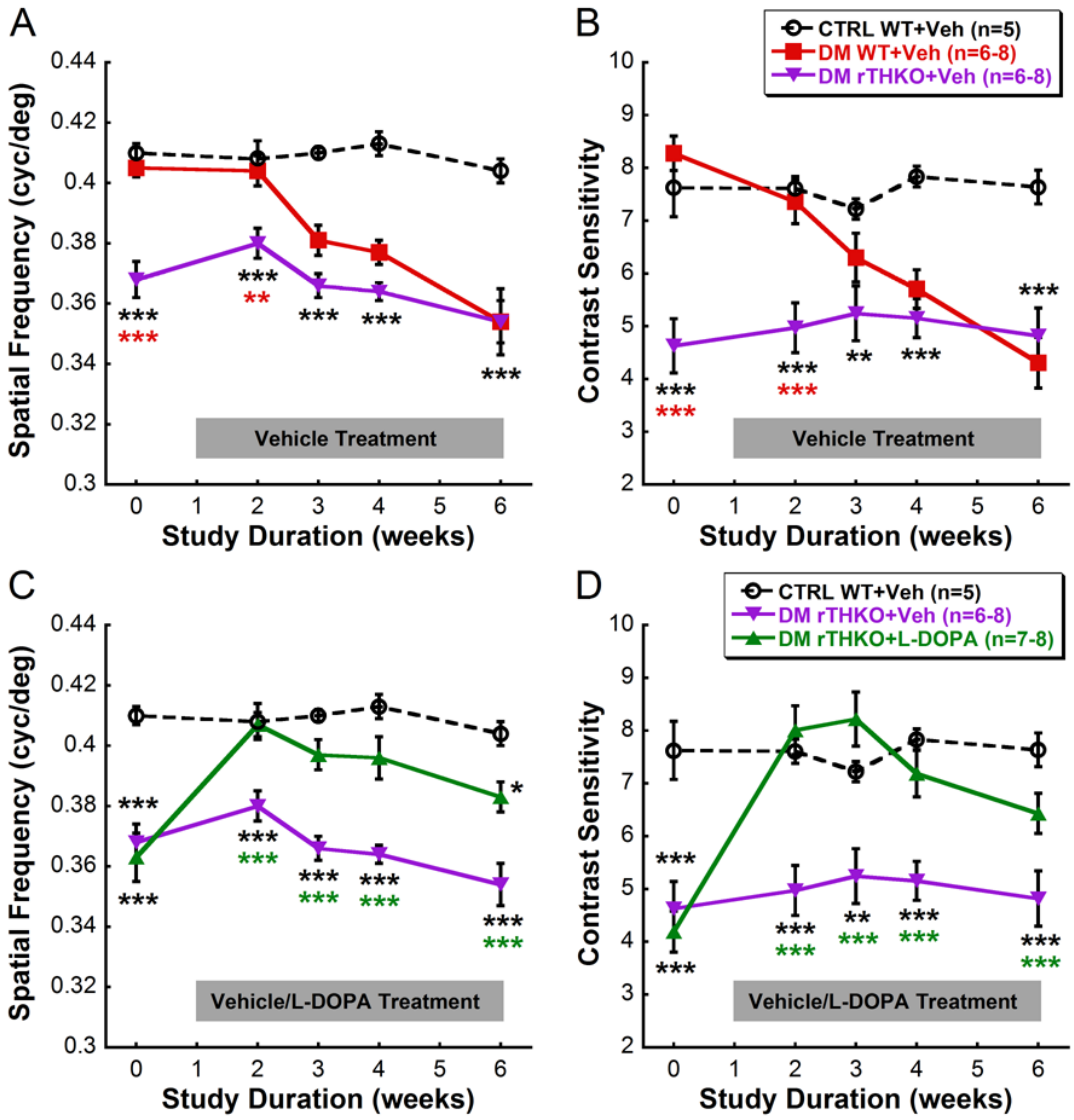

Figure 3-4. Genetic model of retinal DA deficiency (rTHKO) replicated early diabetes-induced visual dysfunction and could be rescued with L-DOPA treatment. (A) Diabetes did not further impair the visual acuity levels of DM rTHKO+Veh mice, and the visual acuity thresholds of DM WT+Veh and DM rTHKO+Veh groups became indistinguishable starting at 3 weeks post-STZ. **(B)** Similarly, the combination of rTHKO and diabetes did not further reduce contrast sensitivity within the time-frame of this study and contrast sensitivities of DM WT+Veh and DM rTHKO+Veh mice were indistinguishable from 3 weeks post-STZ onward. **(C)** Meanwhile, chronic L-DOPA treatment restored the visual acuity thresholds of rTHKO mice (DM rTHKO+L-DOPA group). DM rTHKO+L-DOPA mice had significantly higher visual acuities than DM rTHKO+Veh mice throughout the study duration [post-hoc comparison, $p<0.001$]. Moreover, L-DOPA treatment in rTHKO mice significantly delayed the onset and slowed the progression of diabetes-induced impairment of visual acuity, which was only significant at 6 weeks post-STZ [post-hoc comparison, $p<0.05$]. **(D)** Similar to findings in visual acuity, DM rTHKO+L-DOPA mice exhibited significantly better contrast sensitivities than DM rTHKO+Veh mice [post-hoc comparison, $p<0.001$]. The severity of perturbation in contrast sensitivity due to diabetes was also diminished in DM rTHKO+L-DOPA mice when compared to DM WT+Veh mice [post-hoc comparison, $p<0.05$]. The color of the asterisk indicates the treatment group for which significance was reached. Note that the Y-axis does not start at zero; this is modified to more clearly show the differences between treatment groups.

To validate that daily i.p. injections of L-DOPA were able to increase retinal DA levels, we measured retinal DA contents of the following four groups of animals: CTRL WT+Veh, CTRL WT+L-DOPA, DM rTHKO+Veh, and DM rTHKO+L-DOPA. As expected, the retinal TH deficiency in the rTHKO mice greatly diminished DA levels in comparison to both CTRL groups [Table 3-3, One-way ANOVA with Ranks, $H=12.092$ with 3 degrees of freedom, $p=0.007$]. On the other hand, L-DOPA treatment was able to restore the retina DA contents of rTHKO mice to a level comparable to those of CTRL animals. L-DOPA did not significantly increase the DA levels of CTRL mice. Overall, these results provide evidence that retinal DA reduction contributes to the visual defects in early-stage DR and that restoration of retinal DA content with L-DOPA treatment can slow the onset and progression of visual loss.

Treatment Groups	n	Retinal Dopamine Level (pg/retina)
CTRL WT+Veh	5	400 ± 179*
CTRL WT+L-DOPA	5	399 ± 179*
DM rTHKO+Veh	6	54 ± 22
DM rTHKO+L-DOPA	8	307 ± 109

Table 3-3. Daily L-DOPA injections restored retinal dopamine levels. As expected, rTHKO+Veh mice had significantly reduced DA levels from CTRL mice [post-hoc analysis, $p<0.05$], and daily injections of L-DOPA (10 mg/kg) were able to increase retinal DA contents of DM rTHKO animals, to levels comparable to those of CTRL animals. The asterisk indicates significant difference between the respective treatment group and DM rTHKO+Veh group. Abbreviation used in the table: n = sample size.

To confirm our previous hypothesis that retinal dysfunction in early-stage DR contributes to visual deficits (Aung et al., 2013) and to further support a role for retinal DA deficiency in the visual deficits, we examined if L-DOPA treatment improved retinal function as well (assessed by ERG). Since OKT responses were recorded under photopic conditions, we first examined isolated cone pathway function by exposing light-adapted animals to flicker stimuli. The CTRL group shown here and in subsequent RT-PCR analyses includes both CTRL WT+Veh and CTRL WT+L-DOPA animals as no significant differences were detected between them. We found that flicker responses in DM WT+Veh mice were significantly reduced [Figure 3-5B, Interaction Effect: $F(4,33)=6.032$, $p<0.01$] and delayed [Figure 3-5C, Interaction Effect: $F(4,33)=3.621$, $p<0.05$] compared to the CTRL animals. More importantly, L-DOPA treatment ameliorated these deficits, restoring the flicker responses of DM WT+L-DOPA mice similar to those of CTRL animals (Figure 3-5). In mice with retinal DA deficiency (DM rTHKO+Veh), we observed an even greater reduction [post-hoc comparison, $p<0.001$] and delay [post-hoc comparison, $p<0.01$] in flicker responses when compared to CTRL mice (Figure 3-5). Once again, administering L-DOPA was able to partially restore cone pathway functions of DM rTHKO mice to CTRL levels (Figure 3-5).

To determine if L-DOPA treatment was also beneficial for rod pathway function, we conducted dark-adapted ERGs on the same groups of animals. In regards to the a-wave, no consistent differences were observed, indicating no alterations in the photoreceptoral response at such early stages of diabetes (data not shown). Next, we examined the post-receptoral function, i.e. b-wave, of these animals. We found that DM WT+Veh animals exhibited significantly delayed b-waves from both CTRL and DM

WT+L-DOPA groups under both dim [Figure 3-6A and 3-6B, rods-dominated response: $F(2,20)=3.688$, $p=0.042$] and bright [Figure 3-6C and 3-6D, mixed rods and cones response: $F(2,20)=8.311$, $p=0.002$] flashes. Importantly, L-DOPA treatment reversed the ERG deficits as no significant difference was detected in the implicit times of the b-waves between CTRL and DM WT+L-DOPA groups. When we repeated the experiment with rTHKO animals, we found that the implicit times of the b-wave responses of DM rTHKO+Veh group under both dim (111.6 ± 8.0 msec) and bright (92.9 ± 8.1 msec) flashes were indistinguishable from those of DM WT+Veh group (dim: 110.4 ± 4.4 msec and bright: 91.1 ± 3.1 msec) (Figure 3-6). Administration of L-DOPA to rTHKO mice showed a strong trend, though not statistically significant, for improvement in b-wave implicit times under both dim and bright stimuli (Figure 3-6). In terms of b-wave amplitude, we only found that both groups of DM rTHKO mice (± L-DOPA) showed significantly reduced responses from the CTRL WT animals at both dim [$F(4,34)=4.497$, $p=0.005$] and bright [$F(4,34)=3.197$, $p=0.025$] flash stimuli (data not shown). Nonetheless, these additional analyses replicated our previous findings of early inner retinal dysfunctions in both rod and cone pathways due to diabetes (Aung et al., 2013). Collectively, the ERG data also reinforce our hypotheses that retinal dysfunction may partially underlie early diabetes-associated visual defects, and that L-DOPA therapy was able to improve retinal function and thereby slow the progression of visual loss.

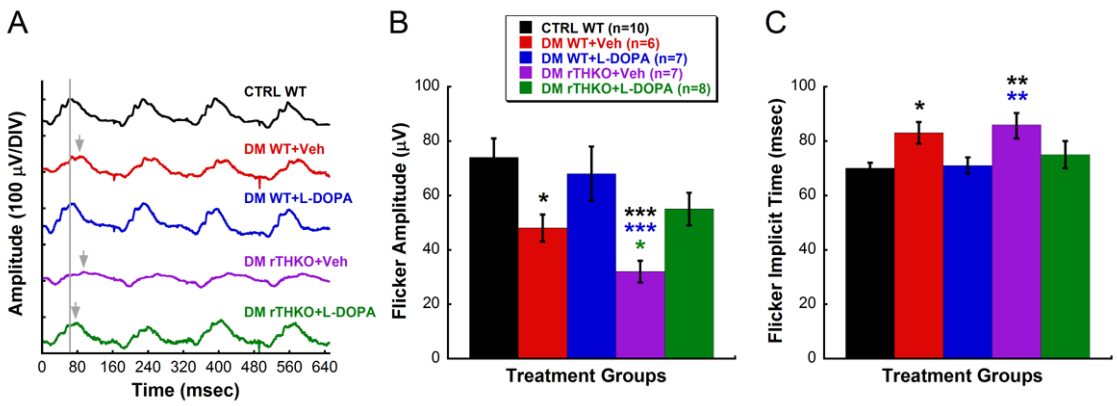

Figure 3-5. **Changes in DA levels due to diabetes affected light-adapted retinal function. (A)** Representative raw waveforms to flicker stimuli (6 Hz) from CTRL WT (**black**), DM WT+Veh (**red**), DM WT+L-DOPA (**blue**), DM rTHKO+Veh (**purple**), and DM rTHKO+L-DOPA (**green**) at 5-week time-point. The grey line indicates the peak of the response in a CTRL WT mouse, while the grey arrows indicate the peak of the response when delayed. **(B, C)** Average amplitudes (B) and implicit times (C) of the responses from experimental groups at 5-week time-point. DM WT+Veh mice had reduced [post-hoc comparison, $p<0.05$] and delayed [post-hoc comparison, $p<0.05$] ERG responses when compared to CTRL WT mice. L-DOPA treatment was able to restore ERG responses of DM WT mice to those of CTRL mice. Moreover, DM rTHKO+Veh mice, with presumed lower DA content, had severely reduced amplitudes in comparison to all other groups [post-hoc comparison, $p<0.05$] except that of DM WT+Veh animals. DM rTHKO+Veh mice also exhibited delayed responses from CTRL WT and DM WT+L-DOPA animals [post-hoc comparison, $p<0.01$]. The color of the asterisk indicates the treatment group to which significance was reached.

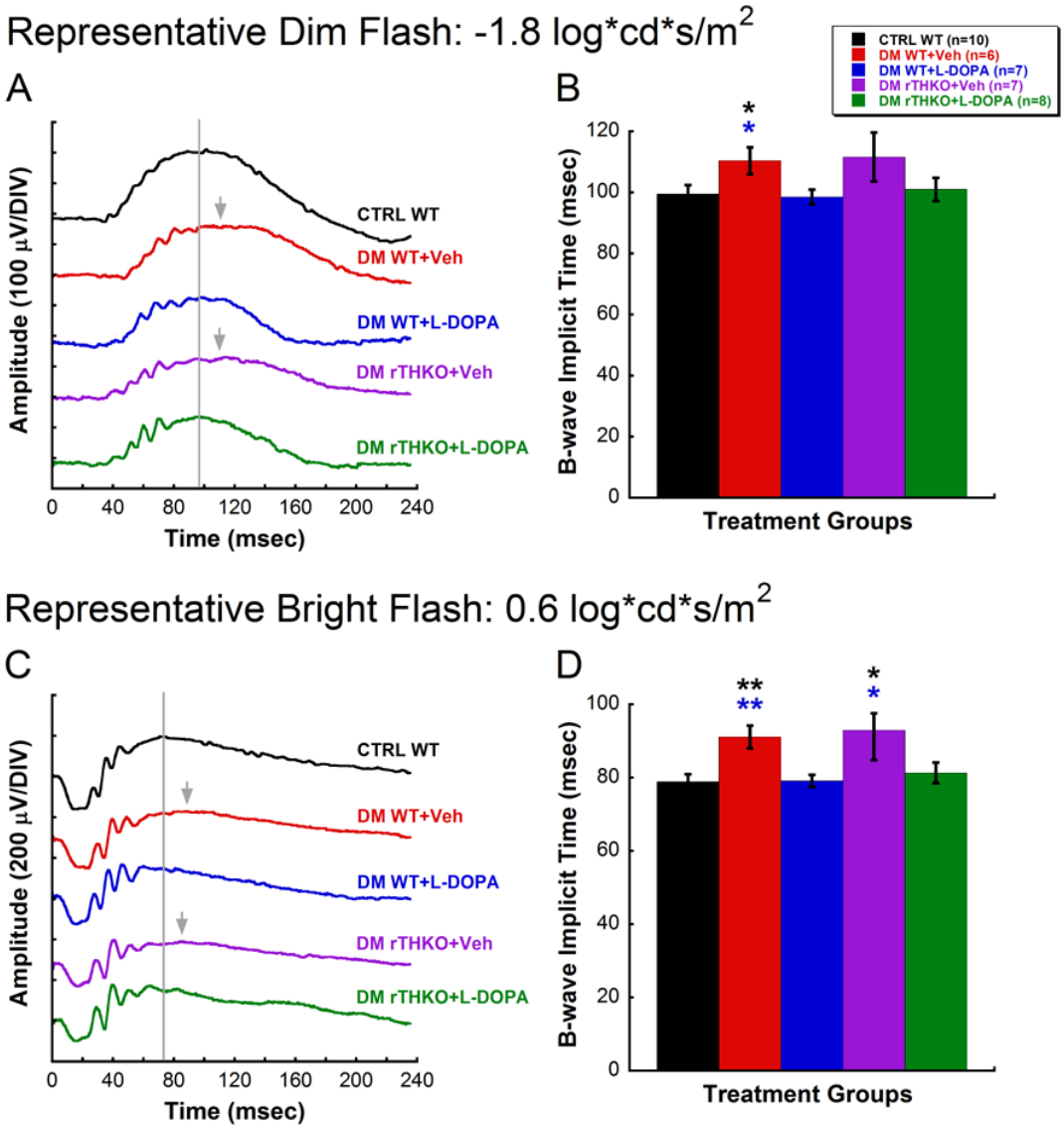

Figure 3-6. Changes in DA levels due to diabetes affected dark-adapted retinal function. (A, B) Representative raw waveforms and average b-wave implicit times in response to a *dim-flash* stimulus (-1.8 log cd s/m^2) at the 5-week time-point. **(C, D)** Representative raw waveforms and average b-wave implicit times in response to a *bright-flash* stimulus (0.6 log cd s/m^2) at the 5-week time-point. Following color lines and bars represent each treatment group: CTRL WT (**black**), DM WT+Veh (**red**), DM WT+L-DOPA (**blue**), DM rTHKO+Veh (**purple**), and DM rTHKO+L-DOPA (**green**). The grey lines indicate the peak of the b-wave in a CTRL WT mouse, while the grey arrows indicate the peak of the response when delayed. DM WT+Veh mice exhibited significantly delayed b-wave responses elicited with both dim [post-hoc comparison, $p<0.05$] and bright [post-hoc comparison, $p<0.01$] flash stimuli in comparison to CTRL WT and DM WT+L-DOPA mice. L-DOPA treatment was able to restore ERG responses of DM WT mice (DM WT+L-DOPA) to those of CTRL WT mice. Similarly, DM rTHKO+Veh mice had severely delayed responses from CTRL WT and DM WT+L-DOPA animals at the bright flash stimulus [post-hoc comparison, $p<0.05$]. The color of the asterisk indicates the treatment group to which significance was reached.

3.4.4 Retinal transcript levels of key dopamine proteins unchanged with diabetes

Since our results showed that diabetes produced retinal DA deficiency, we were interested in determining if changes in *Th* transcript levels may mediate this pathology. Using real-time RT-PCR, we found that diabetes did not significantly alter *Th* levels (Figure 3-7 and Table 3-4), though L-DOPA treatment resulted in a trend for *Th* down-regulation. The specificity of our *Th* primers was confirmed as we found more than 4 fold reduction in *Th* expression in rTHKO mice [Figure 3-7 and Table 3-4, Student's t values: DM rTHKO+Veh=5.964 and DM rTHKO+L-DOPA=5.928, $p<0.01$], regardless of L-DOPA treatment. Next, we were interested if diabetes affected transcript levels of DA receptors, specifically D1 receptor (*Drd1*) and D4 receptor (*Drd4*), which are selectively involved in visual acuity and contrast sensitivity, respectively (Jackson et al., 2012). We found no significant changes in the transcript levels of *Drd1* and *Drd4* (Figure 3-7 and Table 3-4). Interestingly, we found that L-DOPA treatment led to a significant down-regulation of *Drd4* transcript level in DM WT mice [Figure 3-7 and Table 3-4, Student's t value: DM WT+L-DOPA=2.154, $p<0.05$], corresponding to a previous report that suggested DA-dependent regulation of *Drd4* expression level (Jackson et al., 2011).

Treatment Group	n	*Th* Expression	*Drd1* Expression	*Drd4* Expression
CTRL WT	10	1	1	1
DM WT+Veh	5	1.05	1.30	1.08
DM WT+L-DOPA	6	-1.61	1.05	-2.14*
DM rTHKO+Veh	6	-5.38**	-1.28	1.18
DM rTHKO+L-DOPA	6	-4.80**	-1.29	1.27

Table 3-4. Fold changes in mRNA levels of genes of interest for each experimental group compared to CTRL WT group. Significances depicted here reflect those indicated in Figure 6. The asterisk indicates significant difference between the respective treatment group and CTRL WT group. Abbreviation used in the table: n = sample size.

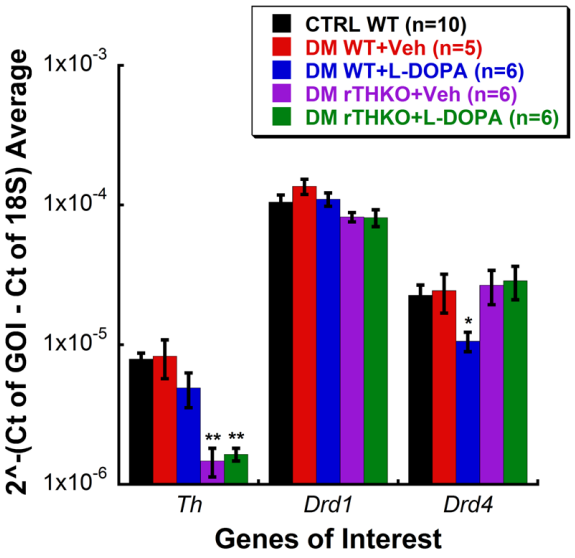

Figure 3-7. mRNA levels of the examined dopaminergic system related genes. rTHKO mice had significantly lower expressions of *Th* than CTRL WT mice [$p<0.01$]. Diabetes in DM WT mice did not induce a significant change in mRNA levels of *Th*, *Drd1*, or *Drd4* when compared to the CTRL WT mice. Interestingly, L-DOPA treatment caused a down-regulation of *Drd4* [$p<0.05$], but not of *Drd1*, in DM WT mice when compared to CTRL WT mice. Note that the Y-axis refers to averaged $2^{-\Delta Ct}$ values, with ΔCt calculated by subtracting cycle threshold (Ct) of 18S from Ct of gene of interest (GOI). The asterisk indicates significant difference between the respective treatment group and CTRL WT group. Abbreviations used in the figure: Ct = cycle threshold; GOI = gene of interest.

3.4.5 Selective improvement in visual function with dopamine receptor agonists

Next, we examined if activation of DA pathways with selective receptor agonists could reverse visual defects in animals with established diabetes. To test this, we induced diabetes in a group of WT mice with STZ and maintained them for 8 weeks. After 8 weeks of diabetes, we injected the animals with vehicle, D1 receptor (D1R) agonist (SKF38393), and D4 receptor (D4R) agonist (PD168077). We found that DA agonist treatment was able to restore both visual acuity [Figure 3-8A, $F(2,10)=8.550$, $p=0.007$] and contrast sensitivity [Figure 3-8B, $F(2,10)=5.321$, $p=0.027$], but not to the CTRL WT levels. More interestingly, we found that administration of D1R agonist only improved visual acuity while administration of D4R agonist only improved contrast sensitivity. These findings replicate those of Jackson et al. (2012) in normoglycemic animals and suggest that diabetes does not alter the distinct roles of D1R and D4R on visual function. More importantly, these results indicate that treatments targeting the dopaminergic system could be beneficial to patients with established diabetes.

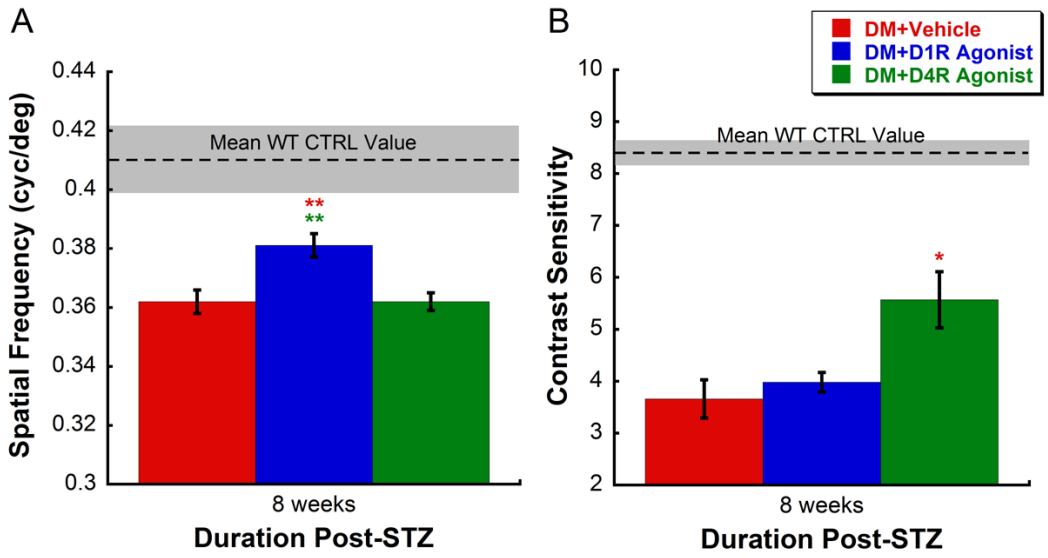

Figure 3-8. Distinct improvement in OKT responses of 8-week DM WT mice (n=7) after treatments with selective dopamine receptor agonists. (A) Visual acuity values of DM WT mice improved significantly when treated with D1 receptor agonist [post-hoc analysis, $p<0.01$]. Treatment with D4 receptor agonist failed to improve visual acuity. **(B)** Conversely, contrast sensitivity levels of DM WT mice were enhanced significantly only when treated with D4 agonist [post-hoc analysis, $p<0.05$]. However, neither treatment restored visual function (visual acuity and contrast sensitivity) to CTRL WT levels [indicated by the dashed lines with their variance (± SEM) represented by grey boxes]. Note that the Y-axis does not start at zero; this is modified to more clearly show the differences between treatment groups.

3.5 Discussion

We conducted noninvasive functional assessments in diabetic rodents as well as post-mortem analyses of the dopaminergic pathways in retinal tissues to examine the overall role of retinal DA in early visual deficits due to diabetes. We found that diabetes produced retinal DA deficiency, and that pharmacologic replacement of DA or stimulation of DA receptors ameliorated diabetes-associated visual dysfunction.

3.5.1 Dopamine Deficiency in Diabetes

In accordance with previous reports (Trulson and Himmel, 1983; Nishimura and Kuriyama, 1985), our data show reduced retinal DA contents in both DM rats and mice, as early as 4 to 5 weeks post-STZ (Figures 3-1 and 3-2). Dysregulation at multiple site(s) of DA metabolic processing has been postulated to reduce DA abundance, but published results show inconsistencies. First, it is possible that retinal DA reduction in diabetes originates from decreased biosynthesis. Several reports have documented diminished L-DOPA accumulations in diabetic retinas with normal activity levels of TH, thereby concluding that DA deficiency is due to reduced tyrosine level in the retina (Fernstrom et al., 1984, 1986). However, others indicate that DA alteration is due to decreased TH activity, leading to reduced rate of tyrosine hydroxylation (Northington et al., 1985). Although the *Th* transcript levels did not change due to diabetes in the present study (Figure 3-7 and Table 3-4), some reports have suggested that retinal TH protein levels are down-regulated (Seki et al., 2004), presumably from increased post-translational processing of the TH proteins or apoptotic loss of dopaminergic neurons (Gastinger et al., 2006). These inconsistencies may be attributed to animal strain differences, variable glycemic controls, or different durations of hyperglycemia across studies (Kirwin et al.,

2009; Kern et al., 2010a; Robinson et al., 2012). A second plausible mechanism for reduced DA levels in diabetic animals is enhanced turnover of DA. Although we did not measure DA turnover rate direclty in this study, we found that metabolism of DA to DOPAC (DOPAC/DA ratio), an indirect assessment of DA turnover (Witkovsky, 2004), was not altered by diabetes (Figures 3-1 and 3-2). Mitochondrial dysfunction (Kowluru, 2005) and oxidative stress associated with diabetes (Kowluru and Chan, 2007; Sasaki et al., 2010) may also result in enhanced oxidation of DA and render it inactive biologically – a possibility that should be explored in future studies.

Aside from dysfunction of the dopaminergic neurons, disturbances in light transmission and/or retinal circadian clock pathways may alter retinal DA content, as retinal DA synthesis and release are tightly regulated by such mechanisms (Iuvone et al., 1978; Doyle et al., 2002). Because cataract is a common complication of diabetes (Obrosova et al., 2010), increased opacity of the lens could attenuate light transmission to the retina, and thereby impair light-induced up-regulation of DA in diabetic retinas. However, we found reduced retinal DA levels starting at 4 weeks after STZ (Figure 3-1A), prior to significant development of cataract at 6 weeks in STZ-induced diabetic rats (Aung et al., 2013). Moreover, despite the lack of cataract development in our STZ mice at the 5-week time-point, we still found reduced retinal DA levels in these mice (Figure 3-2). Therefore, diminished light input is not a likely contributing factor for early diabetes-induced retinal DA deficiency. In regards to altered circadian clocks underling DA deficiency in diabetes, studies have shown that both retinal and peripheral circadian clocks are dysfunctional in diabetic animals (Young et al., 2002; Herichová et al., 2005; Busik et al., 2009; do Carmo Buonfiglio et al., 2011) and mice with circadian clock

mutations recapitulate diabetic phenotypes (Marcheva et al., 2010; Doi, 2012; Bhatwadekar et al., 2013). Therefore, further research is warranted to explore how abnormal circadian pathways in a diabetic retina can lead to alterations in the dopaminergic system and to elucidate other potential upstream mediator(s) (e.g. oxidative stress, inflammation, vascular dysfunction) that can lead to DA deficiency.

3.5.2 Dopamine Deficiency and Visual Deficits

Our data suggest that disruptions in the retinal dopaminergic system due to diabetes produce profound visual deficits. Not only does the onset of DA reductions coincide with the onset of visual defects, the results from L-DOPA and DA receptor agonist treatments provide evidence for the causal role of DA deficiency in visual loss in early-stage DR. These results are consistent with studies on multiple disorders with known abnormalities in DA signaling, such as Parkinson's disease and retinitis pigmentosa, that have been shown to develop visual deficits (Brandies and Yehuda, 2008; Bodis-Wollner, 2009). However, visual symptoms in disorders that involve the brain may not be completely due to local effects of retinal DA deficiency, as DA is involved in multiple levels of mammalian visual processing, including the thalamic and cortical relays. In addition, examining visual defects in retinitis pigmentosa models due to depressed retinal dopaminergic system is complicated by the severe vision loss associated with photoreceptor degeneration (Nir and Iuvone, 1994; Brandies and Yehuda, 2008; Atkinson et al., 2013). Therefore, our findings, especially with the retinal-specific ERG results and the use of rTHKO mice, corroborate the role of diminished retinal DA bioavailability in visual dysfunction. The effect is unlikely due to degeneration of retinal neurons since the examined time-points were before reports of retinal degeneration in

diabetes (Martin et al., 2004; Kern et al., 2010b; Villarroel et al., 2010; Barber et al., 2011). Furthermore, no evidence of retinal degeneration was observed due to deletion of *Th* in the original characterization of the rTHKO mice (Jackson et al., 2012). However, the loss of retinal DA in these mice was incomplete. The retinal DA levels and the numbers of TH-positive cells in the rTHKO mice were approximately 10% of wild type controls (Jackson et al., 2012), similar to the DA levels observed in the present study (Table 3-3). Thus, there may be a small number of dopaminergic amacrine cells in which the gene was not disrupted, resulting in a low level of *Th* expression (Figure 3-7 and Table 3-4). It is unknown whether complete elimination of retinal DA would have a more severe effect on cell survival, retinal function, and ultimately visual function. Nonetheless, examination of the potential neuroprotective effects of chronic activation of DA pathways in a diabetic retina would be interesting because some studies have found that stimulation of DA pathways, especially through D1R activation, could protect retinal neurons from injury due to oxidative stress or glutamate neurotoxicity under *in vitro* conditions (Kashii et al., 1994; Yamauchi et al., 2003; Li et al., 2012).

How, then, does DA deficiency lead to visual deficits? Jackson et al. (2012) reported that the global effects of DA on vision are mediated through actions of D1 and D4 receptors, possibly by uncoupling gap junctions in distinct retinal neurons. D1Rs are expressed on horizontal cells, where their activation uncouples electrical synapses and restricts current flow between these cells. Horizontal cell uncoupling may narrow the ganglion cell center-surround receptive field and thereby produce sharper visual acuity (Witkovsky, 2004; Bloomfield and Völgyi, 2009). Thus, a diabetes-mediated attenuation of DA signaling through D1Rs could expand the receptive fields of ganglion cells and

lead to lower spatial frequency thresholds (Jackson et al., 2012). Conversely, D4Rs are localized to photoreceptors, where the binding of DA to the receptor limits the transmission of signals between rods and cones via electrical synapses (Witkovsky, 2004; Bloomfield and Völgyi, 2009). Therefore, a decrease in D4R activation could enhance coupling of rods and cones and result in shunting of cone signals into rod pathways. Under rod saturating light-adapted conditions, this could diminish contrast sensitivity (Jackson et al., 2012). However, it is important to recognize the possibility of diabetes altering melatonin (do Carmo Buonfiglio et al., 2011; Hikichi et al., 2011), a neuromodulator with a reciprocal and antagonistic relationship to DA, which may potentiate the effects of DA reduction on visual deficits (Tosini et al., 2012). Although the mice used in the study were on C57BL/6 background with minimal melatonin synthesis, future testing should be conducted to understand the contributions of dopamine-melatonin interactions to visual dysfunction in diabetes. Furthermore, although *Drd1* and *Drd4* transcript levels were not affected by diabetes in our model (Figure 3-7 and Table 3-4), it is still possible that dysregulation in the protein or activity levels of DA receptors could augment the effects of DA deficiency on vision.

3.5.3 Diabetes-induced Dopamine Deficiency and Clinical Relevance

In conclusion, we found that reduced retinal DA content is an underlying factor for the early visual deficits observed in diabetic retinopathy. These data support our previous hypothesis that dysfunction in the neural retina due to diabetes is a contributing factor to visual dysfunction as L-DOPA treatment significantly improved retinal function and thereby vision. Importantly, our results have translational relevance as we discovered that restoring DA levels (L-DOPA) or activating DA pathways (DA receptor agonists) in the

retina may serve as therapeutic interventions for early-stage DR. Lastly, exploring how DA deficiency may underlie other diabetes-associated neuropathies and understanding why dopaminergic neurons are one of the retinal cell types susceptible to these diabetic insults may reveal new therapeutic avenues for diabetic retinopathy and other disorders that involve DA deficiency.

CHAPTER 4: DEFECTIVE FUNCTIONAL HYPEREMIA MAY CONTRIBUTE TO EARLY DIABETES-INDUCED VISUAL DEFICITS IN STREPTOZOTOCIN-INDUCED DIABETIC ANIMALS

This chapter is currently prepared to submit as a full-length manuscript to *Experimental Eye Research*.

4.1 Abstract

Purpose: Functional hyperemia is a hemodynamic response utilized by the central nervous system to modulate local blood flow to match neuronal activity during periods of activation. Recent studies have demonstrated a significant reduction in this response in diabetic patients with preclinical diabetic retinopathy. By limiting blood flow during periods of increased neuronal activity, dysregulation of functional hyperemia may impair retinal function and ultimately vision; however, such relationships remain unclear. Therefore, the first objective of this study was to establish the temporal relationship between defective hyperemic response and visual deficits in a rodent model of early-stage diabetic retinopathy. The second objective was to investigate if modulating the bioavailabilities of two vasoactive metabolites of arachidonic acid [20-hydroxyeicosaetraenoic acids (20-HETEs)[1] and epoxyeicosatrienoic acids (EETs)[2]], which have been implicated as potential molecular mediators for the diminished

[1] 20-HETE is a vasoconstrictor.

[2] EETs are a family of vasodilators.

functional hyperemia response, could alleviate the early visual deficits observed in diabetic retinopathy.

Methods: For the first objective, we used two groups of experimental rats: control (CTRL) and diabetic (100 mg/kg streptozotocin, DM). Functional hyperemia (by assessing flicker-induced vasodilatory response) and visual function (by measuring optokinetic response) of the animals were monitored biweekly. For the second objective, DM rats were injected daily either with vehicle or inhibitor (HET0016 for inhibition of 20-HETE synthesis and AUDA for inhibition of EETs degradation) after a week of established diabetes. CTRL rats were also included to receive either vehicle or inhibitor (as described above) to evaluate potential side-effects of the drugs. Rats were assessed at 4- and 6-week time-points for visual function with optokinetic tracking and cataract formation with slit lamp exam.

Results: Significantly diminished flicker-induced vasodilations were found in the retinal arterioles of DM rats when compared to CTRL rats, which occurred 2 weeks prior to the onset of visual deficits (4 weeks post-STZ). For the pharmacologic experiments, administration of HET0016 or AUDA to DM rats delayed the onset of visual deficits, and visual function of drug-treated DM rats remained consistently higher than vehicle-treated DM rats. The beneficial effects of these pharmacological treatments were not due to differences in severity of hyperglycemia or cataract formation.

Conclusions: Our findings show that defects in retinal hyperemic response developed prior to the visual deficits, suggesting the potential of defective functional hyperemia damaging the neural retina and leading to visual dysfunctions. Furthermore, we found that inhibiting 20-HETE production or EETs metabolism improved visual function of

DM animals. These drugs may serve as potential therapeutic options to preserve visual function during early-stage diabetic retinopathy.

4.2 Introduction

Diabetic retinopathy (DR) is a common complication of diabetes and a leading cause of blindness in working-age adults (King et al., 1998; Klein, 2007). Although DR is diagnosed clinically with the observation of major structural lesions in the retinal vasculature (Frank, 2004), there are now studies that show diabetic patients exhibiting defective hemodynamic responses preceding clinical signs of DR. Specifically, several reports have found a dramatic reduction in flicker-induced vasodilation of the retinal vasculature, an assessment of the functional hyperemia response in the retina (Garhofer et al., 2004; Mandecka et al., 2007, 2009; Bek et al., 2008; Nguyen et al., 2009; Pemp et al., 2009; Lecleire-Collet et al., 2011; Lasta et al., 2013). Functional hyperemia, mediated by neurovascular coupling, is a hemodynamic response employed by the retina to match blood flow according to neural activity as the retina is stimulated by light (Riva et al., 2005; Attwell et al., 2010). Insufficient hyperemic response could potentially deprive the active retina of its required nutrients and oxygen, leading to a state of ischemia or hypoxia (Blair et al., 2009; Ly et al., 2011; Qian and Ripps, 2011). Such a dysregulation could ultimately impair retinal function. Mounting evidence shows significant neural deficits in early-stage DR in both diabetic patients and animal models, manifested as alterations in electroretinogram (ERG) (Ghirlanda et al., 1997; Shirao and Kawasaki, 1998; Wolff et al., 2010; Ly et al., 2011) and impairments in visual function (Jackson and Barber, 2010; Kirwin et al., 2011; Akimov and Rentería, 2012; Aung et al., 2013). However, the exact impact of defective hyperemic responses on retinal and visual

dysfunctions in early-stage DR remains unclear. To better understand the relationship of these pathologies, we have chosen animal models due to cost-effectiveness, short follow-up times, the options to utilize pharmacological and genetic manipulations to explore the underlying mechanism(s), and the ability to control for potential confounding variables, such as age, disease onset and duration. Thus, the first part of the study was to develop an imaging setup (Figures 4-1 and 4-2) to assess the associated occurrences of defective functional hyperemia and visual deficits in a rodent model of Type 1 diabetes.

Mechanistically, several recent reports suggest changes in the levels of vasoactive arachidonic acid metabolites synthesized by cytochrome P450 (CYP) enzymes, 20-hydroxyeicosaetraenoic acids (20-HETEs)[3] and epoxyeicosatrienoic acids (EETs)[4], may be the culprits of defective hyperemic response in diabetes (Metea and Newman, 2006; Mishra and Newman, 2010, 2011). Specifically, those studies reasoned that diabetes induced an up-regulation of 20-HETE and/or a down-regulation of EETs, leading to inability of retinal vessels to vasodilate effectively in response to light stimulation. Further supporting this hypothesis, another study shows that inhibition of 20-HETE production attenuated the early diabetes-induced decreases in retinal blood flow (Wang et al., 2011). As proper functional hyperemia response is essential for normal retinal function (Riva et al., 2005), it is highly plausible that diminished hyperemic response is a contributing factor to the visual deficits seen in early-stage DR. By restoring the

[3] 20-HETE is a terminal hydroxylation product of arachidonic acid catalyzed by CYP4A enzyme. It increases smooth muscle tone of the vessels by inhibiting calcium-dependent K^+ (K^+_{Ca}) channels, leading to depolarization of smooth muscle cells, activation of L-type Ca^{2+} channels and subsequently contraction (Fleming, 2001).

[4] EETs are generated by CYP2A enzyme and induce relaxation of the smooth muscle cells by activating K^+_{Ca} channels, resulting in hyperpolarization of the cells and inhibiting L-type Ca^{2+} channels (Fleming, 2001).

imbalance in 20-HETE and EETs levels, we may be able to improve hyperemic responses and ultimately attenuate early visual dysfunction due to diabetes. Therefore, the second purpose of the study was to investigate if daily pharmacological inhibition of 20-HETE synthesis (inhibiting the process of hydroxylation) or upregulation of EETs availability (inhibiting the metabolism) would ameliorate early diabetes-induced visual deficits.

4.3 Materials and Methods

4.3.1 Animals and Experimental Design

Two month old pigmented male Long Evans rats (150-225 g; Charles River, Wilmington, MA) were used in the study and were housed in ventilated cages on a 12 h light-dark cycle with food and water provided *ad libitum*. All procedures were approved by the Atlanta VA Institutional Animal Care and Use Committee and conformed to the ARVO Statement for the Use of Animals in Ophthalmic and Vision Research.

Examining Onset of Defective Hyperemic Response. Diabetes was induced in a group of rats with a single intravenous injection of streptozotocin (STZ: 100 mg/kg; Sigma-Aldrich, St. Louis, MO) dissolved in 8:1 ratio of citrate buffer/50% glucose solution (DM, n=8). Another group of rats was injected with citrate buffer/50% glucose solution to serve as controls (CTRL, n=6). Diabetes was defined as two successive daily blood glucose levels >250 mg/dL (as determined with hand-held blood glucose meter from tail-prick blood), which routinely occurred 2-3 days after STZ administration (Clee and Attie, 2007). If DM rats were not gaining weight, they received pellets of sustained-release subcutaneous insulin (Linplant; Linshin Canada, Scarborough, ON, Canada) at a dose adequate to prevent cachexia, but insufficient to control hyperglycemia (13 ± 3 mg/pellet with a release rate of approximately 2 U/day) (Thulé et al., 2006). Rats were

assessed biweekly for hyperemic response, visual function (acuity and contrast sensitivity), and lens opacity during the 6-week study period to delineate the temporal relationship between these early functional deficits in DR.

Probing the Visual Benefits of Manipulating 20-HETE and EETs levels. To study how modulating the levels of 20-HETE and EETs would affect the overall visual outcome of diabetic animals, we conducted the following two separate studies. For both experiments, rats were assessed at 4 and 6 weeks for visual function with optokinetic tracking (OKT) and cataract formation with slit lamp exam.

Effects of Inhibiting 20-HETE Synthesis on Visual Function. Rats were randomly separated into three groups (n=5 per group): CTRL+Veh, DM+Veh, and DM+HET0016. Diabetes was induced as described above. After STZ-treated animals had maintained hyperglycemia for a week, daily intraperitoneal (i.p.) injection of either vehicle (Veh) or HET0016 (dissolved in DMSO, 2.5 mg/kg; Cayman Chemical, Ann Arbor, MI) was initiated. HET0016 [N-hydroxyl-N'-(4-n-butyl-2methylphenyl)-formamide] is a potent and selective inhibitor of CYP 4A enzyme, leading to reduced formation of 20-HETE (Miyata et al., 2001). HET0016 was not administered to CTRL animals because of previous reports indicating CTRL animals do not tolerate HET0016 well (Wang et al., 2011).

Effects of Preventing EETs Degradation on Visual Function. In this experiment, there were four groups of rats (n=4 per group): CTRL+Veh, CTRL+AUDA, DM+Veh, and DM+AUDA. Diabetes was induced similarly with STZ treatment. Vehicle or AUDA (dissolved in 20% DMSO/PBS solution, 5 mg/kg; Cayman Chemical, Ann Arbor, MI) was administered daily subcutaneously to the rats after 1 week of established diabetes.

AUDA [2-(3-Adamantan-1-yl-ureido)-dodecanoic acid] is a selective inhibitor that efficiently reduces hydrolysis of EETs by soluble epoxide hydrolase, and thereby increases EETs bioavailability (Kim et al., 2004).

4.3.2 Assessing Flicker-induced Vasodilation

Light Stimulation. Filtered light (480-600 nm) from a fiber optic illuminator was gated with an electromechanical shutter (Optical Beam Shutter; Thorlabs, Newton, NJ) to generate 12 Hz flickering green light. Light with wavelength of 480-600 nm and a flicker frequency of 12 Hz were chosen because such wavelength and frequency have been shown to produce maximal functional hyperemia response in many species (Riva et al., 2005). Through a fiber optic bundle, the flicker light was reflected off a 45^0 angle prism mirror (TS Cold Mirror; Edmundoptics, Barrington, NJ) to focus onto the eye (Figure 4-1). The luminance of the light was 4000-5000 lux at the surface of the eye.

Measurement of Flicker-induced Dilation. Each animal was injected i.p. with indocyanine green dye (ICG, 20 mg/kg; IC-Green; Akorn, Lake Forest, IL) to label the blood vessels (Figure 4-2A and 4-2B). The retinal vasculature was imaged with a scanning laser ophthalmoscope (SLO; Heidelberg Spectralis; Heidelberg Engineering, Carlsbad, CA). While the vessels were continuously monitored with the SLO, the retina was stimulated with flickering light. Each stimulation trial consisted of 10 sec of baseline measurement, followed by 15 sec of stimulation with flicker light, and ending with 10 sec of recovery assessment. When needed, stimulation trials were repeated with a 2 min interval period to separate the trials.

Measurement of the flicker-induced vasodilation was performed offline with an imaging processing and analyzing program (ImageJ; NIH, Bethesda, MA). First, a line

was drawn perpendicular to a first-order arteriole or venule at one optic disk distance away from the optic nerve (Figure 4-2B). Then, the lumen of the vessel that intersected with the line was extracted over the entire stimulation trial, generating a distance (vessel diameter) vs. time line scan image (also known as kymograph) (Figure 4-2C). Next, we calculated the vessel caliber at each timeframe by taking the difference in x values with the same y value. The resulting differences vs. y values were used to create luminal diameter vs. time graph. Finally, to calculate the percent vasodilation, we averaged the vessel diameters at 0-5 sec (baseline) and 15-20 sec (stimulation) and measured the percent change in vessel caliber from baseline to stimulation.

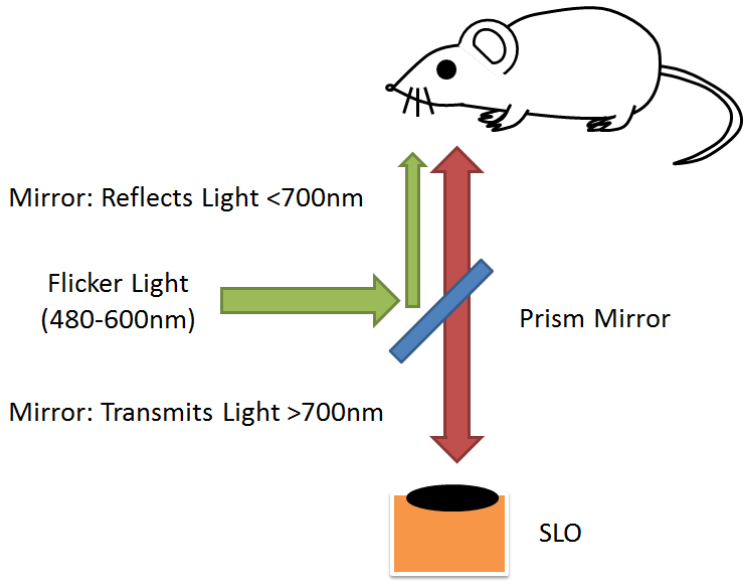

Figure 4-1. Schematic illustrating the imaging setup. The animal is placed on a heated platform with its eye directly facing the scanning laser ophthalmoscope (SLO). SLO is used to image the retinal vasculature that has been filled with indocyanine green (ICG), which has an excitation and emission wavelength of 805 nm and 835 nm, respectively. While the vessels are continuously imaged, filtered green flicker light (at 12 Hz) is reflected off a prism mirror onto the eye to activate the retina. The prism mirror is positioned between the eye and SLO to allow for an even exposure of flicker light to the eye. The prism mirror is designed to reflect light with wavelength less than 700 nm (flicker light) and allow transmission of light with wavelength greater than 700 nm (SLO imaging light). Abbreviation used in the diagram: SLO = scanning laser ophthalmoscope.

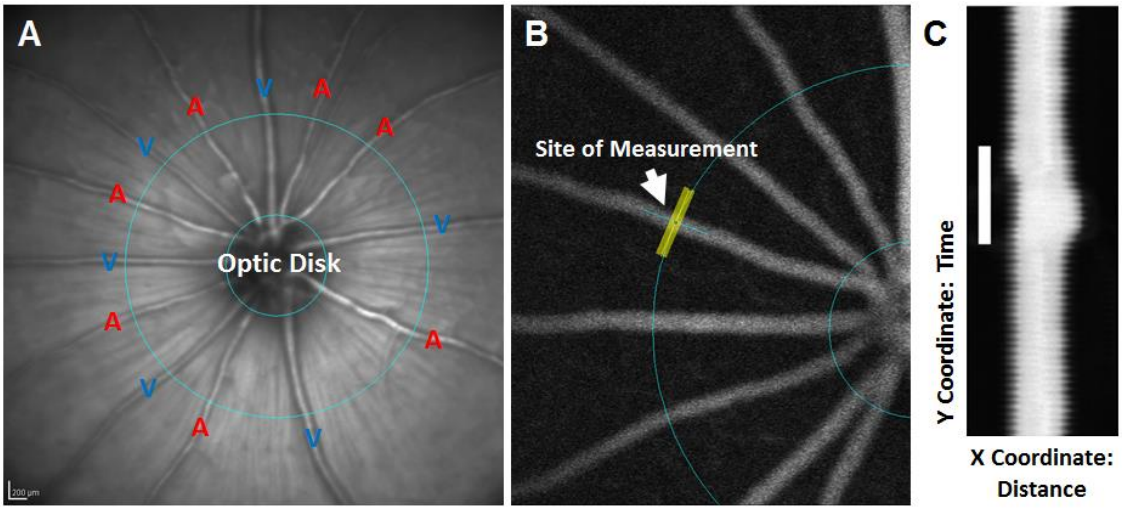

Figure 4-2. Images detailing the process of analyzing flicker-induced vasodilatory response. (A) A fundus image of a rat eye with the focus on the retinal vasculature. The fundus image is used to determine (1) whether a vessel is an arteriole or a venule, (2) the order of the vessel, and (3) the size of the optic disk. **(B)** An image of a rat eye with its retinal vasculature labeled with indocyanine green (ICG). For each vessel of interest, the hyperemic response is assessed at one optic disk distance away. To generate the subsequent kymograph, a line perpendicular to the vessel of interest is drawn and the vessel lumen over the stimulation trial is then extracted. **(C)** A sample kymograph of a vessel over a stimulation trial [modified from (Srienc et al., 2010)]. A kymograph is generated by compiling the image of the line drawn in **(B)** over time. The white space signifies the lumen of the vessel, and the white bar corresponds to the period when flicker light is delivered. The expansion of the lumen indicates the presence of a flicker-induced vasodilatory response. Abbreviations used in the figure: A = arteriolar and V = venular.

4.3.3 Optokinetic Tracking Assessments

Visual function of each animal was tested using the virtual OKT system (OptoMotry system; Cerebral-Mechanics, Lethbridge, AB, Canada), as previously described (Douglas et al., 2005; Aung et al., 2013). In brief, an observer monitored the presence or absence of an animal's tracking motion in real-time through a video camera positioned above the animal. Tracking is defined as slow head movements in the same direction and speed as the rotating gratings. The visual acuity and peak contrast sensitivity were determined with a staircase paradigm, under which the response threshold was crossed three times.

4.3.4 Slit Lamp Cataract Exam

A researcher graded the lens condition (blinded of the treatment condition) using slit lamp illumination on a cataract grade scale described previously (Muranov et al., 2004; Aung et al., 2013). In brief, the classifications were as follows: Grade 0, a clear lens; Grade 1, swollen fibers and subcapsular opacities; Grade 2, nuclear cataract in lens and swollen fibers in lens cortex; Grade 3, severe nuclear cataract with perinuclear area opacity in lens; Grade 4, total opacity of lens. To ensure equivalent assessment of the cataract severity for each observation, the slit lamp illumination was standardized to the same slit width and light intensity for all examinations.

4.3.5 Statistical Analysis

Statistical analysis was performed using commercial statistical software (SigmaStat 3.5; Aspire Software International, Ashburn, VA). For the functional hyperemia assessment, Student's t-test was used to compare between treatment groups. For the remaining comparisons, two-way repeated-measures ANOVAs were used to

compare different parameters between treatment groups over time. P-values reported are the interaction effect, unless otherwise noted. Post-hoc multiple comparisons for all ANOVA tests were performed when appropriate with p-value corrected with Rough False Discovery Rate method [calculated as (p*(#tests+1))/(2*(#tests))]. For visual function assessments and cataract scores, measurements from both eyes were analyzed and averaged prior to averaging for the group means. All analyses were performed with *a priori* significance set at $\alpha<0.05$. For the asterisk symbol: * indicates $p<0.05$, ** defines $p<0.01$, and *** means $p<0.001$. All data are presented as Mean ± SEM.

4.4 Results

4.4.1 Diabetic rats exhibited diminished hyperemic response prior to visual deficits

To determine if a rodent model of diabetes replicated the vascular dysfunctions found in diabetic patients, we developed an imaging setup and analysis to assess flicker-induced vasodilatory response in rat. We found that CTRL rats exhibited approximately 11.7% dilation in their 1st-order arterioles and 5.5% dilation in their 1st-order venules (Figure 4-3); values that were comparable to the levels found in other studies on assessing flicker-induced vasodilation responses in rats (Srienc et al., 2010; Mishra and Newman, 2011). More importantly, we found that the arterioles of DM animals showed a marked decrease in flicker-induced vasodilation when compared to the CTRL animals [Figure 4-3, Student's t-value=1.88, $p<0.05$] at 2 weeks post-STZ. Though not statistically significant, the venular response was also reduced in DM rats when compared to CTRL rats (Figure 4-3). Flicker-evoked vascular responses were not consistently detected in DM rats after 4 weeks post-STZ due to increased lens opacity deteriorating the image quality. In relation to visual dysfunctions, DM rats in this group

showed a significant reduction in their visual acuity starting at 1 month post-STZ (data not shown), similar to our previous report (Aung et al., 2013). Altogether, we found that defective functional hyperemia occurred prior to the onset of visual deficits in STZ-induced DM rats.

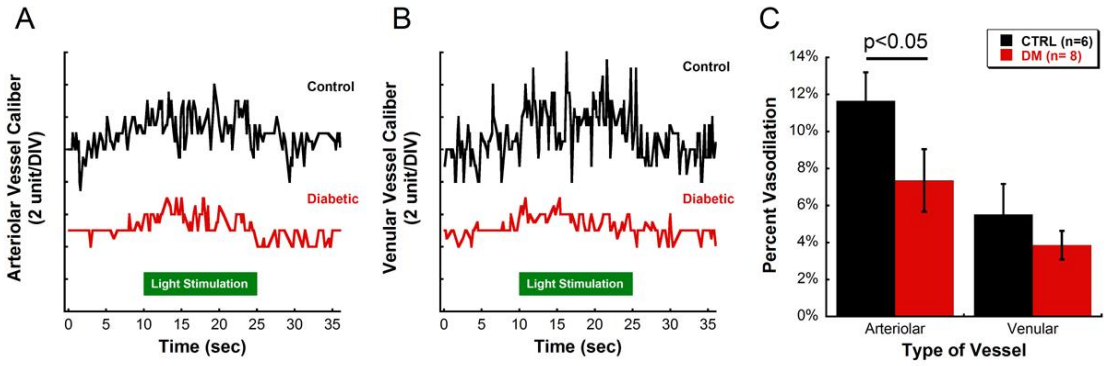

Figure 4-3. STZ-induced DM rats exhibited significant reductions in flicker-induce vasodilation. (A) Representative tracings of *arteriolar* vessel caliber over a stimulation trial between CTRL (**black**) and DM (**red**) rats. **(B)** Representative tracings of *venular* vessel caliber over a stimulation trial between CTRL (**black**) and DM (**red**) rats. **(C)** DM rats had a significant reduction in percent arteriolar vasodilation in comparison to CTRL animals [Student's t-test, $p<0.05$]. Although not statistically significant, DM rats also exhibited a trend of diminished venular dilatory response in comparison to CTRL animals.

4.4.2 HET0016 treatment ameliorated diabetes-induced visual deficits

In this experiment, DM+Veh rats also exhibited significant deficits in visual acuity [Figure 4-4A, $F(4,20)=3.560$, $p=0.024$] and contrast sensitivity [Figure 4-4B, $F(4,20)=8.306$, $p<0.001$] compared to CTRL rats starting at 4 weeks post-STZ. HET0016 treatment was able to delay the onset and lessen the severity of the visual deficits due to diabetes (Figure 4-4). At 4 and 6 weeks post-STZ, DM+HET0016 rats consistently maintained higher visual acuity thresholds and exhibited significantly higher contrast sensitivities when compared to DM+Veh rats [post-hoc comparison, $p<0.01$]. These results indicate that chronic inhibition of 20-HETE synthesis led to visual improvement in DM animals.

4.4.3 AUDA treatment improved visual function of diabetic animals

Similarly, significant reductions in visual acuity [Figure 4-5A, $F(6,21)=6.993$, $p<0.001$] and contrast sensitivity [Figure 4-5B, $F(6,21)=3.320$, $p=0.019$] were found in this group of DM+Veh rats, starting at 4 weeks post-STZ. The deficits, however, seemed to be less severe than the DM+Veh rats in HET0016 experiment (most likely due to the less severe cataract formation, see Figure 4-7 and Section 4.4.5). Daily AUDA administration preserved the visual functions of DM rats (Figure 4-5). Specifically, DM+AUDA rats had significantly higher visual acuity levels at 4 weeks post-STZ [post-hoc comparison, $p<0.001$] and better contrast sensitivities at 4 and 6 weeks post-STZ [post-hoc comparison, $p<0.01$] than DM+Veh rats. Collectively, the data suggest that slowing the degradation of EETs ameliorated the early visual deficits in DM animals.

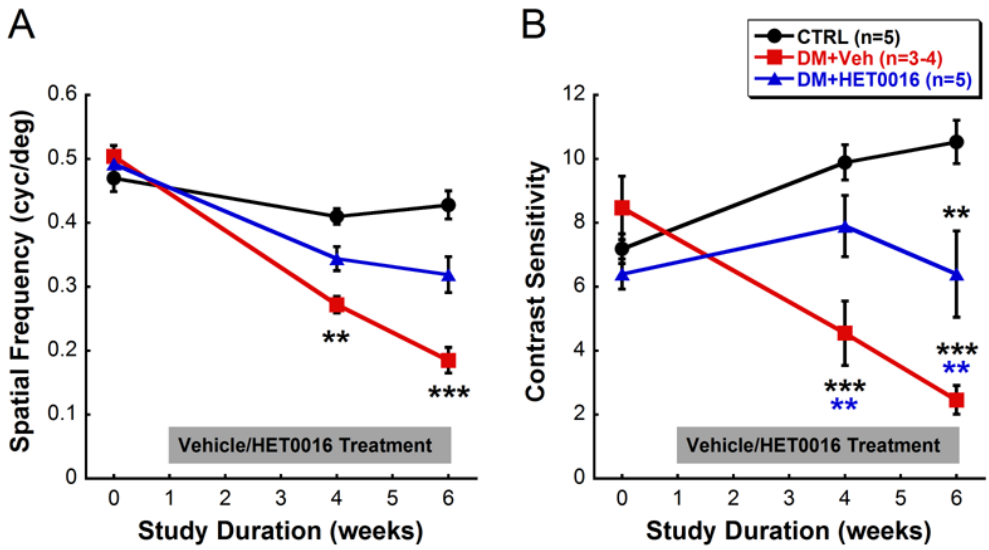

Figure 4-4. Inhibition of 20-HETE synthesis with HET0016 preserved visual functions of DM rats. **(A)** HET0016 treatment significantly delayed the onset of reduced visual acuity due to diabetes, as DM+HET0016 rats did not show a significant drop in spatial frequency threshold, even at the end of the study. On the other hand, DM+Veh had significantly reduced acuity thresholds starting at 4 weeks post-STZ when compared to CTRL+Veh animals [post-hoc comparison, $p<0.01$]. Although not statistically significant, DM+HET0016 rats showed a strong trend for improved visual acuity when compared to DM+Veh rats. **(B)** DM+Veh rats displayed decreased contrast sensitivities at 4 weeks post-STZ, while DM+HET0016 rats had such deficits only at 6 weeks post-STZ. HET0016 treatment significantly preserved contrast sensitivity when compared to DM+Veh rats [post-hoc comparison, $p<0.01$]. The color of the asterisk indicates the treatment group for which significance was reached.

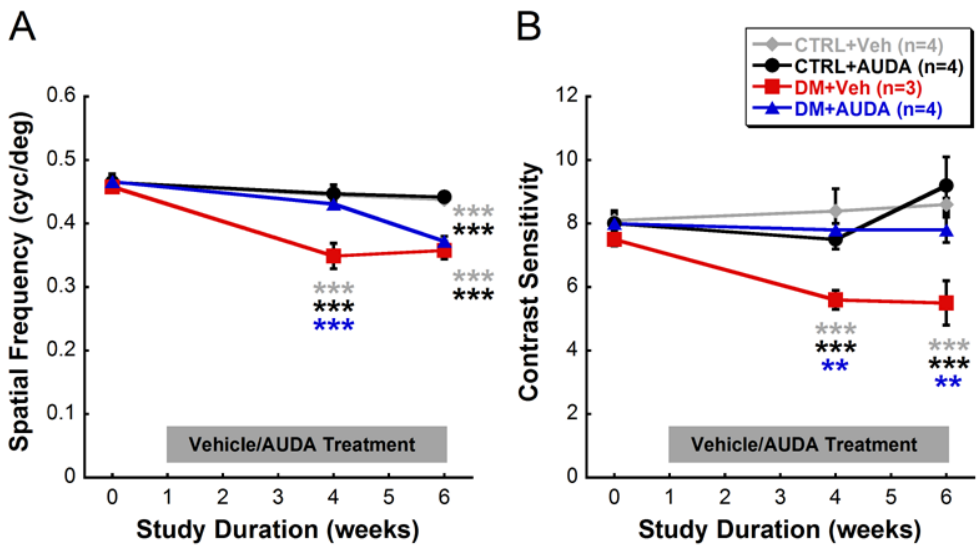

Figure 4-5. Inhibition of EETs degradation with AUDA improved visual functions of DM rats. (A) AUDA treatment significantly delayed the onset of reduction in visual acuity by 2 weeks. DM+Veh rats had significant deficits in their threshold levels at both 4 and 6 weeks post-STZ in comparison to both CTRL groups [post-hoc comparison, $p<0.001$], while DM+AUDA rats only exhibited such deficits at 6 weeks post-STZ [post-hoc comparison, $p<0.001$]. More importantly, DM+AUDA rats showed significant improvement in visual acuity thresholds at 4 weeks post-STZ compared to DM+Veh rats [post-hoc comparison, $p<0.001$]. **(B)** DM+Veh rats displayed decreased contrast sensitivities starting at 4 weeks post-STZ [post-hoc comparison, $p<0.001$], while DM+AUDA rats maintained their contrast sensitivity levels throughout the study period. AUDA treatment also significantly preserved contrast sensitivity when compared to DM+Veh rats [post-hoc comparison, $p<0.01$]. The color of the asterisk indicates the treatment group for which significance was reached.

4.4.4 Comparison of the visual benefits of HET0016 and AUDA treatments

Next, we compared the efficacies of HET0016 and AUDA in preserving visual functions of STZ-induced DM rats (Figure 4-6). To assess this, we calculated the differences in visual function between DM+HET0016 or DM+AUDA rats and their respective vehicle-treated DM rats. In terms of visual acuity, we found that HET0016 and AUDA had similar efficacies prior to 6-week time-point. However, improvements seen in the visual acuity of the DM+AUDA group significantly diminished at 6 weeks, while the DM+HET0016 group maintained its beneficial effects [Figure 4-6A, $F(2,14)=11.393$, $p=0.001$]. On the other hand, both HET0016 and AUDA sustained their beneficial effects on contrast sensitivity for the entire duration of the study [Figure 4-6B, $F(2,14)=6.900$, $p=0.008$], even though DM+HET0016 rats had lower contrast sensitivities than their respective vehicle-treated DM rats [post-hoc comparison, $p<0.05$].

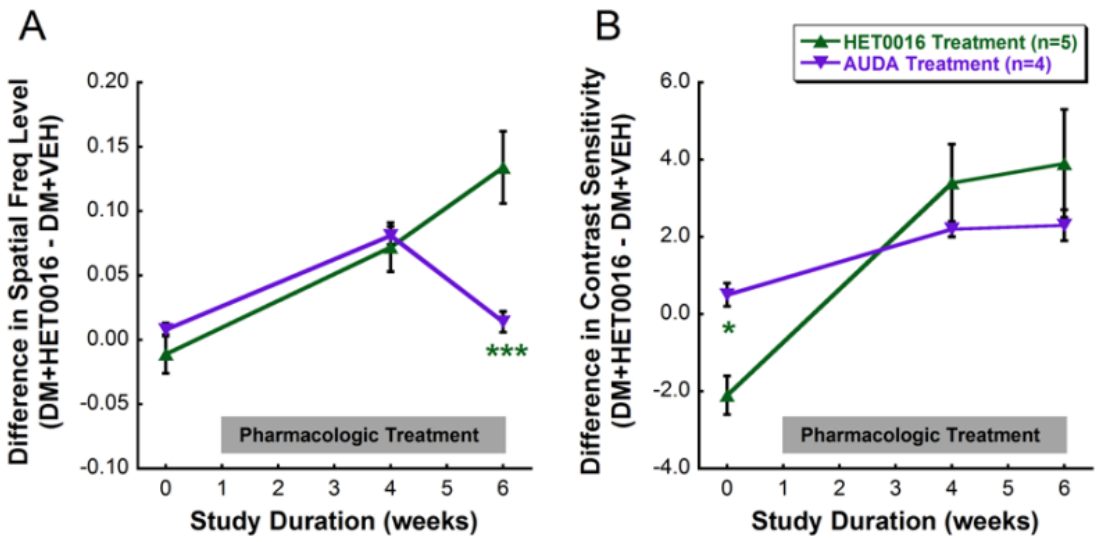

Figure 4-6. Efficacy of HET0016 and AUDA treatments differed in maintenance of visual acuity but was similar in preservation of contrast sensitivity. (A) Although both HET0016 and AUDA treatment led to preservation of visual acuity levels when compared to DM+VEH rats at 4 weeks, the effect of AUDA diminished greatly at 6 weeks while HET0016 continued to provide improvement [post-hoc comparison, $p<0.001$]. **(B)** Although the differences in contrast sensitivity in HET0016 experiment was significantly lower than that in AUDA experiment at baseline [post-hoc comparison, $p<0.05$], both HET0016 and AUDA treatments sustained their beneficial effects till the end of the study (as shown by consistent positive values for the difference between drug-treated and vehicle-treated animals).

4.4.5 HET0016 or AUDA treatment did not alter the general health and lens opacity of the treated diabetic animals

Regardless of treatment (vehicle, HET0016, or AUDA), all DM rats had significantly lower weights than CTRL rats at the end of study [Table 1, HET0016 Expt: $F(2,10)=23.645$, $p<0.001$, AUDA Expt: $F(3,10)=6.123$, $p=0.012$]. In the HET0016 experiment, DM+Veh rats approximately weighed 28% less than CTRL+Veh rats, while DM+HET0016 rats were 30% smaller than CTRL+VEH rats. In the AUDA experiment, AUDA treatment actually led to significant reductions in body weight for both CTRL and DM rats when compared to respective vehicle-treated rats [post-hoc comparison, $p<0.01$]. DM+Veh group were 13% smaller than CTRL+Veh group, while DM+AUDA group were 33% smaller than CTRL+Veh group. In terms of blood glucose (BG) levels, all STZ-treated rats (whether subsequently administered vehicle, HET0016, or AUDA) displayed similar severity of hyperglycemia at the end of study when compared to CTRL rats [Table 1, HET0016 Expt: $F(2,10)=270.664$, $p<0.001$ and AUDA Expt: $F(3,10)=30.700$, $p<0.001$]. In the HET0016 experiment, BG levels of DM+Veh rats and DM+HET0016 rats were 4.21 and 4.77 fold higher, respectively, than BG levels of CTRL+Veh rats. In the AUDA experiment, BG levels of DM+Veh rats and DM+AUDA rats were 3.82 and 3.52 fold higher, respectively, than BG levels of CTRL+Veh rats.

As cataract formation can significantly impact visual function (Aung et al., 2013), we compared the cataract scores between our treatment groups. Although the severity of cataract formation found in DM rats seemed to be higher in HET0016 experiment [Figure 4-7A, $F(4,20)=15.631$, $p<0.001$] than in AUDA experiment [Figure 4-7B, $F(6,22)=3.111$,

p=0.023], there were no differences in cataract scores between vehicle- and drug-treated DM rats (same finding for both HET0016 and AUDA experiments).

Species	Set	Treatment Group	Baseline		End of Study	
			Weight (g)	BG (mg/dl)	Weight (g)	BG (mg/dl)
Rat	1	CTRL	340 ± 15	129 ± 6	587 ± 23	120 ± 6
		DM	319 ± 16	128 ± 1	382 ± 15*	557 ± 22*
Rat	2	CTRL+Veh	211 ± 5	137 ± 7	432 ± 18	124 ± 5
		DM+Veh	226 ± 13	148 ± 9	312 ± 23*	522 ± 26*
		DM+HET0016	221 ± 7	131 ± 6	304 ± 7*	591 ± 9*
Rat	3	CTRL+Veh	165 ± 17	148 ± 14	439 ± 13	130 ± 5
		CTRL+AUDA	135 ± 10	132 ± 3	362 ± 6*	117 ± 3
		DM+Veh	136 ± 3	138 ± 3	383 ± 36	496 ± 74**
		DM+AUDA	129 ± 5	130 ± 3	292 ± 8***	459 ± 33**

Table 4-1. Average weight and blood glucose (BG) levels of the experimental groups (± SEM) used for this project. All STZ-induced DM rats, regardless of subsequent treatment (none, vehicle, HET0016, or AUDA), were significantly smaller [post-hoc comparison, $p<0.05$] and had higher blood glucose (BG) levels [post-hoc comparison, $p<0.001$] than CTRL rats at the end of the study. More importantly, modifying the levels of 20-HETE and EETs did not alter the body weight and severity of hyperglycemia of the DM rats. The color of the asterisk indicates the treatment group for which significance was reached. Abbreviations used in the table: BG = blood glucose.

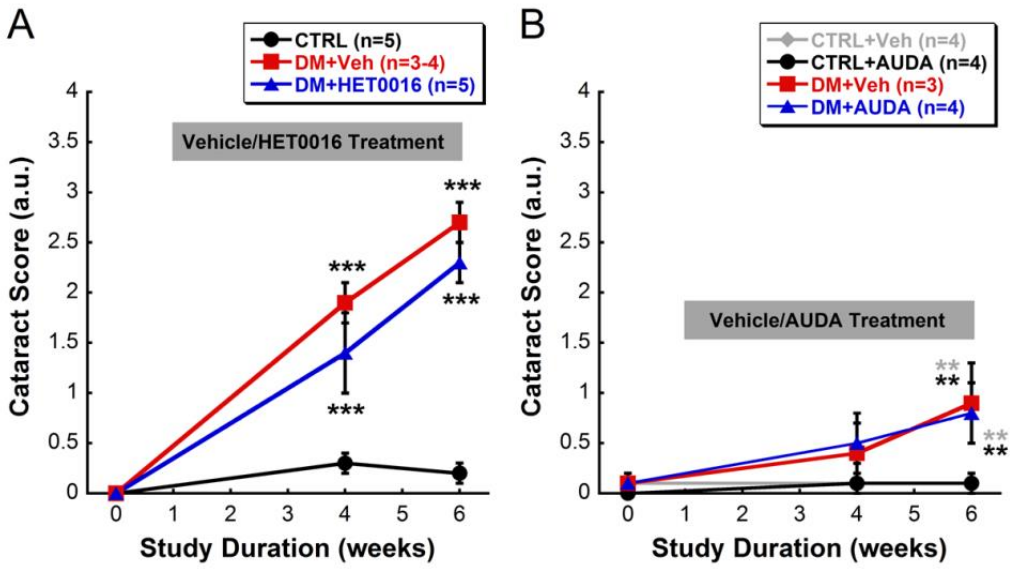

Figure 4-7. Severity of cataract formation in DM animals did not differ due to HET0016 or AUDA treatment. (A) For the HET0016 treatment experiment, both DM groups had significantly higher cataract scores than the CTRL group at 4 and 6 weeks [post-hoc comparison, $p<0.001$]. **(B)** For the AUDA treatment experiment, both DM groups developed significant cataract toward the end of the study, at 6-week time-point [post-hoc comparison, $p<0.01$]. The color of the asterisk indicates the treatment group for which significance was reached.

4.5 Discussion

In this study, we were able to reliably assess flicker-induced vascular responses from rats' retinal vessels and found that DM rats had significantly diminished flicker-evoked responses in their arterioles when compared to CTRL animals. Furthermore, the onset of reduced flicker-induced vascular response occurred 2 weeks prior to the detection of visual dysfunction. Also, we found that modulating levels of 20-HETE and EETs, putative mediators of retinal hyperemic response, improved visual functions of DM animals.

4.5.1 Detecting Functional Hyperemia in Early-stage DR

Reduction in functional hyperemia is one of the earliest retinal changes observed in diabetic patients, occurring before overt signs of clinical retinopathy (Garhofer et al., 2004; Mandecka et al., 2007, 2009; Bek et al., 2008; Nguyen et al., 2009; Lecleire-Collet et al., 2011; Lasta et al., 2013). Consistent with this finding, we found that DM rats exhibited reduced flicker-evoked vasodilation in their arterioles at 2 weeks post-STZ, a time-point prior to the development of microvascular lesions in diabetic rat retina (Curtis et al., 2009; Kern et al., 2010). Moreover, the average severity of reduction in our DM rats, approximately 37% of CTRL animals, was similar to the range of levels found in studies on human patients (from 28% up to 60%) (Garhofer et al., 2004; Mandecka et al., 2007, 2009; Lasta et al., 2013). Our data also replicated those of another research group that has detected diminished flicker-evoked arteriolar dilatory responses in STZ-induced diabetic rats, both in isolated retina preparations (Mishra and Newman, 2010) and in *in vivo* rat retinas (Mishra and Newman, 2011). However, it is interesting that the changes reported in their studies occurred only after 7 months post-STZ. The authors claimed that

this slow onset and the lack of typically observed changes in retinal function (assessed with full-field electroretinography) and lens opacity were due to more rigorous glycemic controls in their studies. Nonetheless, the results show that our imaging system was able to detect changes in hyperemic response due to diabetes and that STZ-induced diabetic rats recapitulate the functional hyperemia dysfunction found in diabetic patients with preclinical DR.

4.5.2 Underlying Causes of Abnormal Functional Hyperemia

Although defective functional hyperemia is a robust finding in early-stage DR, the mechanisms underlying this loss of response are unclear. As functional hyperemia is regulated by complex mechanisms involving coordinated interactions of the neurovascular unit (neurons, glia, and vessels), defects in any one of the components can compromise the response. First, the loss of functional hyperemia could be due to a decrease in light-evoked neuronal activity. However, our results indicate that defective functional hyperemia occurred prior to the earliest detection of retinal dysfunction – delays in oscillatory potentials at 4 weeks post-STZ (Aung et al., 2013). This temporal relationship is consistent with other reports in STZ-induced diabetic rats and in human patients (Mishra and Newman, 2011; Lasta et al., 2013). Still, it is likely that reduced neural activity in later disease stages could further exacerbate the decline in flicker-induced vasodilation (Lecleire-Collet et al., 2011) – a question that we wish to answer in the future as we improve our imaging system to accommodate for the deterioration in image quality due to cataract formation.

It is also possible that abnormal retinal vasculature could account for the reduced hyperemic response in early-stage DR. For instance, loss of vascular responsiveness

could attribute to diminished flicker-induced vasodilation. Although not investigated in this study, others have reported that vascular reactivity to exogenous vasodilator stimulation is unaffected in diabetic patients and animals (Pemp et al., 2009; Mishra and Newman, 2010). Another possibility is that resting retinal vessels in diabetic retina are already dilated such that light stimulation could no longer elicit further dilation. This does not appear to be the case as no significant difference in resting vessel calibers between CTRL and DM groups were found in our study (data not shown) or by another research group (Mishra and Newman, 2011). Still, it is important to note that endothelial dysfunction, a well-documented early pathology in DR, could contribute to defects in functional hyperemia. Specifically, imbalance between endothelium-derived vasodilator and vasoconstrictor substances due to abnormal synthesis and regulation of these molecules could potentially result in inability of the vessels to respond appropriately to light stimulation (Ciulla et al., 2002; Clermont and Bursell, 2007; Lee et al., 2008; Wright et al., 2009; Wang et al., 2010).

Lastly, the diminished hyperemic response could be caused by altered signaling in the neurovascular coupling cascade. Though hyperglycemia alone has been shown to impair functional hyperemia in a diabetic retina (Ernest et al., 1983; Dorner et al., 2003), the exact molecular mediators have yet to be clarified. The second part of this study aimed to tackle that question.

4.5.3 Role of 20-HETE and EETs in Early-stage Diabetic Retinopathy

Although arachidonic acid metabolites have been identified as important pathogenic mediators for cerebral ischemia (i.e. stroke) (Roman, 2002; Poloyac et al., 2006; Tanaka et al., 2007) and diabetes-induced cardiovascular dysfunction (Benter et al.,

2005; Yousif and Benter, 2007; Chen et al., 2008; Yousif et al., 2009a, 2009b), their roles in the normal regulation of retinal vasculature and in early vascular dysfunctions observed in diabetic retinopathy have only been investigated recently. Works by Newman et al. demonstrate that functional hyperemia may be mediated by a feed-forward mechanism in which active neurons release signaling molecules (most likely ATP) that stimulate Müller glial cells to release vasoactive agents, including EETs and 20-HETE, which in turn regulate the vascular tone (Metea and Newman, 2006, 2007; Newman, 2013). Moreover, they show that the type of vasomotor response observed depends on retinal levels of nitric oxide (NO), which modulate the activity of the enzymes responsible for the synthesis of 20-HETE and EETs (Fleming, 2001). Under physiologic conditions, the effects of 20-HETE are outweighed by the production of vasodilators, and the vessels dilate upon light stimulation. However, increased NO abundance due to upregulation of inducible NO synthase (iNOS) was observed in diabetic retinas (Carmo et al., 1999; Toda et al., 2007; Mishra and Newman, 2010). This over-production of NO could lead to an imbalance of 20-HETE and EETs levels and ultimately result in a decrease in flicker-evoked vasodilation (Gugleta et al., 2006; Bek et al., 2008; Mandecka et al., 2009; Nguyen et al., 2009; Pemp et al., 2009; Lecleire-Collet et al., 2011). Indeed, studies have shown that inhibition of iNOS restored functional hyperemia responses in a Type 1 diabetic rodent model in both *ex vivo* whole-mount preparations and *in vivo* (Mishra and Newman, 2010, 2011). Aside from hyperemic responses, Wang et al. (2011) showed that inhibition of 20-HETE synthesis with HET0016 ameliorated the overall hemodynamic functional decline of STZ-treated mice, attenuating the diabetes-induced decrease in retinal red blood cell velocity, shear rate, and blood flow rate (Wang et al.,

2011). Together, these studies suggest that imbalance in vasoactive arachidonic acid metabolites contributes to the vascular deficits observed in early-stage DR.

Results from our study further strengthened the pathogenic roles of imbalance in 20-HETE and EETs and demonstrated the detrimental impact of this imbalance on visual outcome. In particular, we found that chronic inhibition of 20-HETE production or EETs degradation improved the visual functions of DM animals (Figures 4-4 and 4-5). We also found that preservation of visual function in these treated DM animals cannot be completely attributed to differences in general health, hyperglycemia severity, or degree of lens opacity (Table 4-1 and Figure 4-7). To further support our findings, it would be interesting to assess how regulating retinal 20-HETE and EETs content would affect electroretinograms of diabetic animals, in which robust changes have been consistently observed in early-stage DR (Ghirlanda et al., 1997; Shirao and Kawasaki, 1998; Li et al., 2002; Bearse et al., 2006; Wolff et al., 2010). Future studies should also assess retinal 20-HETE and EETs levels under normal and diabetic conditions and correlate visual functions with changes in the levels of these arachidonic acid metabolites.

4.5.4 Regulating Levels of Arachidonic Acid Metabolites and Its Effects on Visual Function

Equally important, findings from this study provide evidence on the potential interplay between the vascular and neuronal pathologies in early-stage DR. Our results indicate that imbalances in 20-HETE and EETs levels may underscore the association of defects in retinal vasculature with impaired visual function. So then, how does regulating 20-HETE and EETs levels affect visual function? One possibility is that vascular dysfunction due to altered 20-HETE and EETs levels induces hypoxia in the retina, as the

retinal vasculature fails to deliver adequate oxygen to meet the increased metabolic demand of an active neural retina (Blair et al., 2009). Numerous studies have indeed shown signs of retinal hypoxia in early-stage DR (Linsenmeier et al., 1998; Arden et al., 2005; de Gooyer et al., 2006; Wright et al., 2010; Ly et al., 2011). Such impairment could then lead to neuronal dysfunction, affecting visual function (Riva et al., 2005; Pournaras et al., 2008; Qian and Ripps, 2011). Therefore, the preservation of visual function observed in our DM animals treated with 20-HETE or AUDA may be secondary to improvement in vascular function, resulting in reduced retinal hypoxia and better neuronal function. It is also plausible that decreased visual deficits in DM rats treated with HET0016 and AUDA may be due to preservation of retinal dopaminergic system as dopamine has been found to play an important role in modulating multiple aspects of light-adapted vision (Jackson et al., 2012). To validate these hypotheses, further examinations of vascular function, presence of retinal hypoxia, retinal dopamine content, and visual function within the same animal model are needed.

Another plausible mechanism by which modulations of 20-HETE and EETs levels led to improvements in visual functions in DM rats may be direct neuroprotection, as inhibiting soluble epoxide hydrolase has been shown to decrease neuronal apoptosis from cerebral ischemia in rats (Zhang et al., 2007; Simpkins et al., 2009). To explore this hypothesis, longer study durations are needed as the time-points examined in this study were earlier than times associated with retinal degeneration in diabetes (Martin et al., 2004; Kern et al., 2010; Villarroel et al., 2010; Barber et al., 2011).

4.5.5 Therapeutic Efficacies of HET0016 and AUDA

With the use of both HET0016 and AUDA, we indirectly confirmed that proper balance of 20-HETE and EETs levels is crucial for the functioning of the retina (Figure 4-6). However, it seemed that modulating 20-HETE levels may be more effective and stable as we found that DM+AUDA rats no longer showed improved spatial frequency thresholds at 6 weeks post-STZ while DM+HET0016 rats still maintained their preserved thresholds. This could be due to the decreased severity in the visual deficits of DM+VEH rats in the AUDA experiment (Figure 4-5), which rendered the benefits of AUDA treatment harder to discern. Also, it is highly possible that we might not be maintaining the therapeutic dosage for AUDA treatment, as the dosage for AUDA was based on previous studies on the use of AUDA in the brain, not the retina (Zhang et al., 2007; Simpkins et al., 2009). Therefore, further studies are needed to titrate the optimal dosage for AUDA and potentially HET0016 that can achieve maximum preservation of visual function. In addition, repeating this study using inhibitors with better water solubility would allow the drugs to be delivered orally; although local administration of HET0016 or AUDA to the eye may have beneficial effects since systemic alterations of 20-HETE and EETs may have unwanted side-effects. Local administration of the inhibitors would also allow us to discern whether visual improvement observed in the drug-treated DM animals were primarily due to local preservation of retinal function or secondary to systemic benefits, as 20-HETE and EETs are involved in other organ systems, such as the heart and the kidney (Falck et al., 1987; Fleming, 2001; Roman, 2002; Chen et al., 2008).

In this study, we also observed more consistent improvements in contrast sensitivity compared to spatial frequency thresholds, due to HET0016 or AUDA.

Although the exact underlying mechanism(s) still need to be further explored, this finding supports the notion that contrast sensitivity measurements are a robust and sensitive biomarker for early-stage DR and can be used to monitor/compare efficacies of different treatments (Kawasaki et al., 1986; Greenstein et al., 1990; Ghirlanda et al., 1997; Jackson and Barber, 2010).

4.5.6 Conclusions

In summary, we found that STZ-induced diabetic rats show similar defects in functional hyperemia as human diabetic patients, in terms of severity and time course. In addition, we discovered that use of inhibitors for 20-HETE production and EETs metabolism was effective in attenuating visual deficits in the initial weeks of STZ-induced diabetes. To the best of our knowledge, this is the first evidence of visual benefits provided by pharmacologically regulating the levels of vasoactive arachidonic acid metabolites in STZ-induced diabetic rats, providing novel therapeutic targets for early diabetes-associated visual deficits. Findings from this study also strengthen the importance of neurovascular coupling for proper visual function and support the hypothesis that disrupted crosstalk between the neural retina and the retinal vasculature may contribute to the pathogenesis of DR (Qian and Ripps, 2011; Newman, 2013).

CHAPTER 5: CONCLUDING REMARKS

5.1 Summary of Findings

Due to the increasing prevalence of diabetes (King et al., 1998), diabetic retinopathy (DR) poses a serious healthcare problem worldwide. Although it is the leading cause of irreversible blindness in working-age adults (Klein et al., 1989; Congdon et al., 2003; Klein, 2007), clinical diagnosis and staging of DR is still based on examination of the fundus to assess the presence and severity of late-stage vascular lesions (Frank, 2004). Better understanding of the preclinical stages of DR is warranted so that earlier diagnosis and intervention can be implemented for this devastating ocular disease.

Research in the past decades on early-stage DR has revealed a neuronal component to the early pathology of the disease, prior to the appearance of clinically significant vascular abnormalities (Barber, 2003; Antonetti et al., 2006). Despite the growing awareness of the early functional and cellular changes in the neural retina of both diabetic patients and animal models, the impact of these neuronal changes on vision and the underlying pathogenic mediators remain elusive. In Chapters 2 through 4, I have described experimental results that hopefully delivered some insight on these questions.

In Chapter 2, I evaluated the importance of detecting early retinal dysfunction by examining its associations with visual defects observed in early-stage DR. Consistent with my hypothesis, I found that the onset of electroretinogram (ERG) alterations coincided with the time-point (4 weeks of diabetes) when the diabetic animals first exhibited reductions in their optokinetic (OKT) responses. The reduced OKT responses could not be completely explained by cataract formation as diabetic rats without cataracts

also displayed decreased OKT values. Furthermore, I found that the levels of visual deficits correlated significantly with not only the severity of cataracts, but also the extent of ERG changes.

In my next set of experiments (as discussed in Chapter 3), I investigated if retinal dopamine (DA) deficiency potentially underlies early diabetes-induced visual changes. Consistent with a published report (Nishimura and Kuriyama, 1985), I found marked reductions in retinal DA contents in both streptozotocin (STZ)-induced diabetic rats and mice within weeks of diabetes onset. Moreover, the finding that chronic L-DOPA treatment improved retinal and visual dysfunctions of diabetic mice confirmed that DA deficiency mediates early functional deficits in DR. The use of retina-specific *tyrosine hydroxylase* knockout (rTHKO) mice also validated that disruptions in the retinal dopaminergic system contribute to the functional deficits in early-stage DR. Lastly, I was able to show the potential of targeting the dopaminergic system therapeutically since acute treatment with agonists of selected DA receptors ameliorated visual dysfunctions in diabetic mice.

In the subsequent Chapter 4, I examined the possibility that vascular dysfunction, specifically defective functional hyperemia, affects the visual function of a diabetic retina. In accordance with my hypothesis, I found that diabetic animals exhibited diminished hyperemic responses prior to the onset of visual loss. More importantly, I discovered that inhibiting the synthesis of 20-HETE or up-regulating the bioavailability of EETs improved visual functions of diabetic animals, suggesting that appropriate vascular response is needed for optimal neural and ultimately visual function.

In this concluding chapter, I would like to discuss the implications of these findings and suggest future directions to address the limitations and questions that may arise from my thesis work.

5.2 Technical Implications for Experimental Study of Diabetic Retinopathy

As mentioned in the closing statement of Chapter 2, a major technical implication of this thesis work is strengthening the validity of using STZ-induced diabetic animals to study early-stage DR. In particular, the consistent findings of early ERG alterations and OKT abnormalities in STZ-induced animals found in this work replicate the functional pathologies found in diabetic patients without clinically diagnosed DR (Ghirlanda et al., 1997). Establishing a reliable model for early-stage DR is beneficial in several aspects. First, future experiments can utilize ERG and OKT responses of STZ-induced diabetic animals to rapidly screen for potential therapeutic drug(s) and monitor longitudinally the effectiveness and safety of the treatment(s). For instance, STZ-injected diabetic animals were successfully used in this work to examine the benefits and potential side-effects of different pharmacological treatments (e.g. L-DOPA, HET0016, and AUDA) for early-stage DR, as described in Chapters 3 and 4. Second, having such a model at our disposal would allow for more in-depth examination of the disease process. For example, the use of diabetic rTHKO mice, as described in Chapter 3, enabled us to isolate the role of retinal DA deficiency in early diabetes-induced visual deficits. Lastly, the ability to control the onset, severity, and progression of diabetes in this model minimizes potential confounding variables that may impact the study, such as age, diet, and glycemic control.

Another important technical advance from this thesis work is the development of an *in vivo* assessment of functional hyperemia in rat. As discussed in Chapters 1 and 4,

appropriate hyperemic response is pivotal for proper retinal function as it supplies necessary oxygen and nutrients to meet the increased metabolic demand of activated retinal neurons. In human subjects, a device called Retinal Vessel Analyzer has been developed to reliably assess functional hyperemia in the retina by monitoring changes in vessel caliber (both arterial and venous) in response to flicker light stimulation (Seifertl and Vilser, 2002). More importantly, numerous studies have shown early deterioration of the flicker-induced vasodilation in diabetic patients without structural abnormalities in the retinal vasculature (Bek et al., 2008; Mandecka et al., 2009; Nguyen et al., 2009; Lecleire-Collet et al., 2011). Such deterioration could lead to neuronal dysfunction as implied by another study showing signs of defective functional hyperemia preceding neuronal dysfunctions as assessed with pattern ERG (Lasta et al., 2013). However, results shown were simply associative and further studies are needed to determine the causal effects of abnormal functional hyperemia on retinal and visual functions of a diabetic retina and to dissect the underlying mechanisms or mediators of the defective response. To do so, an animal model that reliably replicates the pathology and a method sensitive enough to detect the changes are needed. As shown in Chapter 4, the imaging system developed in this thesis work (composed of custom-made devices to deliver filtered green flicker light and Heidelberg scanning laser ophthalmoscope to image the retinal vasculature) was able to measure flicker-induced retinal vascular changes in rats. In addition, the method was sensitive enough to detect reduced flicker-induced vasodilatory response, as early as 2 weeks post-STZ, in diabetic rats. The diminished hyperemic response also occurred prior to the onset of ERG alterations (4 weeks post-STZ), reproducing the finding in human patients described above (Lasta et al., 2013).

It is important to note that we are not the first lab that has developed a method to assess functional hyperemia *in vivo* in experimental animals. For instance, Dr. Newman and his research group have successfully established a technique that combined laser speckle flowmetry with laser scanning confocal microscopy to image *in vivo* blood flow in the rat retina (Srienc et al., 2010). Using such technique, they also found reduced flicker-evoked dilations in STZ-induced diabetic rats; however, the change occurred only after 7 months of diabetes (Mishra and Newman, 2011). Another group has also presented an imaging system to assess the dynamics of retinal vessel in rats (Link et al., 2011). Their system was able to yield highly stable readings for vessel caliber of both arterioles and venules (<1 % coefficient of variation). However, it remains unclear if their system has the capability to detect hyperemic response and the changes due to diabetes as the authors did not demonstrate this in their study. Nonetheless, the active pursuit of establishing reliable measurement of functional hyperemia in animals will aid future studies to elucidate potential mediators for the altered neurovascular coupling cascade in early-stage DR and to develop new DR-specific therapies.

5.3 Insights to the Pathogenesis of Early-stage Diabetic Retinopathy

In the study of DR, one of the main goals has been to elucidate the underlying mechanism(s) of the disease, such that measures to prevent the development of DR or treatments to slow the disease progression could be devised. As a field, we have learned that up-regulation of multiple metabolic pathways (e.g. increased polyol and hexosamine pathways flux, activation of protein kinase C, and formation of glycation end-productions) (Brownlee, 2001) triggered by diabetes (insulin insufficiency and hyperglycemia) plays a crucial role in the pathogenesis of DR. In addition, there is

growing evidence that oxidative stress (Kowluru and Chan, 2007; Giacco and Brownlee, 2010) and inflammation (Tang and Kern, 2011) also contribute to the development of the disease. Results from this thesis project expand upon this knowledge by showing how several retinal systems (i.e. dopaminergic neurotransmission and neurovascular coupling) are potentially affected by these abnormalities, which then lead to the functional deficits manifested in early-stage DR. As shown in Chapter 3, diabetes clearly perturbed the retinal dopaminergic system in rodent models of Type 1 diabetes, resulting in DA deficiency and ultimately visual dysfunctions. Even though DA deficiency could be due to direct defect(s) in multiple site(s) of DA synthesis, release, and metabolism, it is highly plausible that all these defects are secondary to diabetes-induced metabolic changes and associated oxidative stress and inflammation (Figure 5-1). Similarly, these metabolic changes could be the upstream mediators that impair the function of the neurovascular units to elicit appropriate functional hyperemic responses, as evidenced by the retinal abnormalities, gliosis, and endothelial dysfunctions found in early-stage DR (Fletcher et al., 2005, 2007; Bharadwaj et al., 2013). Collectively, these findings add vital pieces to the understanding of the overall pathogenic pathways of diabetes leading to the functional deficits suffered by diabetic patients and animals.

Although this dissertation describes the dysfunctions in the retinal dopaminergic system and neurovascular coupling mechanism seemingly as two distinct abnormalities in diabetes, it is possible that the two deficits may interact and affect one another (Figure 5-2). For instance, retinal DA deficiency due to diabetes may contribute to the diminished functional hyperemic response in the diabetic retina. In addition to being a neuromodulator, DA has been shown to regulate the activity of pericytes, which are the

contractile units responsible for the vascular tone of microvessels (Wu et al., 2001; Huemer et al., 2007). Specifically, binding of DA to the D1 receptors on the pericytes can induce hyperpolarization in the pericytes (via activation of adenylate cyclase and protein kinase A), resulting in the relaxation of the pericytes and increased blood flow. Therefore, DA could potentially contribute to the neurovascular coupling response, and retinal DA deficiency in diabetes could then exacerbate the already reduced functional hyperemia due to other mediators, i.e. imbalance of 20-HETE and EETs, found in this study. Conversely, defective functional hyperemia could also directly impair dopaminergic neurons and worsen the reduction in DA levels in diabetes. As described in Chapter 4, insufficient functional hyperemia may result in retinal hypoxia, which could be most severe in the inner retina due to the relatively low oxygen tension that the inner retina is already exposed to (Linsenmeier, 1986; Yu and Cringle, 2006). Interestingly, signs of retinal hypoxia in diabetic animals are indeed localized mostly to the inner retina (Linsenmeier et al., 1998; de Gooyer et al., 2006a, 2006b; Ly et al., 2011). As the dopaminergic amacrine cells reside in the inner retina, they may be more vulnerable to the hypoxia induced by defective functional hyperemia, possibly impairing the dopaminergic system further and resulting in larger DA reductions. Obviously, further research is needed to elucidate the potential interactions of the two defects as they could lead to a downward spiral and rapidly exacerbate the severity of both defects.

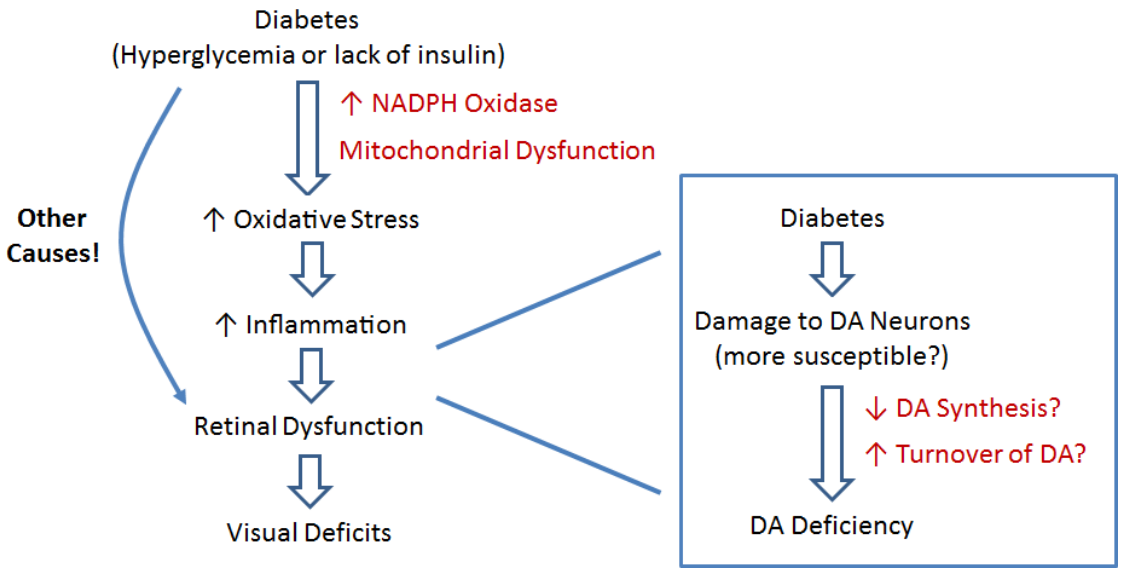

Figure 5-1. Schematic illustrating how dopamine deficiency may fit in the pathogenesis of early diabetes-induced retinal and visual dysfunctions. Oxidative stress and inflammation induced by diabetes may be one of the upstream factors impairing the retinal dopaminergic system, leading to reduced retinal dopamine content. The exact mechanism(s) leading to dopamine deficiency may include decreased dopamine production, enhanced dopamine turnover, and others. Altogether, the resulting dopamine deficiency causes dysfunction in the neural retina, manifesting as early alterations in electroretinograms and visual responses. It is important to be aware of other potential causes for the observed retinal and visual deficits in early-stage DR. Abbreviations used in the diagram: DA = dopamine; NADPH = nicotinamide adenine dinucleotide phosphate.

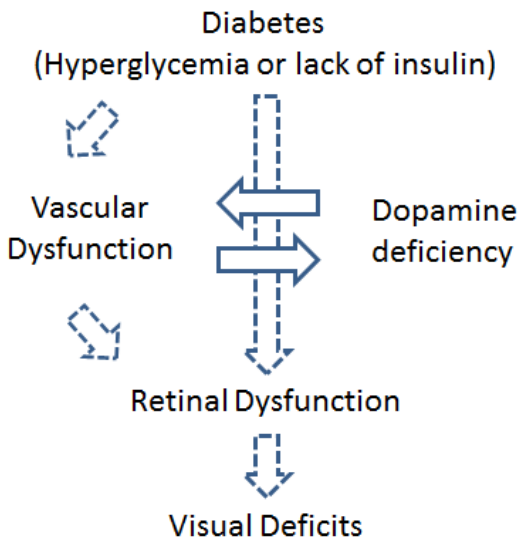

Figure 5-2. Diagram showing the potential interactions between dopamine deficiency and defective functional hyperemia in diabetes.

5.4 Potential Clinical Applications

In terms of clinical relevance, a translational implication of this collection of experiments is the generation of novel biomarkers. For instance, results in Chapter 2 reinforce the possibility of using the optokinetic tracking response and/or other subtle aspects of vision (scotopic vision, visual field, etc.) as markers for screening preclinical DR. It would be interesting to validate this hypothesis in a diabetic patient population and test which visual modality has the highest sensitivity in detecting early retinal abnormalities due to diabetes. Moreover, the finding of diabetes producing retinal DA deficiency in Chapter 3 underscores the potential of using changes in serum DA levels as an indicator for disease progression and initiation of early treatments for DR. Also, the observation of early defective functional hyperemia described in Chapter 4 strengthens the robustness of using this vascular dysfunction to characterize early-stage DR.

Another clinical implication of this work is potential therapy development. Revealing the pathogenic roles of retinal DA deficiency and imbalance of 20-HETE and EETs in early diabetes-induced visual deficits opens a wide range of potential interventions to provide not only symptomatic relief (i.e. visual improvement) but also slowing of disease progression. Since some of the drugs used in this project are already commonly used in the clinics, i.e. L-DOPA and DA receptor agonists for the treatment of Parkinson's disease, it would be very intriguing to study the development and severity of DR in diabetic patients that use these drugs for other disorders. In addition, as diabetes is a systemic disorder that affects all organ systems, current findings of how diabetes impairs the retina could be considered as mechanisms underlying diabetes-induced abnormalities in other parts of central nervous system. Therefore, the potential

therapeutic targets in the retina may be applicable in the brain as well. Lastly, as we found diabetes caused DA deficiency and defective functional hyperemia, these effects of diabetes may explain the observation of additive severity in patients with diabetes and other neurological disorders that share similar underlying mechanisms, such as stroke [known defective functional hyperemia (Fleming, 2001; Pratt et al., 2004; Zhang et al., 2007; Imig et al., 2011)] and Parkinson's disease [known DA deficiency (Nguyen-Legros, 1988; Bodis-Wollner, 2009)] – a possibility that deserves further investigation for better patient care and treatment.

5.5 Limitations, Future Direction, and Final Words

While results from this study advance our understanding of early-stage DR with important clinical implications, because the study focused mainly on rodent models of Type 1 diabetes, it remains unclear how these findings will apply to the development of DR in Type 2 diabetes. Although hyperglycemia and insulin insufficiency are features shared by both Type 1 and Type 2 diabetes and are the key underlying causes for the abnormalities in DR, the metabolic syndrome and insulin resistance that are only associated with Type 2 diabetes may further complicate the pathogenesis and treatment of DR in Type 2 diabetes. Therefore, it is important to study if pathogenic roles of retinal DA deficiency and defective functional hyperemia translate to models of Type 2 diabetes as well. Results from this future direction can yield greater clinical importance as Type 2 diabetes is the more prevalent form of diabetes (King et al., 1998; Klein, 2007). In addition, though rodent models have the advantages of rapid short study duration, ability for genetic manipulation, and easier management, it may be worthwhile to replicate the findings and conclusions drawn in this study on larger mammals, such as pigs or even

primates, which will more adequately reflect human disease (Rees and Alcolado, 2005). Further studies are also needed to examine the effects of early interventions suggested in this thesis work (e.g. DA replacement therapy) on the development of clinical DR, i.e. microvascular lesions, and thus creating relevant preventative treatment strategies.

Aside from the global future directions mentioned above, there are caveats pertinent to each study (i.e. Chapters 2 to 4) that should be noted and addressed. In Study 1 (Chapter 2), though temporal and correlational evidence for the contribution of retinal dysfunction to visual deficits in early-stage DR were provided, these results are still associative and the causal relationship remains elusive. One way to address this issue is by developing neuron-specific therapies for diabetic animals and examining how those treatments may affect the visual outcomes of the treated animals. As antioxidant treatments have consistently shown benefits in ameliorating diabetes-induced abnormalities in the retina (Kowluru et al., 2001; Kowluru and Koppolu, 2002; Kowluru and Chan, 2007; Arnal et al., 2009; Giacco and Brownlee, 2010; Gupta et al., 2011), a potential strategy may entail neuron-specific up-regulation of protein(s) involved in cellular antioxidant mechanism with viral vector or Cre-Lox recombination. By confining the treatment benefit only in retinal neurons, the direct impact of retinal dysfunction on vision in early-stage DR can then be isolated. Also, as discussed in the study, formation of cataracts complicates the attempt to separate the role of retinal dysfunction on vision in diabetic animals. Therefore, it is worthwhile to develop methods to eliminate cataract formation as a confounder in diabetic animals, such as surgical removal of cataract.

In Study 2 (Chapter 3), though restoring DA levels or activating DA pathways are found to be beneficial for the visual functions of diabetic animals, it would be interesting

to explore other means to ameliorate diabetes-induced DA deficiency aside from pharmacological interventions. One potential method is exercise. Numerous reports in the field of Parkinson's disease have shown exercise is neuroprotective for nigrostriatal dopaminergic neurons and enhances DA synthesis (Sutoo and Akiyama, 2003; Sung et al., 2012; Aguiar et al., 2013). With such effects established in the brain, it is highly plausible that the benefits of exercise will translate to a diabetic retina.

Lastly, there are several potential directions that can be undertaken to expand upon the findings in Study 3 (Chapter 4). First, though the temporal relationship between diminished functional hyperemia and visual deficits are delineated, direct evidence linking the impact of reduced hyperemic responses on vision is still missing. To fulfill this knowledge gap, temporal examination of the hypoxic load of a diabetic retina [with the use of oxygen sensitive pimonidazole probe or hypoxia-sensitive protein biomarkers (Wright et al., 2010)] and changes in its flicker-induced vasodilatory response is needed. With such temporal relationship established, further studies can then investigate how treatment targeting functional hyperemia (e.g. HET0016 or AUDA) in a diabetic animal may alter or improve the severity of retinal hypoxia, thereby confirming the causal effect of diabetes-induced functional hyperemia alterations on visual function. Furthermore, improvement in the imaging system described in this thesis work is imperative such that functional hyperemic response at later disease stage (>4 weeks post-STZ) can be assessed and correlated with the retinal health and functional changes. Equally important, levels of 20-HETE and EETs in diabetic retinas need to be measured so that their pathogenic roles in defective functional hyperemia could be validated. To address this issue, we are currently adopting a previously established fluorescent high performance liquid

chromatography (HPLC) assay to measure levels of 20-HETE and EETs in retinal samples (Figure 5-3). By comparing the levels of 20-HETE and EETs between control and diabetic animals with the assay and correlating the metabolites levels with corresponding hyperemic responses, this future study will enable us to assess if imbalance in 20-HETE and EETs levels is truly a mediator for the observed functional hyperemia deficit in early-stage DR.

In summary, this thesis work establishes a close association of retinal dysfunctions and visual deficits in early-stage DR and emphasizes the diagnostic potential of detecting these early changes. Subsequently, this work describes two mechanisms, DA deficiency and defective functional hyperemia, that underlie these early diabetes-induced retinal and visual defects. The elucidation of these novel pathogenic pathways opens up avenues for future development of new treatment(s) and biomarker(s) for DR. Moreover, by showing that defects in a specific neurotransmitter system and in a hemodynamic response could manifest in visual dysfunctions, this work reinforces the importance of viewing DR as a neurovascular disorder in the diagnosis and treatment for this devastating ocular disease.

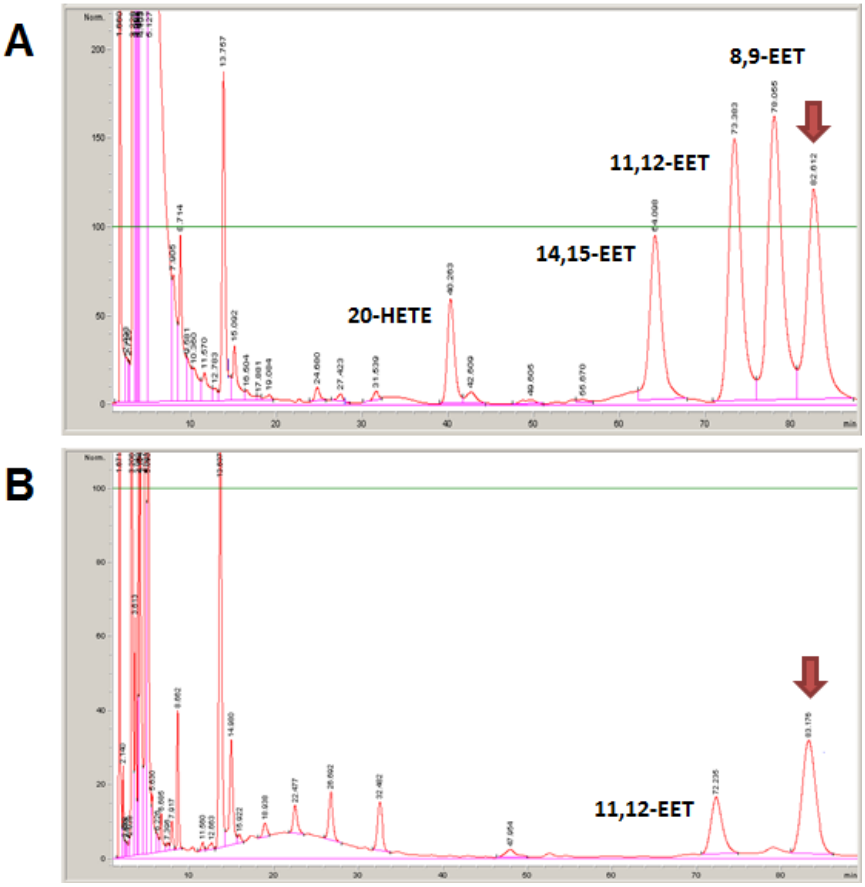

Figure 5-3. Representative HPLC chromatograms illustrating the separation of fluorescently labeled P-450 metabolites of arachidonic acid (A) in a mixture of standards and (B) in a labeled sample of rat retina. The red arrow in each chromatogram indicates the internal standard, WIT-002, that was injected in each HPLC run as a reference to measure the elution time and concentration of the arachidonic acid metabolites of interest. Interestingly, the only prominent arachidonic acid metabolite present in a normal rat retina is 11,12-EET. Abbreviations used in the figure: EET = epoxyeicosatrienoic acid; 20-HETE = 20-hydroxyeicosatetraenoic acid; and WIT-002 = 20-hydroxyeicosa-6(Z),5(Z)-dienoic acid.

REFERENCES

Abu El-Asrar AM, Dralands L, Missotten L, Geboes K (2007) Expression of antiapoptotic and proapoptotic molecules in diabetic retinas. Eye (Lond) 21:238–245.

Abu-El-Asrar AM, Dralands L, Missotten L, Al-Jadaan I a, Geboes K (2004) Expression of apoptosis markers in the retinas of human subjects with diabetes. Invest Ophthalmol Vis Sci 45:2760–2766.

Aguiar a S, Moreira ELG, Hoeller a a, Oliveira P a, Córdova FM, Glaser V, Walz R, Cunha R a, Leal RB, Latini A, Prediger RDS (2013) Exercise attenuates levodopa-induced dyskinesia in 6-hydroxydopamine-lesioned mice. Neuroscience 243:46–53.

Akimov NP, Rentería RC (2012) Spatial frequency threshold and contrast sensitivity of an optomotor behavior are impaired in the Ins2Akita mouse model of diabetes. Behav Brain Res 226:601–605.

Ambati J, Chalam K V, Chawla DK, D'Angio CT, Guillet EG, Rose SJ, Vanderlinde RE, Ambati BK (1997) Elevated gamma-aminobutyric acid, glutamate, and vascular endothelial growth factor levels in the vitreous of patients with proliferative diabetic retinopathy. Arch Ophthalmol 115:1161–1166.

Antonetti D a, Klein R, Gardner TW (2012) Diabetic retinopathy. N Engl J Med 366:1227–1239.

Antonetti DA, Barber AJ, Bronson SK, Freeman WM, Gardner TW, Jefferson LS, Kester M, Kimball SR, Krady JK, LaNoue KF, Norbury CC, Quinn PG, Sandirasegarane L, Simpson IA (2006) Diabetic retinopathy: seeing beyond glucose-induced microvascular disease. Diabetes 55:2401–2411.

Arden GB, Sidman RL, Arap W, Schlingemann RO (2005) Spare the rod and spoil the eye. Br J Ophthalmol 89:764–769.

Arnal E, Miranda M, Johnsen-Soriano S, Alvarez-Nölting R, Díaz-Llopis M, Araiz J, Cervera E, Bosch-Morell F, Romero FJ (2009) Beneficial effect of docosahexanoic acid and lutein on retinal structural, metabolic, and functional abnormalities in diabetic rats. Curr Eye Res 34:928–938.

Atkinson CL, Feng J, Zhang D-Q (2013) Functional integrity and modification of retinal dopaminergic neurons in the rd1 mutant mouse: roles of melanopsin and GABA. J Neurophysiol 109:1589–1599.

Attwell D, Buchan AM, Charpak S, Lauritzen M, Macvicar BA, Newman EA (2010) Glial and neuronal control of brain blood flow. Nature 468:232–243.

Aung MH, Kim MK, Olson DE, Thule PM, Pardue MT (2013) Early visual deficits in streptozotocin-induced diabetic long evans rats. Invest Ophthalmol Vis Sci 54:1370–1377.

Aylward GW (1989) The scotopic threshold response in diabetic retinopathy. Eye (Lond) 3 (Pt 5):626–637.

Barber a J, Lieth E, Khin S a, Antonetti D a, Buchanan a G, Gardner TW (1998) Neural apoptosis in the retina during experimental and human diabetes. Early onset and effect of insulin. J Clin Invest 102:783–791.

Barber AJ (2003) A new view of diabetic retinopathy: a neurodegenerative disease of the eye. Prog Neuropsychopharmacol Biol Psychiatry 27:283–290.

Barber AJ, Gardner TW, Abcouwer SF (2011) The significance of vascular and neural apoptosis to the pathology of diabetic retinopathy. Invest Ophthalmol Vis Sci 52:1156–1163.

Bearse M a, Adams AJ, Han Y, Schneck ME, Ng J, Bronson-Castain K, Barez S (2006) A multifocal electroretinogram model predicting the development of diabetic retinopathy. Prog Retin Eye Res 25:425–448.

Bek T, Hajari J, Jeppesen P (2008) Interaction between flicker-induced vasodilatation and pressure autoregulation in early retinopathy of type 2 diabetes. Graefes Arch Clin Exp Ophthalmol 246:763–769.

Bengtsson B, Heijl a, Agardh E (2005) Visual fields correlate better than visual acuity to severity of diabetic retinopathy. Diabetologia 48:2494–2500.

Benter IF, Yousif MHM, Canatan H, Akhtar S (2005) Inhibition of Ca2+/calmodulin-dependent protein kinase II, RAS-GTPase and 20-hydroxyeicosatetraenoic acid attenuates the development of diabetes-induced vascular dysfunction in the rat carotid artery. Pharmacol Res 52:252–257.

Bharadwaj AS, Appukuttan B, Wilmarth PA, Pan Y, Stempel AJ, Chipps TJ, Benedetti EE, Zamora DO, Choi D, David LL, Smith JR (2013) Role of the retinal vascular endothelial cell in ocular disease. Prog Retin Eye Res 32:102–180.

Bhatwadekar AD, Yan Y, Qi X, Thinschmidt JS, Neu MB, Li Calzi S, Shaw LC, Dominiguez JM, Busik J V, Lee C, Boulton ME, Grant MB (2013) Per2 mutation recapitulates the vascular phenotype of diabetes in the retina and bone marrow. Diabetes 62:273–282.

Björklund A, Dunnett SB (2007) Dopamine neuron systems in the brain: an update. Trends Neurosci 30:194–202.

Blair NP, Wanek JM, Mori M, Shahidi M (2009) Abnormal retinal vascular oxygen tension response to light flicker in diabetic rats. Invest Ophthalmol Vis Sci 50:5444–5448.

Bloodworth JM (1962) Diabetic retinopathy. Diabetes 11:1–22.

Bloomfield S a, Völgyi B (2009) The diverse functional roles and regulation of neuronal gap junctions in the retina. Nat Rev Neurosci 10:495–506.

Bodis-Wollner I (2009) Retinopathy in Parkinson Disease. J Neural Transm 116:1493–1501.

Brandies R, Yehuda S (2008) The possible role of retinal dopaminergic system in visual performance. Neurosci Biobehav Rev 32:611–656.

Bresnick GH, Palta M (1987) Oscillatory potential amplitudes. Relation to severity of diabetic retinopathy. Arch Ophthalmol 105:929–933.

Bron AJ, Cheng H (1986) Cataract and retinopathy: screening for treatable retinopathy. Clin Endocrinol Metab 15:971–999.

Brownlee M (2001) Biochemistry and molecular cell biology of diabetic complications. Nature 414:813–820.

Brownlee M (2005) The pathobiology of diabetic complications: a unifying mechanism. Diabetes 54:1615–1625.

Bursell SE, Clermont AC, Kinsley BT, Simonson DC, Aiello LM, Wolpert UA, Wolpert HA (1996) Retinal blood flow changes in patients with insulin-dependent diabetes mellitus and no diabetic retinopathy. Invest Ophthalmol Vis Sci 37:886–897.

Busik J V et al. (2009) Diabetic retinopathy is associated with bone marrow neuropathy and a depressed peripheral clock. J Exp Med 206:2897–2906.

Cabrera DeBuc D, Somfai GM (2010) Early detection of retinal thickness changes in diabetes using Optical Coherence Tomography. Med Sci Monit 16:MT15–21.

Cai J, Boulton M (2002) The pathogenesis of diabetic retinopathy: old concepts and new questions. Eye (Lond) 16:242–260.

Cao X, Yasuda T, Uthayathas S, Watts RL, Mouradian MM, Mochizuki H, Papa SM (2010) Striatal overexpression of DeltaFosB reproduces chronic levodopa-induced involuntary movements. J Neurosci 30:7335–7343.

Carmo A, Carvalho AP, Lopes MC (2000) Nitric Oxide Synthase Activity in Retinas from Non-Insulin- Dependent Diabetic Goto-Kakizaki Rats: Correlation with Blood – Retinal Barrier Permeability. Nitric Oxide 4:590–596.

Carmo A, Cunha-vaz JG, Carvalho AP, C M, Lopes MC (1999) L-arginine transport in retinas from streptozotocin diabetic rats: correlation with the level of IL-1 beta and NO synthase activity. Vision Res 39:3817–3823.

Carrasco E, Hernández C, de Torres I, Farrés J, Simó R (2008) Lowered cortistatin expression is an early event in the human diabetic retina and is associated with apoptosis and glial activation. Mol Vis 14:1496–1502.

Chen Y-J, Li J, Quilley J (2008) Deficient renal 20-HETE release in the diabetic rat is not the result of oxidative stress. Am J Physiol Heart Circ Physiol 294:H2305–12.

Christie WW (2013) Hydroxyeicosatetraenoic acids and related compounds. AOCS Lipid Libr Available at: http://lipidlibrary.aocs.org/Lipids/eic_hete/index.htm [Accessed January 8, 2014].

Ciavatta VT, Kim M, Wong P, Nickerson JM, Shuler RK, McLean GY, Pardue MT (2009) Retinal expression of Fgf2 in RCS rats with subretinal microphotodiode array. Invest Ophthalmol Vis Sci 50:4523–4530.

Ciulla TA, Harris A, Latkany P, Piper HC, Arend O, Garzozi H, Martin B (2002) Ocular perfusion abnormalities in diabetes. Acta Ophthalmol Scand 80:468–477.

Clee SM, Attie AD (2007) The genetic landscape of type 2 diabetes in mice. Endocr Rev 28:48–83.

Clermont AC, Bursell S-E (2007) Retinal blood flow in diabetes. Microcirculation 14:49–61.

Congdon NG, Friedman DS, Lietman T (2003) Important causes of visual impairment in the world today. JAMA 290:2057–2060.

Curtis TM, Gardiner TA, Stitt AW (2009) Microvascular lesions of diabetic retinopathy: clues towards understanding pathogenesis? Eye (Lond) 23:1496–1508.

Curtis TM, Hamilton R, Yong P-H, McVicar CM, Berner A, Pringle R, Uchida K, Nagai R, Brockbank S, Stitt AW (2010) Müller glial dysfunction during diabetic retinopathy in rats is linked to accumulation of advanced glycation end-products and advanced lipoxidation end-products. Diabetologia.

Darwin CR (1959) On the Origin of Species by Means of Natural Selection, or the Preservation of Favoured Races in the Struggle for Life, 1st ed. London: John Murray.

De Gooyer TE, Stevenson K a, Humphries P, Simpson D a C, Curtis TM, Gardiner T a, Stitt AW (2006a) Rod photoreceptor loss in Rho-/- mice reduces retinal hypoxia and hypoxia-regulated gene expression. Invest Ophthalmol Vis Sci 47:5553–5560.

De Gooyer TE, Stevenson K a, Humphries P, Simpson D a C, Gardiner T a, Stitt AW (2006b) Retinopathy is reduced during experimental diabetes in a mouse model of outer retinal degeneration. Invest Ophthalmol Vis Sci 47:5561–5568.

Do Carmo Buonfiglio D, Peliciari-Garcia RA, do Amaral FG, Peres R, Nogueira TCA, Afeche SC, Cipolla-Neto J (2011) Early-stage retinal melatonin synthesis impairment in streptozotocin-induced diabetic wistar rats. Invest Ophthalmol Vis Sci 52:7416–7422.

Doi M (2012) Circadian clock-deficient mice as a tool for exploring disease etiology. Biol Pharm Bull 35:1385–1391.

Dong C-J, Agey P, Hare W a (2004) Origins of the electroretinogram oscillatory potentials in the rabbit retina. Vis Neurosci 21:533–543.

Dorner GT, Garhöfer G, Huemer KH, Riva CE, Wolzt M, Schmetterer L (2003) Hyperglycemia affects flicker-induced vasodilation in the retina of healthy subjects. Vision Res 43:1495–1500.

Douglas RM, Alam NM, Silver BD, McGill TJ, Tschetter WW, Prusky GT (2005) Independent visual threshold measurements in the two eyes of freely moving rats and mice using a virtual-reality optokinetic system. Vis Neurosci 22:677–684.

Doyle SE, McIvor WE, Menaker M (2002) Circadian rhythmicity in dopamine content of mammalian retina: role of the photoreceptors. J Neurochem 83:211–219.

Ernest JT, Goldstick TK, Engerman RL (1983) Hyperglycemia impairs retinal oxygen autoregulation in normal and diabetic dogs. Invest Ophthalmol Vis Sci 24:985–989.

Falck JR, Schueler VJ, Jacobson HR, Siddhanta a K, Pramanik B, Capdevila J (1987) Arachidonate epoxygenase: identification of epoxyeicosatrienoic acids in rabbit kidney. J Lipid Res 28:840–846.

Feit-Leichman RA, Kinouchi R, Takeda M, Fan Z, Mohr S, Kern TS, Chen DF (2005) Vascular damage in a mouse model of diabetic retinopathy: relation to neuronal and glial changes. Invest Ophthalmol Vis Sci 46:4281–4287.

Fernstrom JD, Fernstrom MH (2007) Tyrosine, phenylalanine, and catecholamine synthesis and function in the brain. J Nutr 137:1539S–1547S; discussion 1548S.

Fernstrom MH, Volk EA, Fernstrom JD (1984) In vivo tyrosine hydroxylation in the diabetic rat retina: effect of tyrosine administration. Brain Res 298:167–170.

Fernstrom MH, Volk EA, Fernstrom JD, Iuvone PM (1986) Effect of tyrosine administration on dopa accumulation in light- and dark-adapted retinas from normal and diabetic rats. Life Sci 39:2049–2057.

Fleming I (2001) Cytochrome p450 and vascular homeostasis. Circ Res 89:753–762.

Fletcher EL, Downie LE, Hatzopoulos K, Vessey KA, Ward MM, Chow CL, Pianta MJ, Vingrys AJ, Kalloniatis M, Wilkinson-Berka JL (2010) The significance of neuronal and glial cell changes in the rat retina during oxygen-induced retinopathy. Doc Ophthalmol 120:67–86.

Fletcher EL, Phipps JA, Ward MM, Puthussery T, Wilkinson-Berka JL (2007) Neuronal and glial cell abnormality as predictors of progression of diabetic retinopathy. Curr Pharm Des 13:2699–2712.

Fletcher EL, Phipps JA, Wilkinson-Berka JL (2005) Dysfunction of retinal neurons and glia during diabetes. Clin Exp Optom J Aust Optom Assoc 88:132–145.

Fortune B, Schneck ME, Adams AJ (1999) Multifocal electroretinogram delays reveal local retinal dysfunction in early diabetic retinopathy. Invest Ophthalmol Vis Sci 40:2638–2651.

Frank RN (1995) Diabetic retinopathy. Prog Retin Eye Res 14:361–392.

Frank RN (2004) Diabetic retinopathy. N Engl J Med 350:48–58.

Frank RN (2009) Treating diabetic retinopathy by inhibiting growth factor pathways. Curr Opin Investig Drugs 10:327–335.

Franze K, Grosche J, Skatchkov SN, Schinkinger S, Foja C, Schild D, Uckermann O, Travis K, Reichenbach A, Guck J (2007) Muller cells are living optical fibers in the vertebrate retina. Proc Natl Acad Sci U S A 104:8287–8292.

Garcia-Ramírez M, Hernández C, Villarroel M, Canals F, Alonso M a, Fortuny R, Masmiquel L, Navarro a, García-Arumí J, Simó R (2009) Interphotoreceptor retinoid-binding protein (IRBP) is downregulated at early stages of diabetic retinopathy. Diabetologia 52:2633–2641.

Garhofer G, Zawinka C, Resch H, Kothy P, Schmetterer L, Dorner GT, Garhöfer G (2004) Reduced response of retinal vessel diameters to flicker stimulation in patients with diabetes. Br J Ophthalmol 88:887–891.

Gastinger MJ, Singh RSJ, Barber AJ (2006) Loss of cholinergic and dopaminergic amacrine cells in streptozotocin-diabetic rat and Ins2Akita-diabetic mouse retinas. Invest Ophthalmol Vis Sci 47:3143–3150.

Ghafour IM, Foulds WS, Allan D, McClure E (1982) Contrast sensitivity in diabetic subjects with and without retinopathy. Br J Ophthalmol 66:492–495.

Ghirlanda G, Di Leo M a, Caputo S, Cercone S, Greco a V (1997) From functional to microvascular abnormalities in early diabetic retinopathy. Diabetes Metab Rev 13:15–35.

Giacco F, Brownlee M (2010) Oxidative stress and diabetic complications. Circ Res 107:1058–1070.

Giolli RA, Blanks RHI, Lui F (2006) The accessory optic system: basic organization with an update on connectivity, neurochemistry, and function. Prog Brain Res 151:407–440.

Giove TJ, Deshpande MM, Gagen CS, Eldred WD (2009) Increased neuronal nitric oxide synthase activity in retinal neurons in early diabetic retinopathy. Mol Vis 15:2249–2258.

Goldstein IM, Ostwald P, Roth S (1996) Nitric oxide: a review of its role in retinal function and disease. Vision Res 36:2979–2994.

Goto R, Doi M, Ma N, Semba R, Uji Y (2005) Contribution of nitric oxide-producing cells in normal and diabetic rat retina. Jpn J Ophthalmol 49:363–370.

Greenstein V, Sarter B, Hood D, Noble K, Carr R (1990) Hue discrimination and S cone pathway sensitivity in early diabetic retinopathy. Invest Ophthalmol Vis Sci 31:1008–1014.

Gugleta K, Zawinka C, Rickenbacher I, Kochkorov A, Katamay R, Flammer J, Orgul S (2006) Analysis of retinal vasodilation after flicker light stimulation in relation to vasospastic propensity. Invest Ophthalmol Vis Sci 47:4034–4041.

Gupta SK, Kumar B, Nag TC, Agrawal SS, Agrawal R, Agrawal P, Saxena R, Srivastava S (2011) Curcumin Prevents Experimental Diabetic Retinopathy in Rats Through Its Hypoglycemic, Antioxidant, and Anti-Inflammatory Mechanisms. J Ocul Pharmacol Ther 0.

Häggström M (2012) Fundus photograph of normal left eye. Wikimedia Common Available at: http://en.wikipedia.org/wiki/File:Fundus_photograph_of_normal_left_eye.jpg [Accessed January 8, 2014]. This file is made available under the Creative Commons CC0 1.0 Universal Public Domain Dedication.

Han Y, Bearse MA, Schneck ME, Barez S, Jacobsen CH, Adams AJ (2004) Multifocal electroretinogram delays predict sites of subsequent diabetic retinopathy. Invest Ophthalmol Vis Sci 45:948–954.

Hansen SH (2001) The role of taurine in diabetes and the development of diabetic complications. Diabetes Metab Res Rev 17:330–346.

Hardy KJ, Lipton J, Scase MO, Foster DH, Scarpello JH (1992) Detection of colour vision abnormalities in uncomplicated type 1 diabetic patients with angiographically normal retinas. Br J Ophthalmol 76:461–464.

Hardy KJ, Scarpello JH, Foster DH, Moreland JD (1994) Effect of diabetes associated increases in lens optical density on colour discrimination in insulin dependent diabetes. Br J Ophthalmol 78:754–756.

Harris A, Arend O, Danis RP, Evans D, Wolf S, Martin BJ (1996) Hyperoxia improves contrast sensitivity in early diabetic retinopathy. Br J Ophthalmol 80:209–213.

Harrison WW, Bearse M a, Ng JS, Jewell NP, Barez S, Burger D, Schneck ME, Adams AJ (2011) Multifocal electroretinograms predict onset of diabetic retinopathy in adult patients with diabetes. Invest Ophthalmol Vis Sci 52:772–777.

Herichová I, Zeman M, Stebelová K, Ravingerová T (2005) Effect of streptozotocin-induced diabetes on daily expression of per2 and dbp in the heart and liver and melatonin rhythm in the pineal gland of Wistar rat. Mol Cell Biochem 270:223–229.

Herrmann R, Heflin SJJ, Hammond T, Lee B, Wang J, Gainetdinov RRR, Caron MGG, Eggers EDD, Frishman LJJ, McCall MA a, Arshavsky VYY (2011) Rod vision is controlled by dopamine-dependent sensitization of rod bipolar cells by GABA. Neuron 72:101–110.

Hikichi T, Tateda N, Miura T (2011) Alteration of melatonin secretion in patients with type 2 diabetes and proliferative diabetic retinopathy. Clin Ophthalmol 5:655–660.

Hill M (2014) Eye and retina. Available at: http://embryology.med.unsw.edu.au/embryology/index.php?title=Eye_and_retina_cartoon.jpg [Accessed January 8, 2014].

Holfort SK, Klemp K, Kofoed PK, Sander B, Larsen M (2010) Scotopic electrophysiology of the retina during transient hyperglycemia in type 2 diabetes. Invest Ophthalmol Vis Sci 51:2790–2794.

Holopigian K, Seiple W, Lorenzo M, Carr R (1992) A comparison of photopic and scotopic electroretinographic changes in early diabetic retinopathy. Invest Ophthalmol Vis Sci 33:2773–2780.

Honda M, Inoue M, Okada Y, Yamamoto M (1998) Alteration of the GABAergic neuronal system of the retina and superior colliculus in streptozotocin-induced diabetic rat. Kobe J Med Sci 44:1–8.

Hood DC (2000) Assessing retinal function with the multifocal technique. Prog Retin Eye Res 19:607–646.

Hood DC, Birch DG (1990) A quantitative measure of the electrical activity of human rod photoreceptors using electroretinography. Vis Neurosci 5:379–387.

Hotta N, Koh N, Sakakibara F, Nakamura J, Hara T, Hamada Y, Fukasawa H, Kakuta H, Sakamoto N (1997) Effect of an aldose reductase inhibitor on abnormalities of electroretinogram and vascular factors in diabetic rats. Eur J Pharmacol 326:45–51.

Huemer K-H, Zawinka C, Garhöfer G, Golestani E, Litschauer B, Dorner GT, Schmetterer L (2007) Effects of dopamine on retinal and choroidal blood flow parameters in humans. Br J Ophthalmol 91:1194–1198.

Imig JD, Simpkins AN, Renic M, Harder DR (2011) Cytochrome P450 eicosanoids and cerebral vascular function. Expert Rev Mol Med 13:e7.

Ishikawa A, Ishiguro S, Tamai M (1996a) Changes in GABA metabolism in streptozotocin-induced diabetic rat retinas. Curr Eye Res 15:63–71.

Ishikawa A, Ishiguro S, Tamai M (1996b) Accumulation of gamma-aminobutyric acid in diabetic rat retinal Müller cells evidenced by electron microscopic immunocytochemistry. Curr Eye Res 15:958–964.

Iuvone PM, Galli CL, Garrison-Gund CK, Neff NH (1978) Light stimulates tyrosine hydroxylase activity and dopamine synthesis in retinal amacrine neurons. Science 202:901–902.

Jackson CR, Chaurasia SS, Hwang CK, Iuvone PM (2011) Dopamine D4 receptor activation controls circadian timing of the adenylyl cyclase 1/cyclic AMP signaling system in mouse retina. Eur J Neurosci 34:57–64.

Jackson CR, Ruan G-X, Aseem F, Abey J, Gamble K, Stanwood G, Palmiter RD, Iuvone PM, McMahon DG (2012) Retinal dopamine mediates multiple dimensions of light-adapted vision. J Neurosci 32:9359–9368.

Jackson DM, Ross SB, Hashizume M (1988) Further studies on the interaction between bromocriptine and SKF38393 in reserpine and alpha methyl-para-tyrosine-treated mice. Psychopharmacology (Berl) 94:321–327.

Jackson GR, Barber AJ (2010) Visual dysfunction associated with diabetic retinopathy. Curr Diab Rep 10:380–384.

Kandel ER, Schwartz JH, Jessell TM (2000) Principles of Neural Science, 4th ed. New York: McGraw-Hill Medical.

Kashii S, Takahashi M, Mandai M, Shimizu H, Honda Y, Sasa M, Ujihara H, Tamura Y, Yokota T, Akaike a (1994) Protective action of dopamine against glutamate neurotoxicity in the retina. Invest Ophthalmol Vis Sci 35:685–695.

Kawasaki K, Yonemura K, Yokogawa Y, Saito N, Kawakita S (1986) Correlation between ERG oscillatory potential and psychophysical contrast sensitivity in diabetes. Doc Ophthalmol 64:209–215.

Kern TS, Barber AJ (2008) Retinal ganglion cells in diabetes. J Physiol 586:4401–4408.

Kern TS, Miller CM, Tang J, Du Y, Ball SL, Berti-Matera L (2010a) Comparison of three strains of diabetic rats with respect to the rate at which retinopathy and tactile allodynia develop. Mol Vis 16:1629–1639.

Kern TS, Tang J, Berkowitz BA (2010b) Validation of structural and functional lesions of diabetic retinopathy in mice. Mol Vis 16:2121–2131.

Kim I-H, Morisseau C, Watanabe T, Hammock BD (2004) Design, synthesis, and biological activity of 1,3-disubstituted ureas as potent inhibitors of the soluble epoxide hydrolase of increased water solubility. J Med Chem 47:2110–2122.

Kim YH, Kim YS, Noh HS, Kang SS, Cheon EW, Park SK, Lee BJ, Choi WS, Cho GJ (2005) Changes in rhodopsin kinase and transducin in the rat retina in early-stage diabetes. Exp Eye Res 80:753–760.

King H, Aubert RE, Herman WH (1998) Global burden of diabetes, 1995-2025: prevalence, numerical estimates, and projections. Diabetes Care 21:1414–1431.

Kirwin SJ, Kanaly ST, Hansen CR, Cairns BJ, Ren M, Edelman JL (2011) Retinal gene expression and visually evoked behavior in diabetic long evans rats. Invest Ophthalmol Vis Sci 52:7654–7663.

Kirwin SJ, Kanaly ST, Linke NA, Edelman JL (2009) Strain-dependent increases in retinal inflammatory proteins and photoreceptor FGF-2 expression in streptozotocin-induced diabetic rats. Invest Ophthalmol Vis Sci 50:5396–5404.

Kizawa J, Machida S, Kobayashi T, Gotoh Y, Kurosaka D (2006) Changes of oscillatory potentials and photopic negative response in patients with early diabetic retinopathy. Jpn J Ophthalmol 50:367–373.

Klein BEK (2007) Overview of epidemiologic studies of diabetic retinopathy. Ophthalmic Epidemiol 14:179–183.

Klein R, Klein BE, Moss SE (1989) The Wisconsin epidemiological study of diabetic retinopathy: a review. Diabetes Metab Rev 5:559–570.

Koehler RC, Roman RJ, Harder DR (2009) Astrocytes and the regulation of cerebral blood flow. Trends Neurosci 32:160–169.

Kohzaki K, Vingrys AJ, Bui B V (2008) Early inner retinal dysfunction in streptozotocin-induced diabetic rats. Invest Ophthalmol Vis Sci 49:3595–3604.

Kowluru A, Kowluru RA, Yamazaki A (1992) Functional alterations of G-proteins in diabetic rat retina: a possible explanation for the early visual abnormalities in diabetes mellitus. Diabetologia 35:624–631.

Kowluru R a, Chan P-S (2007) Oxidative stress and diabetic retinopathy. Exp Diabetes Res 2007:43603.

Kowluru R a, Engerman RL, Case GL, Kern TS (2001) Retinal glutamate in diabetes and effect of antioxidants. Neurochem Int 38:385–390.

Kowluru RA (2005) Diabetic retinopathy: mitochondrial dysfunction and retinal capillary cell death. Antioxid Redox Signal 7:1581–1587.

Kowluru RA, Koppolu P (2002) Diabetes-induced activation of caspase-3 in retina: effect of antioxidant therapy. Free Radic Res 36:993–999.

Lamb TD, Pugh EN (2006) Phototransduction, dark adaptation, and rhodopsin regeneration the proctor lecture. Invest Ophthalmol Vis Sci 47:5137–5152.

Lasta M, Pemp B, Schmidl D, Boltz A, Kaya S, Palkovits S, Werkmeister R, Howorka K, Popa-Cherecheanu A, Garhöfer G, Schmetterer L (2013) Neurovascular dysfunction precedes neural dysfunction in the retina of patients with type 1 diabetes. Invest Ophthalmol Vis Sci 54:842–847.

Lau JCM, Kroes R a, Moskal JR, Linsenmeier R a (2013) Diabetes changes expression of genes related to glutamate neurotransmission and transport in the Long-Evans rat retina. Mol Vis 19:1538–1553.

Lecleire-Collet A, Audo I, Aout M, Girmens J-F, Sofroni R, Erginay A, Le Gargasson J-F, Mohand-Saïd S, Meas T, Guillausseau P-J, Vicaut E, Paques M, Massin P (2011) Evaluation of retinal function and flicker light-induced retinal vascular response in normotensive patients with diabetes without retinopathy. Invest Ophthalmol Vis Sci 52:2861–2867.

Lee S, Morgan GA, Harris NR (2008) Ozagrel reverses streptozotocin-induced constriction of arterioles in rat retina. Microvasc Res 76:217–223.

Li G-Y, Li T, Fan B, Zheng Y-C, Ma T-H (2012) The D1 dopamine receptor agonist, SKF83959, attenuates hydrogen peroxide-induced injury in RGC-5 cells involving the extracellular signal-regulated kinase/p38 pathways. Mol Vis 18:2882–2895.

Li Q, Puro DG (2002) Diabetes-induced dysfunction of the glutamate transporter in retinal Müller cells. Invest Ophthalmol Vis Sci 43:3109–3116.

Li Q, Zemel E, Miller B, Perlman I (2002) Early retinal damage in experimental diabetes: electroretinographical and morphological observations. Exp Eye Res 74:615–625.

Lieth E, Barber AJ, Xu B, Dice C, Ratz MJ, Tanase D, Strother JM (1998) Glial reactivity and impaired glutamate metabolism in short-term experimental diabetic retinopathy. Penn State Retina Research Group. Diabetes 47:815–820.

Lieth E, LaNoue KF, Antonetti D a, Ratz M (2000) Diabetes reduces glutamate oxidation and glutamine synthesis in the retina. The Penn State Retina Research Group. Exp Eye Res 70:723–730.

Link D, Strohmaier C, Seifert BU, Riemer T, Reitsamer H a, Haueisen J, Vilser W (2011) Novel non-contact retina camera for the rat and its application to dynamic retinal vessel analysis. Biomed Opt Express 2:3094–3108.

Linsenmeier RA (1986) Effects of light and darkness on oxygen distribution and consumption in the cat retina. J Gen Physiol 88:521–542.

Linsenmeier RA, McRipley MA, Braun RD, Lutty GA, Padnick LB, Ahmed J, Hatchell DL, McLeod DS (1998) Retinal hypoxia in long-term diabetic cats. Invest Ophthalmol Vis Sci 39:1647–1657.

Livak KJ, Schmittgen TD (2001) Analysis of relative gene expression data using real-time quantitative PCR and the 2(-Delta Delta C(T)) Method. Methods 25:402–408.

Lopes de Faria JM, Katsumi O, Cagliero E, Nathan D, Hirose T (2001) Neurovisual abnormalities preceding the retinopathy in patients with long-term type 1 diabetes mellitus. Graefe's Arch Clin Exp Ophthalmol 239:643–648.

Lorenzi M, Gerhardinger C (2001) Early cellular and molecular changes induced by diabetes in the retina. Diabetologia 44:791–804.

Ly A, Yee P, Vessey K a, Phipps J a, Jobling AI, Fletcher EL (2011) Early inner retinal astrocyte dysfunction during diabetes and development of hypoxia, retinal stress, and neuronal functional loss. Invest Ophthalmol Vis Sci 52:9316–9326.

Mandecka A, Dawczynski J, Blum M, Muller N, Kloos C, Wolf G, Müller N, Vilser W, Hoyer H, Müller UA (2007) Influence of flickering light on the retinal vessels in diabetic patients. Diabetes Care 30:3048–3052.

Mandecka A, Dawczynski J, Vilser W, Blum M, Müller N, Kloos C, Wolf G, Müller UA (2009) Abnormal retinal autoregulation is detected by provoked stimulation with

flicker light in well-controlled patients with type 1 diabetes without retinopathy. Diabetes Res Clin Pract 86:51–55.

Mao J, Liu S, Qin W, Li F, Wu X, Tan Q (2010) Levodopa inhibits the development of form-deprivation myopia in guinea pigs. Optom Vis Sci 87:53–60.

Marcheva B, Ramsey KM, Buhr ED, Kobayashi Y, Su H, Ko CH, Ivanova G, Omura C, Mo S, Vitaterna MH, Lopez JP, Philipson LH, Bradfield C a, Crosby SD, JeBailey L, Wang X, Takahashi JS, Bass J (2010) Disruption of the clock components CLOCK and BMAL1 leads to hypoinsulinaemia and diabetes. Nature 466:627–631.

Martin PM, Roon P, Ells V, T.k, Ganapathy V, Smith SB, Van Ells TK (2004) Death of retinal neurons in streptozotocin-induced diabetic mice. Invest Ophthalmol Vis Sci 45:3330–3336.

Matsubara H, Kuze M, Sasoh M, Ma N, Furuta M, Uji Y (2006) Time-dependent course of electroretinograms in the spontaneous diabetic Goto-Kakizaki rat. Jpn J Ophthalmol 50:211–216.

Metea MR, Newman EA (2006) Glial cells dilate and constrict blood vessels: a mechanism of neurovascular coupling. J Neurosci 26:2862–2870.

Metea MR, Newman EA (2007) Signalling within the neurovascular unit in the mammalian retina. Exp Physiol 92:635–640.

Mishra A, Newman E a (2010) Inhibition of inducible nitric oxide synthase reverses the loss of functional hyperemia in diabetic retinopathy. Glia 58:1996–2004.

Mishra A, Newman E a (2011) Aminoguanidine reverses the loss of functional hyperemia in a rat model of diabetic retinopathy. Front Neuroenergetics 3:10.

Miyata N, Taniguchi K, Seki T, Ishimoto T, Sato-Watanabe M, Yasuda Y, Doi M, Kametani S, Tomishima Y, Ueki T, Sato M, Kameo K (2001) HET0016, a potent and selective inhibitor of 20-HETE synthesizing enzyme. Br J Pharmacol 133:325–329.

Mizutani M, Gerhardinger C, Lorenzi M (1998) Müller cell changes in human diabetic retinopathy. Diabetes 47:445–449.

Molday RS (2011) Phototransduction in rod outer segments. Available at: http://research.biochem.ubc.ca/fac_research/faculty/Molday_2011/Research/Research.html [Accessed January 8, 2014].

Moreland RB, Patel M, Hsieh GC, Wetter JM, Marsh K, Brioni JD (2005) A-412997 is a selective dopamine D4 receptor agonist in rats. Pharmacol Biochem Behav 82:140–147.

Mowat FM, Luhmann UFO, Smith AJ, Lange C, Duran Y, Harten S, Shukla D, Maxwell PH, Ali RR, Bainbridge JWB (2010) HIF-1alpha and HIF-2alpha are differentially activated in distinct cell populations in retinal ischaemia. PLoS One 5:e11103.

Muir ER, Rentería RC, Duong TQ (2012) Reduced ocular blood flow as an early indicator of diabetic retinopathy in a mouse model of diabetes. Invest Ophthalmol Vis Sci 53:6488–6494.

Muranov K, Poliansky N, Winkler R, Rieger G, Schmut O, Horwath-Winter J (2004) Protection by iodide of lens from selenite-induced cataract. Graefe's Arch Clin Exp Ophthalmol 242:146–151.

Newman E a (2013) Functional hyperemia and mechanisms of neurovascular coupling in the retinal vasculature. J Cereb Blood Flow Metab 33:1685–1695.

Nguyen TT, Kawasaki R, Kreis AJ, Wang JJ, Shaw J, Vilser W, Wong TY (2009) Correlation of light-flicker-induced retinal vasodilation and retinal vascular caliber measurements in diabetes. Invest Ophthalmol Vis Sci 50:5609–5613.

Nguyen-Legros J (1988) Functional neuroarchitecture of the retina: hypothesis on the dysfunction of retinal dopaminergic circuitry in Parkinson's disease. Surg Radiol Anat 10:137–144.

Nir I, Haque R, Iuvone PM (2000) Diurnal metabolism of dopamine in the mouse retina. Brain Res 870:118–125.

Nir I, Iuvone PM (1994) Alterations in light-evoked dopamine metabolism in dystrophic retinas of mutant rds mice. Brain Res 649:85–94.

Nishimura C, Kuriyama K (1985) Alterations in the retinal dopaminergic neuronal system in rats with streptozotocin-induced diabetes. J Neurochem 45:448–455.

Northington FK, E!amill RW, Banerjee SP, Hamill RW (1985) Dopamine-stimulated adenylate cyclase and tyrosine hydroxylase in diabetic rat retina. Brain Res 337:151–154.

Obrosova IG, Chung SSM, Kador PF (2010) Diabetic cataracts: mechanisms and management. Diabetes Metab Res Rev 26:172–180.

Oshitari T, Hanawa K, Adachi-Usami E (2009) Changes of macular and RNFL thicknesses measured by Stratus OCT in patients with early stage diabetes. Eye (Lond) 23:884–889.

Ostroy SE, Frede SM, Wagner EF, Gaitatzes CG, Janle EM (1994) Decreased rhodopsin regeneration in diabetic mouse eyes. Invest Ophthalmol Vis Sci 35:3905–3909.

Ozawa Y, Kurihara T, Sasaki M, Ban N, Yuki K, Kubota S, Tsubota K (2011) Neural degeneration in the retina of the streptozotocin-induced type 1 diabetes model. Exp Diabetes Res 2011:108328.

Pannicke T, Iandiev I, Wurm A, Uckermann O, vom Hagen F, Reichenbach A, Wiedemann P, Hammes H-P, Bringmann A (2006) Diabetes alters osmotic swelling characteristics and membrane conductance of glial cells in rat retina. Diabetes 55:633–639.

Pemp B, Garhofer G, Weigert G, Karl K, Resch H, Wolzt M, Schmetterer L (2009) Reduced retinal vessel response to flicker stimulation but not to exogenous nitric oxide in type 1 diabetes. Invest Ophthalmol Vis Sci 50:4029–4032.

Pemp B, Schmetterer L (2008) Ocular blood flow in diabetes and age-related macular degeneration. Can J Ophthalmol 43:295–301.

Penn RD, Hagins WA (1969) Signal transmission along retinal rods and the origin of the electroretinographic a-wave. Nature 223:201–204.

Phipps J a, Yee P, Fletcher EL, Vingrys AJ (2006) Rod photoreceptor dysfunction in diabetes: activation, deactivation, and dark adaptation. Invest Ophthalmol Vis Sci 47:3187–3194.

Poloyac SM, Zhang Y, Bies RR, Kochanek PM, Graham SH (2006) Protective effect of the 20-HETE inhibitor HET0016 on brain damage after temporary focal ischemia. J Cereb Blood Flow Metab 26:1551–1561.

Pournaras CJ, Rungger-Brändle E, Riva CE, Hardarson SH, Stefansson E (2008) Regulation of retinal blood flow in health and disease. Prog Retin Eye Res 27:284–330.

Pozdeyev N, Tosini G, Li L, Ali F, Rozov S, Lee RH, Iuvone PM (2008) Dopamine modulates diurnal and circadian rhythms of protein phosphorylation in photoreceptor cells of mouse retina. Eur J Neurosci 27:2691–2700.

Pratt PF, Medhora M, Harder DR (2004) Mechanisms regulating cerebral blood flow as therapeutic targets. Curr Opin Investig Drugs 5:952–956.

Prusky GT, Alam NM, Beekman S, Douglas RM (2004) Rapid quantification of adult and developing mouse spatial vision using a virtual optomotor system. Invest Ophthalmol Vis Sci 45:4611–4616.

Prusky GT, Alam NM, Douglas RM (2006) Enhancement of vision by monocular deprivation in adult mice. J Neurosci 26:11554–11561.

Prusky GT, West PW, Douglas RM (2000) Behavioral assessment of visual acuity in mice and rats. Vision Res 40:2201–2209.

Puk O, Dalke C, Hrabé de Angelis M, Graw J (2008) Variation of the response to the optokinetic drum among various strains of mice. Front Biosci 13:6269–6275.

Pulido JSE, Erie JC, Arroyo J, Bertram K, Lu M-J, Shippy S a (2007) A role for excitatory amino acids in diabetic eye disease. Exp Diabetes Res 2007:36150.

Qian H, Ripps H (2011) Neurovascular interaction and the pathophysiology of diabetic retinopathy. Exp Diabetes Res 2011:693426.

Ramsey DJ, Ripps H, Qian H (2006) An electrophysiological study of retinal function in the diabetic female rat. Invest Ophthalmol Vis Sci 47:5116–5124.

Ramsey DJ, Ripps H, Qian H (2007) Streptozotocin-induced diabetes modulates GABA receptor activity of rat retinal neurons. Exp Eye Res 85:413–422.

Rees D a, Alcolado JC (2005) Animal models of diabetes mellitus. Diabet Med 22:359–370.

Riva CE, Logean E, Falsini B (2005) Visually evoked hemodynamical response and assessment of neurovascular coupling in the optic nerve and retina. Prog Retin Eye Res 24:183–215.

Robinson R, Barathi V a, Chaurasia SS, Wong TY, Kern TS (2012) Update on animal models of diabetic retinopathy: from molecular approaches to mice and higher mammals. Dis Model Mech 5:444–456.

Robson JG, Frishman LJ (1999) Dissecting the dark-adapted electroretinogram. Doc Ophthalmol 95:187–215.

Roman RJ (2002) P-450 metabolites of arachidonic acid in the control of cardiovascular function. Physiol Rev 82:131–185.

Roy CS, Sherrington CS (1890) On the Regulation of the Blood-supply of the Brain. J Physiol 11:85–158.17.

Roy MS, Gunkel RD, Podgor MJ (1986) Color vision defects in early diabetic retinopathy. Arch Ophthalmol 104:225–228.

Roy MS, Klein R, O'Colmain BJ, Klein BEK, Moss SE, Kempen JH (2004) The prevalence of diabetic retinopathy among adult type 1 diabetic persons in the United States. Arch Ophthalmol 122:546–551.

Rungger-Brändle E, Dosso a a, Leuenberger PM (2000) Glial reactivity, an early feature of diabetic retinopathy. Invest Ophthalmol Vis Sci 41:1971–1980.

Santiago AR, Cristóvão AJ, Santos PF, Carvalho CM, Ambrósio AF (2007) High glucose induces caspase-independent cell death in retinal neural cells. Neurobiol Dis 25:464–472.

Santiago AR, Gaspar JM, Baptista FI, Cristóvão AJ, Santos PF, Kamphuis W, Ambrósio AF (2009) Diabetes changes the levels of ionotropic glutamate receptors in the rat retina. Mol Vis 15:1620–1630.

Sasaki M, Ozawa Y, Kurihara T, Kubota S, Yuki K, Noda K, Kobayashi S, Ishida S, Tsubota K (2010) Neurodegenerative influence of oxidative stress in the retina of a murine model of diabetes. Diabetologia 53:971–979.

Saszik SM, Robson JG, Frishman LJ (2002) The scotopic threshold response of the dark-adapted electroretinogram of the mouse. J Physiol 543:899–916.

Schiller PH (2010) Parallel information processing channels created in the retina. Proc Natl Acad Sci U S A 107:17087–17094.

Schmittgen TD, Livak KJ (2008) Analyzing real-time PCR data by the comparative C(T) method. Nat Protoc 3:1101–1108.

Schupp C, Olano-Martin E, Gerth C, Morrissey BM, Cross CE, Werner JS (2004) Lutein, zeaxanthin, macular pigment, and visual function in adult cystic fibrosis patients. Am J Clin Nutr 79:1045–1052.

Seifertl BU, Vilser W (2002) Retinal Vessel Analyzer (RVA)--design and function. Biomed Tech (Berl) 47 Suppl 1:678–681.

Seki M, Tanaka T, Nawa H, Usui T, Fukuchi T, Ikeda K, Abe H, Takei N (2004) Involvement of brain-derived neurotrophic factor in early retinal neuropathy of streptozotocin-induced diabetes in rats: therapeutic potential of brain-derived neurotrophic factor for dopaminergic amacrine cells. Diabetes 53:2412–2419.

Shirao Y, Kawasaki K (1998) Electrical Responses from Diabetic Retina. Prog Retin Eye Res 17:59–76.

Sieving PA, Frishman LJ, Steinberg RH (1986) Scotopic threshold response of proximal retina in cat. J Neurophysiol 56:1049–1061.

Silva KC, Rosales M a B, de Faria JBL, de Faria JML (2010) Reduction of inducible nitric oxide synthase via angiotensin receptor blocker prevents the oxidative retinal damage in diabetic hypertensive rats. Curr Eye Res 35:519–528.

Simó R, Hernández C (2013) Neurodegeneration in the diabetic eye: new insights and therapeutic perspectives. Trends Endocrinol Metab:1–11.

Simpkins AN, Rudic RD, Schreihofer D a, Roy S, Manhiani M, Tsai H-J, Hammock BD, Imig JD (2009) Soluble epoxide inhibition is protective against cerebral ischemia via vascular and neural protection. Am J Pathol 174:2086–2095.

Sokol S, Moskowitz a, Skarf B, Evans R, Molitch M, Senior B (1985) Contrast sensitivity in diabetics with and without background retinopathy. Arch Ophthalmol 103:51–54.

Speros P, Price J (1981) Oscillatory potentials. History, techniques and potential use in the evaluation of disturbances of retinal circulation. Surv Ophthalmol 25:237–252.

Srienc AI, Kurth-Nelson ZL, Newman EA (2010) Imaging retinal blood flow with laser speckle flowmetry. Front Neuroenergetics 2:1–10.

Storch K-F, Paz C, Signorovitch J, Raviola E, Pawlyk B, Li T, Weitz CJ (2007) Intrinsic circadian clock of the mammalian retina: importance for retinal processing of visual information. Cell 130:730–741.

Sung Y-H, Kim S-C, Hong H-P, Park C-Y, Shin M-S, Kim C-J, Seo J-H, Kim D-Y, Kim D-J, Cho H-J (2012) Treadmill exercise ameliorates dopaminergic neuronal loss through suppressing microglial activation in Parkinson's disease mice. Life Sci 91:1309–1316.

Sutoo D, Akiyama K (2003) Regulation of brain function by exercise. Neurobiol Dis 13:1–14.

Tanaka Y, Omura T, Fukasawa M, Horiuchi N, Miyata N, Minagawa T, Yoshida S, Nakaike S (2007) Continuous inhibition of 20-HETE synthesis by TS-011 improves neurological and functional outcomes after transient focal cerebral ischemia in rats. Neurosci Res 59:475–480.

Tang J, Kern TS (2011) Inflammation in diabetic retinopathy. Prog Retin Eye Res 30:343–358.

Thaung C, Arnold K, Jackson IJ, Coffey PJ (2002) Presence of visual head tracking differentiates normal sighted from retinal degenerate mice. Neurosci Lett 325:21–24.

The Diabetes Control and Complications Trial (DCCT) Research Group (1993) The effect of intensive treatment of diabetes on the development and progression of long-term complications in insulin-dependent diabetes mellitus. N Engl J Med 329:977–986.

Thomas BB, Seiler MJ, Sadda SR, Coffey PJ, Aramant RB (2004) Optokinetic test to evaluate visual acuity of each eye independently. J Neurosci Methods 138:7–13.

Thulé PM, Campbell AG, Kleinhenz DJ, Olson DE, Boutwell JJ, Sutliff RL, Hart CM (2006) Hepatic insulin gene therapy prevents deterioration of vascular function and improves adipocytokine profile in STZ-diabetic rats. Am J Physiol Endocrinol Metab 290:E114–E122.

Toda N, Toda MN, Nakanishi-Toda M (2007) Nitric oxide: ocular blood flow, glaucoma, and diabetic retinopathy. Prog Retin Eye Res 26:205–238.

Tosini G, Baba K, Hwang CK, Iuvone PM (2012) Melatonin: an underappreciated player in retinal physiology and pathophysiology. Exp Eye Res 103:82–89.

Troger J, Neyer S, Heufler C, Huemer H, Schmid E, Griesser U, Kralinger M, Kremser B, Baldissera I, Kieselbach G (2001) Substance P and vasoactive intestinal polypeptide in the streptozotocin-induced diabetic rat retina. Invest Ophthalmol Vis Sci 42:1045–1050.

Trulson ME, Himmel CD (1983) Decreased brain dopamine synthesis rate and increased [3H]spiroperidol binding in streptozotocin-diabetic rats. J Neurochem 40:1456–1459.

Tuitoek PJ, Ritter SJ, Smith JE, Basu TK (1996a) Streptozotocin-induced diabetes lowers retinol-binding protein and transthyretin concentrations in rats. Br J Nutr 76:891–897.

Tuitoek PJ, Ziari S, Tsin AT, Rajotte R V, Suh M, Basu TK (1996b) Streptozotocin-induced diabetes in rats is associated with impaired metabolic availability of vitamin A (retinol). Br J Nutr 75:615–622.

Tummala SR, Benac S, Tran H, Vankawala A, Zayas-Santiago A, Appel A, Derwent JJK, Kang Derwent JJ (2009) Effects of inhibition of neuronal nitric oxide synthase on basal retinal blood flow regulation. Exp Eye Res 89:801–809.

Turner P V, Albassam MA (2005) Susceptibility of rats to corneal lesions after injectable anesthesia. Comp Med 55:175–182.

UK Prospective Diabetes Study (UKPDS) Group (1998) Intensive blood-glucose control with sulphonylureas or insulin compared with conventional treatment and risk of complications in patients with type 2 diabetes (UKPDS 33). Lancet 352:837–853.

VanGuilder HD, Brucklacher RM, Patel K, Ellis RW, Freeman WM, Barber AJ (2008) Diabetes downregulates presynaptic proteins and reduces basal synapsin I phosphorylation in rat retina. Eur J Neurosci 28:1–11.

Villarroel M, Ciudin A, Hernández C, Simó R (2010) Neurodegeneration: An early event of diabetic retinopathy. World J Diabetes 1:57–64.

Wachtmeister L (1998) Oscillatory potentials in the retina: what do they reveal. Prog Retin Eye Res 17:485–521.

Waisbourd M, Goldstein M, Loewenstein A (2011) Treatment of diabetic retinopathy with anti-VEGF drugs. Acta Ophthalmol 89:203–207.

Wang Z, Yadav AS, Leskova W, Harris NR (2010) Attenuation of streptozotocin-induced microvascular changes in the mouse retina with the endothelin receptor A antagonist atrasentan. Exp Eye Res 91:670–675.

Wang Z, Yadav AS, Leskova W, Harris NR (2011) Inhibition of 20-HETE attenuates diabetes-induced decreases in retinal hemodynamics. Exp Eye Res 93:108–113.

Ward MM, Jobling a I, Kalloniatis M, Fletcher EL (2005) Glutamate uptake in retinal glial cells during diabetes. Diabetologia 48:351–360.

Wässle H (2004) Parallel processing in the mammalian retina. Nat Rev Neurosci 5:747–757.

Witkovsky P (2004) Dopamine and retinal function. Doc Ophthalmol 108:17–40.

Wolff BE, Bearse M a, Schneck ME, Barez S, Adams AJ (2010) Multifocal VEP (mfVEP) reveals abnormal neuronal delays in diabetes. Doc Ophthalmol 121:189–196.

Wolter JR (1961) Diabetic retinopathy. Am J Ophthalmol 51:1123–1141.

Wright WS, McElhatten RM, Messina JE, Harris NR (2010) Hypoxia and the expression of HIF-1alpha and HIF-2alpha in the retina of streptozotocin-injected mice and rats. Exp Eye Res 90:405–412.

Wright WS, Messina JE, Harris NR (2009) Attenuation of diabetes-induced retinal vasoconstriction by a thromboxane receptor antagonist. Exp Eye Res 88:106–112.

Wu DM, Kawamura H, Li Q, Puro DG (2001) Dopamine activates ATP-sensitive K+ currents in rat retinal pericytes. Vis Neurosci 18:935–940.

Yamauchi T, Kashii S, Yasuyoshi H, Zhang S, Honda Y, Ujihara H, Akaike A (2003) Inhibition of glutamate-induced nitric oxide synthase activation by dopamine in cultured rat retinal neurons. Neurosci Lett 347:155–158.

Young ME, Wilson CR, Razeghi P, Guthrie PH, Taegtmeyer H (2002) Alterations of the circadian clock in the heart by streptozotocin-induced diabetes. J Mol Cell Cardiol 34:223–231.

Yousif MHM, Benter IF (2007) Role of cytochrome P450 metabolites of arachidonic acid in regulation of corporal smooth muscle tone in diabetic and older rats. Vascul Pharmacol 47:281–287.

Yousif MHM, Benter IF, Dunn KMJ, Dahly-Vernon a J, Akhtar S, Roman RJ (2009a) Role of 20-hydroxyeicosatetraenoic acid in altering vascular reactivity in diabetes. Auton Autacoid Pharmacol 29:1–12.

Yousif MHM, Benter IF, Roman RJ (2009b) Cytochrome P450 metabolites of arachidonic acid play a role in the enhanced cardiac dysfunction in diabetic rats following ischaemic reperfusion injury. Auton Autacoid Pharmacol 29:33–41.

Yu D-Y, Cringle SJ (2006) Oxygen distribution in the mouse retina. Invest Ophthalmol Vis Sci 47:1109–1112.

Yu X, Xu Z, Mi M, Xu H, Zhu J, Wei N, Chen K, Zhang Q, Zeng K, Wang J, Chen F, Tang Y (2008) Dietary taurine supplementation ameliorates diabetic retinopathy via anti-excitotoxicity of glutamate in streptozotocin-induced Sprague-Dawley rats. Neurochem Res 33:500–507.

Zeng K, Xu H, Chen K, Zhu J, Zhou Y, Zhang Q, Mantian M (2010) Effects of taurine on glutamate uptake and degradation in Müller cells under diabetic conditions via antioxidant mechanism. Mol Cell Neurosci 45:192–199.

Zeng XX, Ng YK, Ling E a (2000) Neuronal and microglial response in the retina of streptozotocin-induced diabetic rats. Vis Neurosci 17:463–471.

Zhang W, Koerner IP, Noppens R, Grafe M, Tsai H-J, Morisseau C, Luria A, Hammock BD, Falck JR, Alkayed NJ (2007) Soluble epoxide hydrolase: a novel therapeutic target in stroke. J Cereb Blood Flow Metab 27:1931–1940.

Zheng L, Kern TS (2009) Role of nitric oxide, superoxide, peroxynitrite and PARP in diabetic retinopathy. Front Biosci 14:3974–3987.